BERM BREAKWATERS WITH CONCRETE BLOCKS AS ARMOUR UNITS

Altea Camara Aguilera

TASK DESCRIPTION

NTNU
Det skapende universitet

MASTERKONTRAKT
– uttak av masteroppgave

1. Studentens personalia

Etternavn, fornavn	Fødselsdato
Camara Aguilera, Altea	**19. apr 1988**
E-post	Telefon
alteac@stud.ntnu.no	**45174476**

2. Studieopplysninger

Fakultet
Fakultet for Ingeniørvitenskap og teknologi
Institutt
Institutt for bygg, anlegg og transport
Studieprogram
Diverse studier ved IVT

3. Masteroppgave
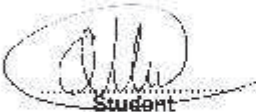
Oppstartsdato	Innleveringsfrist
14. jan 2013	**10. jun 2013**

Oppgavens (foreløpige) tittel
Berm breakwaters with concrete cubes as armour unit

Oppgavetekst/Problembeskrivelse
The Master Thesis will consist in the study of the stability of a modification of the Sirevåg breakwater replacing the class I stone with concrete cubes of 26 tons. The tests will be carried out in a 2D wave flume with irregular waves. The design wave will be Hs,100 = 7.0 m, Tz=10.6 s, HoTo=53. The model scale will be 1:70-1:80. The first part will be the test of the modified breakwater. The results will be compared with previous tests in order to conclude in which degree this modification is advantageous. The result will also be compared with the different recession formulae to know the usefulness of the formulae when using concrete blocks.

Hovedveileder ved institutt	Medveileder(e) ved institutt
Førsteamanuensis Øivind Asgeir Arntsen	**Alf Tørum**

Merknader
1 uke ekstra p.g.a påske.

4. Underskrift

Student: Jeg erklærer herved at jeg har satt meg inn i gjeldende bestemmelser for mastergradsstudiet og at jeg oppfyller kravene for adgang til å påbegynne oppgaven, herunder eventuelle praksiskrav.

Partene er gjort kjent med avtalens vilkår, samt kapitlene i studiehåndboken om generelle regler og aktuell studieplan for masterstudiet.

Trondheim 21/1-2013
Sted og dato

Student

Hovedveileder

Originalen lagres i NTNUs elektroniske arkiv. Kopi av avtalen sendes til institullet og studenten.

Side 7 av 2

PREFACE

This Master Thesis investigates the behaviour of berm breakwaters with concrete units in the armour layer. This topic of investigation is very new, as there are only a few studies about it.

The conclusions reached in this investigation are favourable to the use of concrete units in berm breakwaters. This could solve the problem of building breakwaters in some locations. Nevertheless, further investigations in the topic should follow the ones carried out in this thesis in order to know the viability of these structures entirely.

This report contains the explanation of all the work done during this semester, from the construction of the breakwater models, to the data analysis and the conclusions reasoning. The important data collected on the tests in also found in the appendices to help the work of possible future investigations.

ACKNOWLEDGEMENTS

During this semester I have learned lots of things. I have worked in very interesting and challenging tasks, from building a breakwater model to write Matlab scripts. I have had the opportunity to work in a very interesting topic that made me feel that all my work and effort spend in this project are worthy further beyond my personal learning.

All this could not have been possible without the Erasmus studentship program. I want to thank the European Commission for giving me the opportunity to come to Norway.

I am very grateful to all the people that helped me during this semester; I could not have been the same without all the support received.

First, I would like to thank Alf Tørum for his constant interest in the project and his great advices that reflected his enormous knowledge in the area. I am very lucky to have worked with you.

Second, I thank Esther Gómez for it also constant interest and high involvement in the investigation. Without her experience in model test with concrete units, this thesis would not be the same.

I want to also thank Øivind Arntsen for his help with the wave generation and analysis and to Gustav Jakobsen for his great and essential assistance in the laboratory.

And last, thanks to all the people who have contributed to any extent in this project.

CONTENTS

LIST OF TABLES

LIST OF FIGURES

ENGLISH SUMMARY

The objective of this thesis is to test the hydraulic stability of berm breakwaters with concrete armour units. To achieve this, five breakwater models were tested with the same wave program. All the models were modifications of the Sirevåg berm breakwater. The modifications consisted in the replacement of the class I stone form the armour layer by two different concrete units, cubes and cubipods

The design waves were $H_{s,100}$=7.0 m, T_z=10.6 s. HoTo=48. The wave program consisted in 7 different wave steps contained a total of 16.000 waves approximately. The tests were carried out with irregular waves. The test runs are based on replicas of the two major storms recorded close to the Sirevåg harbour, and had been used before for other berm breakwater studies at NTNU.

The results from the different model tests were compared with each other and with a previous investigation with berm breakwater built with rocks. The results were also compared with Tørum recession equation to know the usefulness of the equation with concrete blocks.

Finally, it was concluded that, based on the data obtained during the tests, concrete cubes have a very good behaviour in berm breakwater structures. The tests shown that models built with concrete cubes in the armour layer experience the same recession than the same model built with rock when they were exposed to low waves. In addition, they experienced lower recession than the models with rock when they were exposed to high waves.

It was also observed that the continuity of the armour layer until a deeper level reduced the recession when the front slope was continuous.

In addition, the results reflected that the layer porosity is a critical factor in layers made of concrete units. Because, a small change on it led to a completely different behaviour.

In this investigation, the models with concrete cubipods underwent more recession than the models with cubes under the same Ho, HoTo and HoVTo circumstances. This result contradicts other tests made with cubipods that proved that cubipods have more hydraulic stability than cubes. A cause could be the lower density of the cubipod units, as some experiments had proved that

light concrete elements have less hydraulic stability than according to the stability number.

Further investigations could analyse the behaviour of berm breakwater with concrete cubipods with concrete densities closer to the values used in prototype construction (around 2.4 t/m3).

During the tests, it was observed that the deeper rows of concrete blocks were the most unstable. Giving more stability to these rows will significantly increase the stability of the whole structure, making it tougher and probably reducing dramatically the recession. A way to improve the structure's behaviour would be to build a toe berm were the concrete units' layer starts. This could be investigated in further thesis.

Moreover, profiles in which the concrete units are lying over rock with lower Dn50 could also be tested. This way the rocks will fit better between the units, increasing the friction of the armour layer with the underlying rock layer and therefore increasing the stability.

Other issues that could be investigated are the influence of the storm length, the ice action and the economic viability.

SPANISH SUMMARY

Está comprobado que los diques berma son más estables que los diques en talud en ciertas situaciones. Además, tienen la ventaja de requerir unidades de escollera más ligeras en el manto principal, haciendo más sencilla la construcción del mismo.

En algunos lugares, las grandes piezas de roca necesarias para formar dicho manto son difíciles de adquirir. En estas zonas, el uso de unidades de hormigón puede solucionar el problema de la construcción de diques berma.

El objetivo de este proyecto es probar la estabilidad hidráulica de diques berma con unidades hormigón en el manto exterior. Para ello, se han ensayado cinco modelos de diques berma.

Las secciones de estos modelos están basadas en el dique berma construido en Sirevåg, una población en la costa suroeste de Noruega, sobre el que se han realizado anteriores investigaciones. Las modificaciones sobre este prototipo consisten en reemplazar los bloques de roca del manto principal por unidades de hormigón. En este proyecto han sido utilizados cubos y cubípodos.

El oleaje de diseño utilizado en los ensayos está basado en réplicas de dos grandes tormentas registradas cerca del puerto de Sirevåg. Este programa de oleaje ha sido utilizado anteriormente en otras investigaciones llevadas a cabo en NTNU (Universidad Noruega de Ciencia y Tecnología). Los valores de diseño de oleaje utilizado son: $H_{s,100}$=7.0 m, T_z=10.6 s. HoTo=48. Este oleaje es irregular. El programa de oleaje ha consistido en siete escalones diferentes, con aproximadamente 16.000 olas en total. Todos los modelos han sido ensayados con el mismo programa de oleaje.

Los resultados obtenidos en los ensayos de los distintos modelos han sido comparados entre sí y con una investigación anterior realizada sobre modelos similares construidos con roca en todas sus capas. También han sido comparados con la fórmula de recesión en diques berma desarrollada por Tørum.

Tras analizar los datos obtenidos durante los ensayos, se puede concluir que el uso cubos de hormigón en el manto principal da buenos resultados en diques berma. Los modelos construidos con cubos experimentan la misma recesión que los mismos modelos construidos con roca cuando son expuestos a oleajes con

bajas alturas de ola. Con oleaje más agresivo, es decir, mayores alturas de ola y periodos, los modelos construidos con cubos experimentan menores recesiones que los de roca.

Además se ha observado una menor recesión en los modelos en los que la capa con unidades de hormigón empezaba a mayores profundidades y tenían una pendiente continua.

Otra conclusión a la que se ha llegado es la importancia de la porosidad de capa en las construcciones con unidades de hormigón. Esta conclusión se obtuvo tras observar el gran cambio producido en el comportamiento de un modelo cuando la porosidad de capa fue reducida en sólo 0.06 puntos.

En los ensayos realizados en este proyecto, en igualdad de número de estabilidad, sección y porosidad de capa, los modelos construidos con cubípodos han sufrido una mayor recesión que los modelos construidos con cubos. Este resultado contradice otros experimentos realizados con cubípodos en los que éstos han sido mucho más estables que los cubos. Una causa de este inesperado comportamiento puede ser la menor densidad del hormigón de los cubípodos utilizados en los ensayos en comparación con la de los cubos. Existen investigaciones acerca de la estabilidad de unidades de hormigón de baja densidad, en las que se comprueba que estas piezas tienen menos estabilidad hidráulica que la representada por el número de estabilidad.

En futuras investigaciones podría comprobarse el comportamiento de diques berma construidos con cubípodos de densidad más cercana a la utilizada en la construcción de diques (aproximadamente 2.4 t/m3).

Durante los ensayos, se observó que las filas de la capa de unidades de hormigón más profundas eran las más inestables, pues los bloques se desplazaban en los primeros minutos de ensayo. Dando más estabilidad a estas filas se podría aumentar significativamente la estabilidad del conjunto de la capa, y con ello reducir la recesión de la estructura. Con tal fin, podría construirse una berma de pie en el lugar en el que la capa de unidades de hormigón empieza.

Otra modificación posible con el objetivo de mejorar el comportamiento de estos modelos, es el uso de roca con menor diámetro nominal bajo la capa de unidades de hormigón. De esta forma las rocas encajarán mejor entre las

unidades, aumentando la fricción entre las dos capas y por lo tanto la estabilidad del conjunto.

Otros temas que podrían ser investigados son: la influencia de la duración de la tormenta, la acción del hielo y la viabilidad económica.

1. INTRODUCTION

It has been tested that berm breakwaters are more stable under certain conditions than conventional breakwaters, Subba Rao et al. (2012). They have also the advantages of its great tolerance in placement accuracy and the lower mass of the individual armour stones that makes the construction with less specialized equipment and labour possible (Tørum et al., 2012). The acquisition of large armour stones can be difficult in some locations. A solution to this problem could be the use of concrete blocks in the armour layer, where the largest rocks are needed.

Only a few experimental studies about berm breakwaters with concrete blocks have been performed, as the one by Subba Rao et al. (2012). They studied the influence in the stability of the berm breakwater produced by the change in different wave parameters and storm duration.

The objective of this thesis is to test the hydraulic stability of berm breakwaters with concrete armour units. To achieve this, tests will be carried out on different modified scale models of the Sirevåg berm breakwater. This prototype has been chosen in order to compare the results with the several investigations completed about it. Some of these studies are the theses carried out by Menze (2000), Myhra (2005) and Westeng (2011) at NTNU. The most relevant of these studies to the investigation carried out in the current thesis is Myhra (2005). He investigated the recession of two berm breakwaters with different construction design, in two models, one from the Sirevåg breakwater and an Alternative model with narrower and higher berm and at which the armour layer started at a level of -7.0m.

All the test runs are based on replicas of the two major storms recorded close to the Sirevåg harbour. As we will work at the same wave flume that Myhra (2005), our test will be similar to his, which slightly changed the test of Menze so as to the largest wave could be generated with the available wave generator.

A laser is used to profile the breakwater before and after each run. The data of the laser is first being smoothened and then the maximum recession at six profiles of the breakwater is calculated. The maximum value of the recession is defined to be within a peak of a width of at least Dn50. This is a usual procedure to calculate the recession. Westeng (2011) also calculated the recession as its

more general definition, that is, at the top of the berm. He concluded that the two methods gave to a large extent equal result.

Visual observations and pictures were also taken after each run. This helps to have a better idea of the alterations in the breakwater. In addition, all moved stones were counted and their actual positions noted. The visual observations were supported by painting each layer of stones and some concrete units in a different colour.

Our task is to test five modified models of the Sirevåg breakwater replacing the class I stone with two different concrete units, cubes and cubipods. The design waves are $H_{s,100}$=7.0 m, T_z=10.6 s. HoTo=48. The models are tested with the same wave conditions used by Myhra (2005). The results of the different models are compared with each other and with previous investigations in order to conclude if this modification in a berm breakwater is favourable or at least has the same behaviour than the traditional berm breakwater. We will also compare the result with Tørum recession equation to know the usefulness of the equation with concrete blocks.

This thesis is the beginning of a whole study. Other tests that study different performances and aspects of the breakwater should follow it, such as a different layer configuration and different morphology that suits better to a berm breakwater with concrete cubes, different concrete armours, and the permeability and overtopping in each of them, ice, costs, blocks strength…

2. BERM BREAKWATERS

The berm breakwater concept is fairly old, but was not used very much until the 1980's when it was "reinvented" to provide wave protection for an airport runway extension into the sea in Dutch Harbor, Alaska in the Aleutian Islands (Rauw, 1987). The concept was also used later for the design of the berm breakwater at Keflavik, Iceland in 1983 (Baird and Woodrow, 1987). Since that time, many berm breakwaters have been built throughout the world. (PIANC, 2003)

Table 1. Number of berm breakwater that had been constructed in the world in 2003 (Sigurdarson et al., 2006)

Country	Number of berm breakwaters constructed
Iceland	29
Iran	8
Norway	6
Canada	5
USA	4
Australia	4
Brazil	2
Faeroe Islands	1
Madeira	1
China	1
India	1
Denmark	1
TOTAL	63

Berm breakwaters are different from conventional rubble mounded breakwater in profile shape, as can be seen in the figure bellow.

Conventional rubble mound breakwater.   Berm rubble mound breakwater
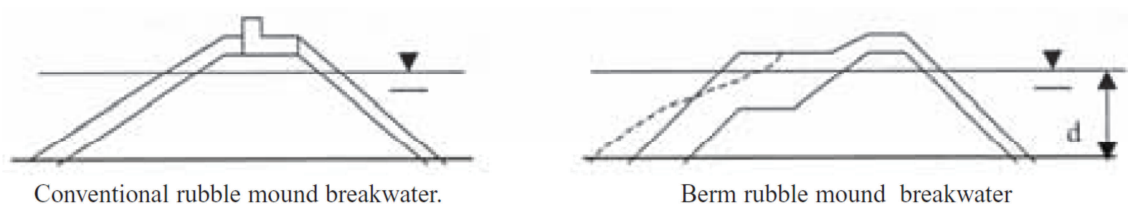
Figure 1. Difference between conventional rubble mound breakwater and berm breakwater (PIANC, 2003)

Berm breakwaters are normally constructed with a berm that is allowed to reshape into an S-shape. It has been considered that it is cheaper to construct the breakwater with a berm that will reshape than with the final S-shape.

The main advantage of the berm breakwater is that the armour stones have a lower mass than in a conventional rubble mound breakwater. Another of the primary benefits of berm breakwaters, when compared with conventional rubble mound breakwaters, is their greater acceptance tolerances with respect to placement accuracy. Hence, the berm breakwater can be constructed with commonly available heavy construction equipment and from local quarry sites at a cheaper cost.

The first berm breakwaters were built with homogenous berms. Multilayer breakwaters were first established in Iceland. Experience from many berm breakwaters has shown that working with several stone classes and placement of stones leads to a better utilization of the quarry material with a low increase of construction cost.

Berm breakwaters behave differently from conventional rubble mound breakwater. A conventional rubble mound breakwater is required to be almost static stable for the design wave conditions, while the berm breakwater has traditionally been allowed to reshape. Non-reshaping static stable berm breakwaters have also lately been considered. Three different categories of berm breakwaters are defined (PIANC, 2003):

- Non-reshaped static stable berm breakwater: only some few stones are allowed to move similar to what is allowed on a conventional rubble mound breakwater.
- Reshaped static stable berm breakwater: the profile is reshaped into a stable profile where the individual stones are also stable.
- Reshaped dynamic stable berm breakwater: the profile is reshaped into a stable profile, but the individual stones may move up and down the slope.

Most of the recent berm breakwaters constructed are designed as statically stable reshaped like Sirevåg or statically stable non-reshaped. Dynamic stable reshaped berm breakwaters should be avoided, because this may lead to excessive stone crushing, Tørum et al. (1999).

The most used parameters in relation to the stability and reshaping of berm breakwaters are the following:

Stability number,

$$Ho \equiv N_s = \frac{H_s}{\Delta D_{n50}}$$ (1)

Period stability number,

$$HoTo = \frac{H_s}{\Delta D_{n50}}\sqrt{\frac{g}{D_{n50}}}T_z$$ (2)

$$Ho\sqrt{To} = \frac{H_s}{\Delta D_{n50}}\sqrt[4]{\frac{g}{D_{n50}}}\sqrt{T_z}$$ (3)

$$To = \sqrt{\frac{g}{D_{n50}}}T_z,$$ (4)

$$\Delta = \frac{\rho_s}{\rho_w} - 1,$$ (5)

Gradation factor

$$f_{g=\frac{D_{n85}}{D_{n15}}}$$ (6)

where

H_s = significant wave height, W_{50} = median stone mass, i.e. 50% of the stones are larger (or smaller) than W_{50}, T_z = mean wave period, g = acceleration of gravity, ρ_s = density of stone, ρ_w = density of water.
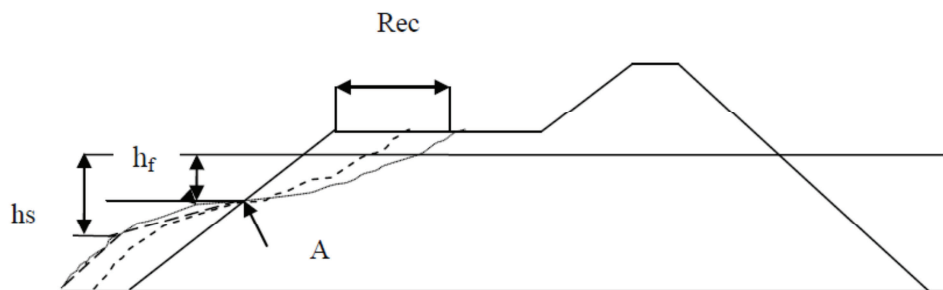
Figure 2. Recession in berm breakwaters

Tørum et al. (2003), Tørum (2007b) arrived at the following equation for the mean non-dimensional recession for berm breakwaters, with the results from the test on the model of the Sirevåg multilayer berm breakwater as the major data basis:

$$\frac{Rec}{D_{n50}} = 0.0000027(HoTo)^3 + 0.000009(HoTo)^2 + 0.11(HoTo)$$
$$- \left(f_{Dn}(f_g)\right) + f_d(\frac{d}{D_{n50}})) \frac{HoTo}{120} \tag{7}$$

Gradation factor function,

$$f_{Dn}(f_g) = -9.9f_g^2 + 23.9f_g - 10.5 \; for \; 1.3 < f_g < 1.8 \tag{8}$$

Depth function for $12.5 < d/D_{n50} < 25$,

$$f_d\left(\frac{d}{D_{n50}}\right) = -0.16\left(\frac{d}{D_{n50}}\right) + 4.0 \tag{9}$$

$$\frac{h_f}{D_{n50}} = 0.2\frac{d}{D_{n50}} + 0.5 \tag{10}$$

The stability criteria for different categories of berm breakwaters are in Table 2.

Table 2. Stability criterion for different categories of berm breakwaters for modest angle of attack, β0=±20° (the criterion depends to some extent on stone gradation). Partly based on PIANC 2003

Category	Ho	HoTo
Non reshaping	< 1.75-2.0	<30-55
Reshaping, static stable	1.75-2.7	55-70
Reshaping, dynamic stable	>2.7	>70

2.1 THE SIREVÅG BERM BREAKWATER

Sirevåg is small village (385 inhabitants in 2005) in the municipality of Hå, in the south-west of Norway, approximately 50 km south of Stavanger. Its industry is mostly related to fishery; consequently the harbour is a vital infrastructure for the inhabitants. This harbour is located in a narrow bay, without any reefs or shoals that give shelter from waves. In 2000-2001 a new breakwater was constructed to protect the harbour facilities and improve the sailing conditions. The breakwater has been exposed to several storms since it was built;

experiencing a smaller reshaping than what was expected from previous model tests.
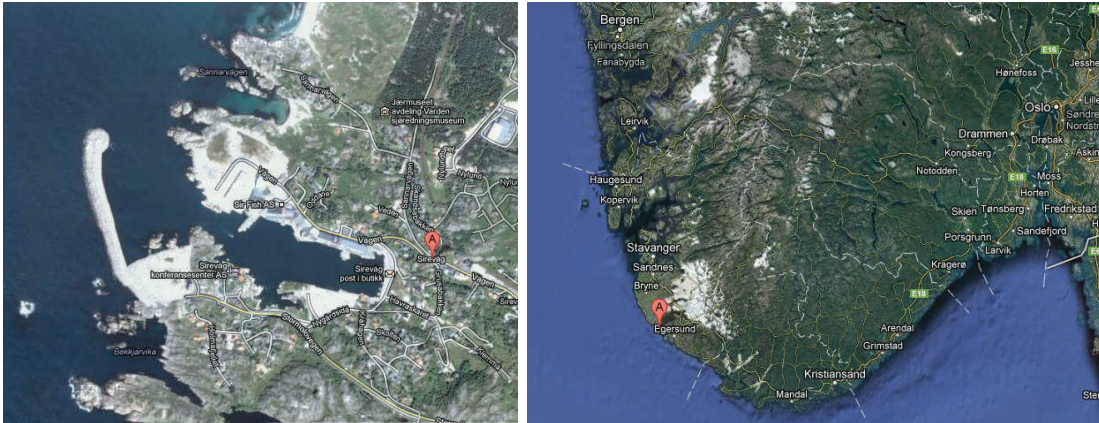
Figure 3. Sirevåg overview (maps.google.com)

The breakwater was designed as statically stable. It was designed with the 100 years return period wave height and it should withstand a wave height with 1000 year return period without total damage.

The cross section designed is the one in Figure 4.
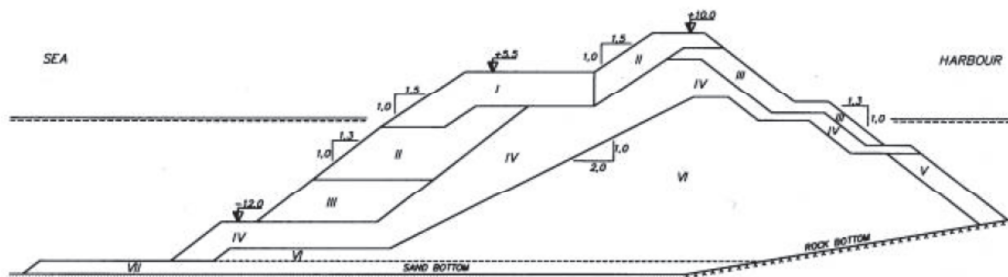
Figure 4. Cross section of the Sirevåg berm breakwater (Sigurdarson et al., 2006)

2.1.1 PHYSICAL CONDITIONS IN SIREVÅG

The design wave conditions for the Sirevåg Breakwater are listed in Table 3.

Table 3. Design wave conditions for the Sirevåg Breakwater

Recurrent period (years)	Significant wave height H_s (m)	Mean wave period T_z (s)
100	7.0	10.6
1,000	8.2	11.0
10,000	9.3	11.8

These design conditions were obtained from the hindcast studies and wave reflection analysis. The wave direction of the larger waves towards the outer end of the breakwater is estimated to be approximately normal to the longitudinal axis of the breakwater, (Myhra, 2005). The wave data was observed with a wave rider in a rather shallow water depth (17 m) close to the breakwater (Menze, 2000).

Wave measurements were started at the beginning of December 1998. Measurements were taken every half-hour. Two large storms with waves close to the design storm were recorded during the winter 1998 to 1999, on December 27th with H_s = 7.0 m and T_p = 14 s and on February 4th with H_s = 6.7 m and T_p = 15 s. (Sigurdarson et al., 2003)

The velocity of the current outside Sirevåg is not known, but some estimates of the current in the area based on the drift of floats were made by SINTEF in 1998. A maximum velocity of 0.20 m/s was observed during this short measurement campaign. Tidal variations in Sirevåg are based on a tide gauge in Stavanger. There are in the range of ±0.35 m around the mean water level. The maximum observed water level has been measured to 1.12 m above the mean water level, during storm surge. (Myhra, 2005)

3. EXPERIMENTAL SET-UP

The model tests were performed in the laboratories of NTNU/SINTEF in Trondheim. They were carried out in a two-dimensional wave flume with a length of 26.5 m and a width of 0.595m. A slope of 1:30 was constructed at the bottom. The maximum water depth at the flume at median water level was 59.5 cm, and at the breakwater model was 25.8 cm.

Seven resistant type wave gauges were installed, five at the bottom of the slope, one at the top and one in the middle on the slope. The wave gauge at the top was situated 1.60 m in front of the toe of the breakwater and the wave gauge in the slope at 4.40 m from the breakwater's toe. The bottom gauges have also a fixed position. In Myhra (2005) the wave gauges situated in deep water were placed with distance between them that changed with the wave length. Nevertheless, as a suggestion of the experts of DHI (Danish Hydraulic Institute), we decided to fix the position of them. The distances between them are:

Δl_{12}=40 cm, Δl_{13}=75 cm, Δl_{14}=100 cm, Δl_{15}=110 cm

Being the wave gauge number 1 the closest to the wave paddle. The wave gauge number five is situated at the bottom edge of the slope.
The use of five wave gauges at deep water has the purpose of separate the incoming and reflected wave spectrums. Then, determine the incoming wave properties and the reflection coefficient. This calculus was made by a computer program from DHI that also recorded all the wave data. The wave generator was also from DHI. All the tests were run with irregular waves.

The distance between the wave paddle and the centreline of the breakwater was approximately 19.05m. The distance between the wave paddle and the beginning of the slope was 6.60m and between the centreline of the breakwater and the absorption beach about 5.60 m. A sketch of the wave flume can be seen in the figure 5.
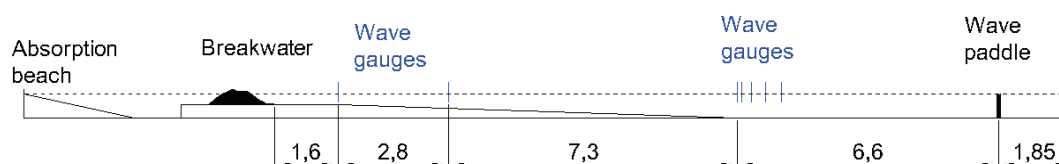
Figure 5. Experimental setup

The wave flume and some of the setting used are the same that Myhra (2005) used.

A laser was utilized to profile the breakwater before starting the wave runs and between each run. The laser was running on a beam placed over the breakwater and supported by a trolley that moved in the longitudinal and transversal axis automatically. In the first two setups, the scanner took samples with an interval of 5mm in profiles distant 5mm from each other. At the following setups the scanner accuracy was changed to interval of 10mm in profiles distant 5mm, because it had been seen that this accuracy was not necessary because the data had to be smothered afterwards. The data of these profiling was registered on a computer, and profile graphics were built.

4. THE BREAKWATER MODELS

Five different models were tested. All of them are variations of the profile of the Sirevåg breakwater, in which the armour stones had been replaced by concrete units. This change is made in order to test the possibility of building berm breakwaters with these characteristics at locations where larger rocks are not available or are difficult to acquire. More detailed plans of the models can be found in Appendix C.

In the first model, the class I stones and the class II stones of the crest that are in the Sirevåg breakwater profile, were replaced by concrete cubes. In order to maintain the Sirevåg breakwater profile, the armour layer had different thicknesses. The horizontal parts (crest and berm) had double layer of cubes while the slopes have one layer.

Concrete cubes   Class II rock   Class III rock   Class IV rock   Class V rock
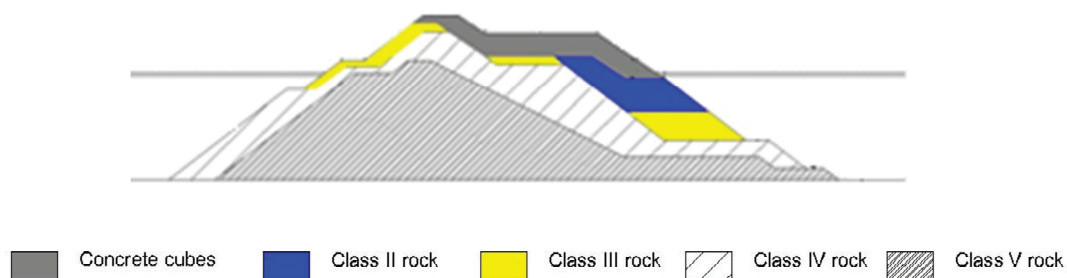
Figure 6. Prototype and model cross section of the breakwater in the setup 1.

In the second model, every rock from class I and II was replaced by two layers of concrete cubes.

Concrete cubes   Class III rock   Class IV rock   Class V rock

Figure 7. Prototype and model cross section of the breakwater in the setup 2.

Master Thesis, spring 2013   Altea Cámara Aguilera   NTNU

After testing the second model, we realized that the underwater berm was a weak point as it made the waves break in this point, producing higher erosion in this area. As a result, we decided to test a model with a profile mixture of model 1 and the model 2. This model had cubic blocks until 10 cm underwater (in model scale), but instead of the berm there was a continuous slope, as in the first model.

| Concrete cubes | Class II rock | Class III rock | Class IV rock | Class V rock |
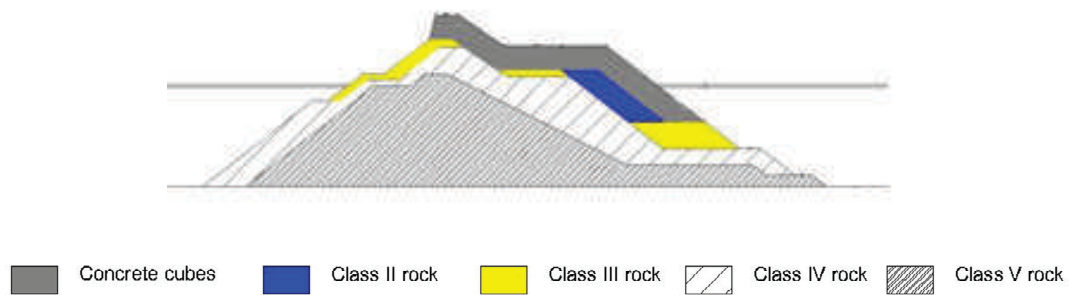
Figure 8. Prototype and model cross section of the breakwater in the setup 3.

The fourth and fifth models had the same profile as the third model but instead of concrete cubes, cubipods were used. The difference between models four and five was in the porosity of the armour layer (see 4.2 Armour porosity).

| Cubipods | Class II rock | Class III rock | Class IV rock | Class V rock |
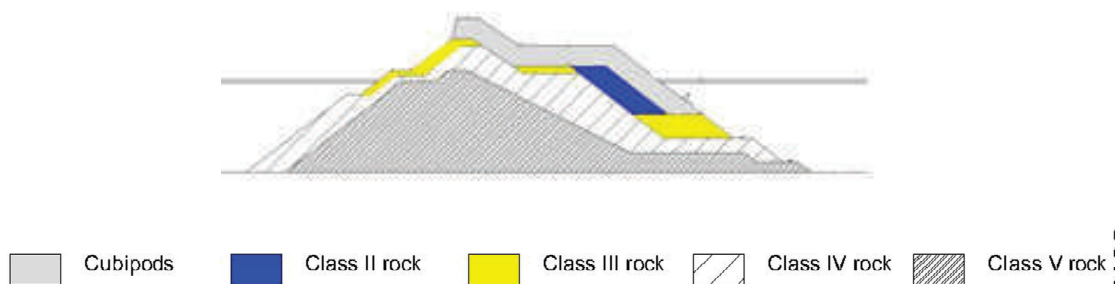
Figure 9. Prototype and model cross section of the breakwater in the setup 4 and 5.

4.1 MATERIALS

4.1.1 STONE MATERIALS

In general, multi-layer berm structures are build-up of several size-graded layers. The largest stones are placed on top of the berm and sometimes also at its front, where they are most effective in order to reinforce the structure. Smaller stones are used in the inner layers of the berm increasing the utilization of the quarried material. The reinforcement of the berm makes possible the reduction of the berm width, which reduces the volume of the structure. The use of larger stones more narrowly graded on top and at the front of the berm

has been proved in model tests to decrease reshaping of the berm (Sigurdarson et al, 2001).

The Sirevåg berm breakwater was constructed with seven different stone classes. The stone classes and quarry yield predictions for the first for classes are shown in table 4.

Table 4. Stone classes and quarry yield predictions at the Sirevåg berm breakwater

Stone Class	W_{min}-W_{max} (tonnes)	W_{mean} (tonnes)	W_{max}/W_{min}	d_{max}/d_{min}	Expected quarry yield
I	20.0–30.0	23.3	1.5	1.14	5.6%
II	10.0–20.0	13.3	2.0	1.26	9.9%
III	4.0 – 10.0	6.0	2.5	1.36	13.7%
IV	1.0 – 4.0	2.0	4.0	1.59	19.3%

Generally a distinction between core material, filter layer and armour layer can be done.

- The core material is made by stone classes VI and VII. In the models, only one stone class was used to build the core.
- The filter layer prevents the core material to mix with the armour layer. In this model it is made by stone class IV.
- The armour layer is made by stone classes II and III and the concrete blocks. This layer has the most important role in the experiment; therefore the different stone classes were coloured to better visualize their movements, yellow the class III and blue the class II.

The model has a scale of 1:70 as Menze (2000) and Myhra (2005). To build this model, the same stone class was used for class V and IV, because these layers are not decisive for this specific experiment.

The stone material used to construct our model is originally from the Fossberga quarries in Stjørdal. The density of the stones according with Menze (2000) was $\rho_s \approx 2700 kg/m^3$. The stone density corresponds also to the one in the prototype. The different stone weights in the model are shown in Table 5.

Table 5. Stone weights (Westeng, 2011)

Stone class	Model weights
I	0.058 – 0.087 kg
II	0.029 - 0.058 kg
III	0.012 – 0.029 kg
IV	0.0036 kg

Menze (2000) calculated the stone distribution of the stones class II and III. As can be seen in the figures at Appendix A, the distribution does not resemble the typical S-curve. Menze (2000) says that "this is caused by the procedure of picking the stones by hand and later by sorting them further into their corresponding class. Hereby stones shifted from smaller to bigger fractions and vice versa, causing the distribution curvature to flatten out."

Menze (2000) also calculated the volume reduction factor k from samples of 200 stones, defined as:

$$k = \frac{V}{V_{dim}} \tag{11}$$

Where

$$V = \frac{m_s}{\rho_s} \tag{12}$$

$$V_{dim} = l_s w_s h_s \tag{13}$$

m_s the mass of the single stone, ρ_s the density of the stones, l_s the length of the single stone, w_s the width of the single stone and h_s the height of the single stone.

The k value was 0.43 for the class II stones and 0.42 for the class III.

This factor says something about the void porosity in the armour layer that has an impact on the movement of the rocks. This was investigated by Newberry et al. (2002) that concluded that the typical porosity for double and single layers was 34% and that the placement method affects the porosity by 2-4%.

The effect of the rock shape in the reshaping was investigated by Frigaard et al. (1996). In this test no significant difference was observed between models with different stone types, both in reshaping and overtopping.

In this investigation, no further measurements over the stones used in the model were done.

4.1.2 CONCRETE CUBES

The concrete cube armour unit has many structural and logistic advantages, some of them are:

- it has a high structural strength
- it can be manufactured using efficient vertical formworks
- it can be handled with pressure clamps
- it does not require much space for manufacturing and stacking.

The concrete cubes used to construct the model were built in the laboratory. Fresh concrete was poured into rubber moulds with wanted shape. After one day the pieces were removed from its mould ready to be used.

These concrete cubes have a nominal diameter D_n=3.25 cm and a weight W=80g that corresponds in prototype to 2.275 m and 28 tones. The density of the concrete is 2.33 g/cm^3. In Appendix B there is more information about these values. With these values we obtain a design Ho of 2.313.

$$Ho = \frac{H_s}{\Delta D_{n50}} = \frac{7}{\left(\frac{2330}{1000} - 1\right) * 2.275} = 2.313 \qquad (14)$$

4.1.3 CUBIPODS

The cubipods are a recently developed armour unit developed to counteract the disadvantages of the cubic block while keeping its advantages (Pardo, 2012). We have listed some of the advantages of cubic blocks before. On the other hand, its main drawback is the tendency to face-to-face fitting that result in heterogeneous packing and loss of friction with the layer below.

The cubipod is a cubic element with protuberances on its faces. The protuberances must be small and robust to prevent breakage; the truncated square pyramid is ideal because it avoids the bending and twisting during the impacts that might occur during its construction and manufacturing while allowing for the use of efficient vertical forms. By maintaining a significant cubic core, it can be handled with pressure clamps and requires little stacking space. In addition, the small protuberances are similar in size to the gaps in the rocks of the lower layer, thereby increasing the friction of the armour layer with the lower filter layer. Cubipods can only be placed randomly (it is self-positioning) and can be used in the construction of one layer or two layer.
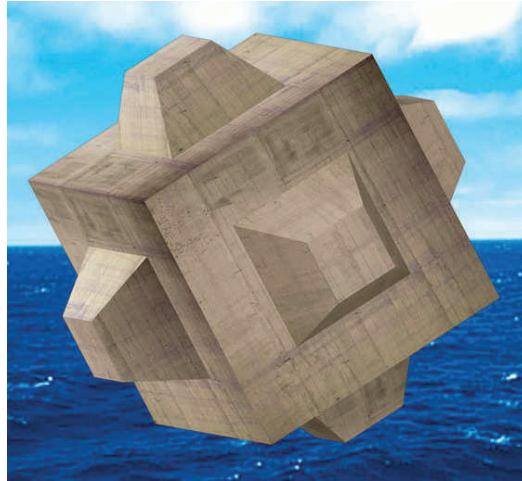
Figure 10. Cubipod (Cubípodo, 2013b)

Summing up, the advantages of the cubipod against the cube block are (Cubipod, 2013):

- Withstand higher drops
- Higher hydraulic stability in the roundhead and a much higher hydraulic stability in the trunk, without the problems of face-to-face fitting and heterogeneous packing.
- Lower overtopping rates

All the concrete units were manufactured in the laboratory, with the same procedure that the cubes. The cubipods used in the model have a nominal diameter D_n=3.10 cm and a weight W=61.75 g that corresponds in prototype to 2.17 m and 21.18 tones. The density of the concrete is 2.07 g/cm^3. In Appendix B there is more information about these values. With these values we obtain a design Ho of 2.313.

$$Ho = \frac{H_s}{\Delta D_{n50}} = \frac{7}{\left(\frac{2070}{1000} - 1\right) * 2.17} = 3.01 \qquad (15)$$

In some models, the concrete units were coloured depending on its position in order to better visualize the movement of the blocks of different parts.

4.2 ARMOUR POROSITY

Armour porosity affects energy dissipation, wave reflection, hydraulic stability, run-up, overtopping and heterogeneous-packing. The construction of armour layers at prototype scale is restricted and affected by available equipment, visibility, wind and waves, while small-scale laboratory construction is unrestricted with an optimal environment. Therefore the porosity value tested

in the laboratory has to be reachable in prototype construction. It has been tested that heterogeneous packing is more likely if actual armour porosity is higher than designed, and run-up and overtopping rates may increase when armour porosity decreases. Furthermore, armour hydraulic stability seems to significantly increase when armour porosity decreases, for massive, bulky and slender concrete armour units, as is the case of cubes and cubipods (Medina, 2010).

Medina et al. (2010) estimated achievable armour porosities at prototype scale. They used Cartesian Blind Placement System (CBPS) and small-scale crawler cranes in a wave tank to emulate realistic concrete armour units' placement at prototype scale. The maximum and minimum single-layer armour porosity estimated on 3/2 slope was 35%<p%<45% for cube armours and 37%<p%<51% for Cubipod armours. They also said that armour layers of conventional cubes placed randomly by hand are not realistic if porosity is p%<35% and have more hydraulic stability than the higher porosity armours which can be constructed with crawler cranes at prototype scale.

Thus, we can say that armour porosity is critical in the behaviour of marine structures built with concrete units. Consequently, the amount of blocks per row needed to have certain porosity was calculated beforehand to the construction of the models. This method allows controlling de porosity of the armour layer at the same time that controls the homogeneity of the armour layer. At each model, the following values were calculated at the concrete blocks layer.

- Layer porosity (p)

$$p = 1 - \frac{N\,Dn_{50}^2}{A_t} \tag{16}$$

N= number of blocks placed in an area A_t in one layer.

Dn_{50}= nominal diameter of the blocks

A_t= total area where the blocks are placed

- Packing density (ɸ)

$$ɸ = n\,(1 - p) \tag{17}$$

n= number of layers
- Placing density (φ)

$$φ = \frac{ɸ}{Dn_{50}^2} \tag{18}$$

These parameters have different values at each model (the location of the sections can be consulted in figure 10):

SETUP 1

		Area	N	Layer porosity	Packing density	Placing density
Two layers	Section 1	505.75	30	0.37	1.27	0.12
	Section 2	1666	100	0.37	1.27	0.12
	Section 3	255.85	15	0.37	1.27	0.12
One layer	Section 4	428.4	26	0.37	0.63	0.06
	Section 5	957.95	58	0.37	0.63	0.06
	Average			0.37	1.02	0.10
	Total	3813.95	375			

SETUP 2

	Area	N	Layer porosity	Packing density	Placing density
Section 1	702.1	35	0.48	1.04	0.10
Section 2	523.6	35	0.30	1.39	0.13
Section 3	1005.55	58	0.40	1.21	0.11
Section 4	1356.6	81	0.37	1.25	0.12
Section 5	1213.8	69	0.40	1.20	0.11
Average			0.39	1.22	0.12
Total	4801.65	552			

SETUP 3

	Area	N	Layer porosity	Packing density	Placing density
Section 1	714	46	0.320	1.361	0.129
Section 2	654.5	34.5	0.443	1.114	0.105
Section 3	1487.5	80.5	0.428	1.143	0.108
Section 4	1398.25	80.5	0.392	1.216	0.115
Section 5	714	46	0.320	1.361	0.129
Average			**0.381**	**1.239**	**0.117**
Total	4968.25	575			

SETUP 4

	Area	N	Layer porosity	Packing density	Placing density
Section 1	714	46	0.381	1.238	0.129
Section 2	654.5	34.5	0.493	1.013	0.105
Section 3	1487.5	80.5	0.480	1.040	0.108
Section 4	1398.25	80.5	0.447	1.107	0.115
Section 5	714	46	0.381	1.238	0.129
Average			**0.436**	**1.127**	**0.117**
Total	4968.25	575			

SETUP 5

	Area	N	Layer porosity	Packing density	Placing density
Section 1	535.5	37.5	0.327	1.346	0.140
Section 2	654.5	37.5	0.449	1.101	0.115
Section 3	1487.5	87.5	0.435	1.131	0.118
Section 4	1398.25	87.5	0.399	1.203	0.125
Section 5	714	50	0.327	1.346	0.140
Average			**0.387**	**1.225**	**0.128**
Total	4789.75	600			
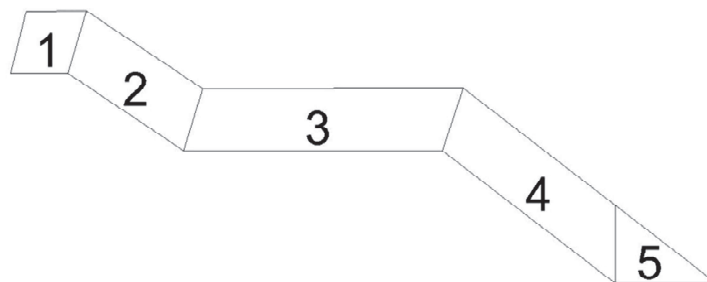
Figure 11. Location of the different sections of the armour layer

5. CONSTRUCTION OF THE MODEL

To begin with the construction of the breakwater models, the profile layers were drawn in the walls of the flume. Afterwards, the model was constructed by layers, starting for the deeper ones, making the top of each layer fit in the lines drawn on the walls. To help in this task, a flat wooden stick with a length equal to the flume width was used.

All the stones were placed pell-mell. The concrete blocks, cubes and cubipods, were placed one-by-one. The number of blocks in each row was calculated beforehand in order to acquire armour porosity similar to the ones acquired in the field. A first layer of concrete blocks was located and after that, a second layer was built over it. The blocks are located at chessboard order with reference to the rows next to them and over them. The blocks where placed by hand one by one. The positioning technic and the construction process were chosen in order to simulate the usual construction processes of breakwaters with concrete blocks.

The first rows of the concrete blocks layer are the most critical. If they are placed in an unstable position the stability of the whole structure will we lower, because the blocks will be easily displaced by the waves once they do not have support from the front row. Consequently, it is very important to place this row carefully. It is also important that the surface over which these blocks are placed is as regular as possible.

From the experience acquired during the construction and testing of these models, it can be said that the most stable way to place the first row of the second layer is in the holes existent between the first and the second row of the first layer (see figure 12). However, this is an issue that could be deeply studied. A change on the profile in order to increase the stability would be also recommendable. This issue is further discuss in Chapter 11, conclusions.

Figure 12. Detail of the placement of the first rows of concrete blocks

The same construction method was used in the construction of all the models.

Myhra (2005) studied the difference on reshaping of two models of the Sirevåg breakwater, one with pell-mell placed armour stones, and another with orderly placement. He concluded that no significant difference was found above -1 m of the Sirevåg breakwater. Nevertheless, no tests on this issue were made with concrete blocks.

6. WAVES

6.1 WAVES CALIBRATION

Before building the model in the flume and starting with the test, having the flume completely empty, some wave tests were run in order to measure the significant wave height produced with different amplitude factor of the wave paddle.

Afterwards the slope was constructed and the waves were calibrated again, obtaining the relation between the input and output wave height and wave period. The wave height was measured on the wave gauge situated at the top edge of the slope. The water level during these tests was 0.595m, the main water level. The output data was calculated by the down-cross method. This data can be seen in the table below.

Table 6. Input and Output values during wave calibration

Input		Output	
Tp [s]	Amplitude factor	Tp[s]	Hs[m]
1.29	0.054	1.272	0.0427
1.43	0.068	1.422	0.0574
1.57	0.087	1.563	0.0755
1.70	0.105	1.569	0.0931
1.84	0.118	1.837	0.1120
1.70	0.129	1.743	0.1163

The waves for these test and the ones after, are generated with the program provided by DHI. The wave spectrum produced followed a JONSWAP wave spectrum with a peak enhance factor of γ=2.2, the same as Myhra (2005). The JONSWAP (Joint North Sea Wave Project) spectrum is a well-known and much used spectrum. The JONSWAP spectrum includes the wind speed as the parameter for the purpose of wave forecasting, but can be rewritten according to Goda (2000) in an approximate form in terms of wave height, period and peak enhancement factor. The peak enhancement factor controls the sharpness of the spectra peak.

The input data for the wave program was:

- Peak period (T_p), different for each wave step
- Seed, 12345 for all the tests
- Amplitude factor, input significant wave height
- Duration, 1500 s

The duration of the calibration tests was decided to be the same as the duration used for the subsequent tests. The reason for that was that variations in the wave height are likely to occur when using the same wave parameters, but differences in the time series. This is due to the statistical variability on the random waves. Goda (1994) observed fluctuations owing to this phenomenon between a continuous 14 hours record and 27 segments of 30 minutes duration. Myhra (2005) made some experiments in order to control the variations in the wave series. He compared series of 25 minutes with five series of five minutes for different wave heights. He concluded that in order to know "exactly" the wave parameters, the wave analysis should be based on the whole time series, which are the 25 minutes time series.

6.2 WAVES IN THE MODEL TESTS

The wave conditions during the model tests are bases on the ones used by Myhra (2005), which are a slight modification of the ones used by Menze (2000). Menze (2000) based his test in previous test in EU research programs on berm breakwaters, as Tørum (1997). His tests had a target wave steepness of s_m=0.04, value that was observed during two major storms in Sirevåg during the winters of 1998/1999 and 1999/2000 (Menze 2000). Myhra (2005) changed the program of testing due to a stroke limitations of the wave generator. As the same wave flume and wave paddle than Myhra (2005) are used, the limitations are the same. With the first model, the same program that Myhra (2005) was followed. Then, it was observed that the values of Ho and To of the sixth step were lower than the ones at the fifth step. As these values are supposed to be proportional to the recession and be higher when the recession grows, it was decided that the sixth step will be done with an input value of Tp=1.84s, as at the fifth step. The same was applied to the last sub step at the seventh step.

In the next table, the wave inputs to the program are shown (in model scale).

Table 7. Wave inputs in the different setups and steps

	Step	Duration [s]	Setup 1		Setup 2,3,4 and 5	
			Tp [s]	Hs [m]	Tp [s]	Hs [m]
Water level 0.0 m	Step 1	1500	1.29	0.054	1.29	0.054
		1500	1.29	0.054	1.29	0.054
	Step 2	1500	1.43	0.068	1.43	0.068
		1500	1.43	0.068	1.43	0.068
	Step 3	1500	1.57	0.087	1.57	0.087
		1500	1.57	0.087	1.57	0.087
	Step 4	1500	1.70	0.105	1.70	0.105
		1500	1.70	0.105	1.70	0.105
	Step 5	1500	1.84	0.118	1.84	0.118
		1500	1.84	0.118	1.84	0.118
	Step 6	1500	1.70	0.129	1.84	0.129
		1500	1.70	0.129	1.84	0.129
0.014 m model (1 m prototype)	Step 7	1500	1.29	0.054	1.29	0.054
		1500	1.43	0.068	1.43	0.068
		1500	1.57	0.087	1.57	0.087
		1500	1.7	0.105	1.7	0.105
		1500	1.84	0.118	1.84	0.118
		1500	1.7	0.129	1.84	0.129

Every wave step was divided in 25 minutes tests in order to obtain the same values than during the calibration tests, as was explained before. Thus, the first 6 wave steps with about 2000 waves consist in two 25 minutes tests, one right after the other, while the seventh wave step consist in six tests of 25 minutes each.

The waves impacting in the breakwater were obtained with the data recorded by the five gauges situated at deep water. A reflection analysis was made, as explained in chapter 8, reflection. From this analysis, different parameters from the incoming wave spectrum were obtained, as the significant wave height in deep water, the mean wave period, the peak wave period and the number of waves. These data is registered in the tables at Appendix E. Afterwards, the shoaling effect due to the slope existing between the deep water wave gauges and the structure was calculated. Ks was extracted from the figure 13.
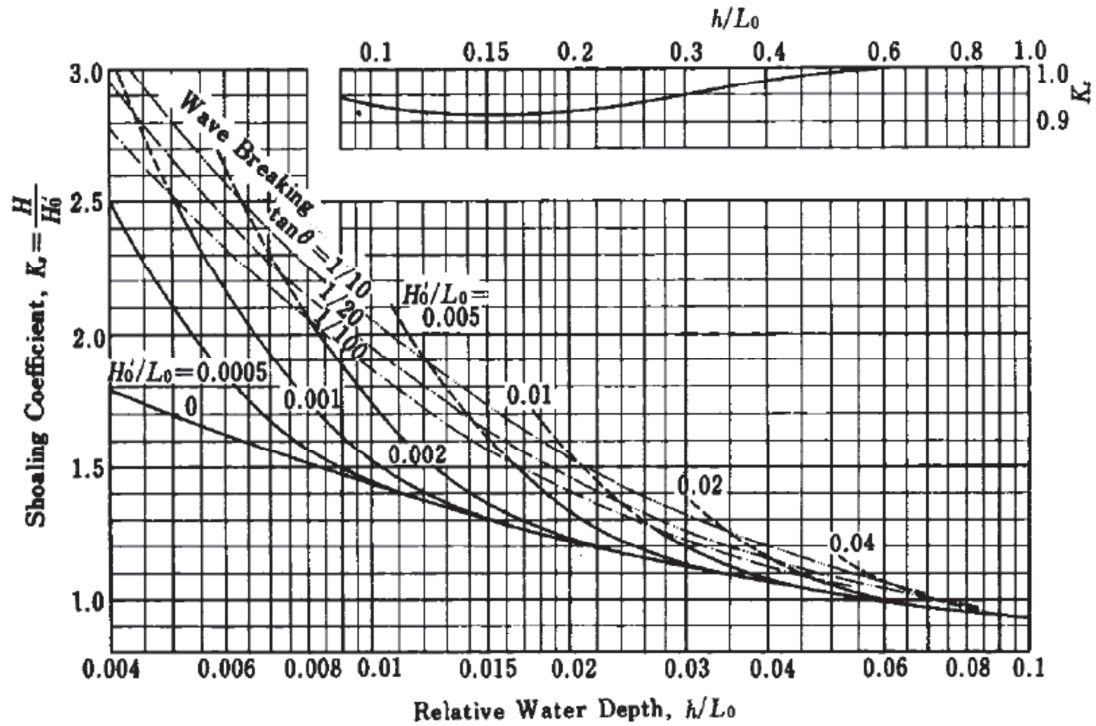
Figure 13. Diagram of nonlinear wave shoaling from Goda (2000)

The formulas used for the shoaling calculation were:

Wave length at deep water

$$L_0 = 1.56 Tz^2 \qquad (19)$$

Wave height impacting at the breakwater

$$H = K_s * H_0 \qquad (20)$$

7. RECESSION MEASUREMENT

At each setup, seven different wave steps were run, as described in chapter 6. The model was scanned before the test started and after each wave step in order to calculate the recession experienced at each wave step. With the data obtained, six profiles for each run were calculated. The profiles started at five centimetres from the walls and had a distance between them of 10 centimetres (see appendix D). First, an outer envelope was made through Matlab for each profile in order to eliminate the spikes. This envelope follows the original profile as the slope is positive or zero and keeps being horizontal at the height of the last peak when the slope in negative.
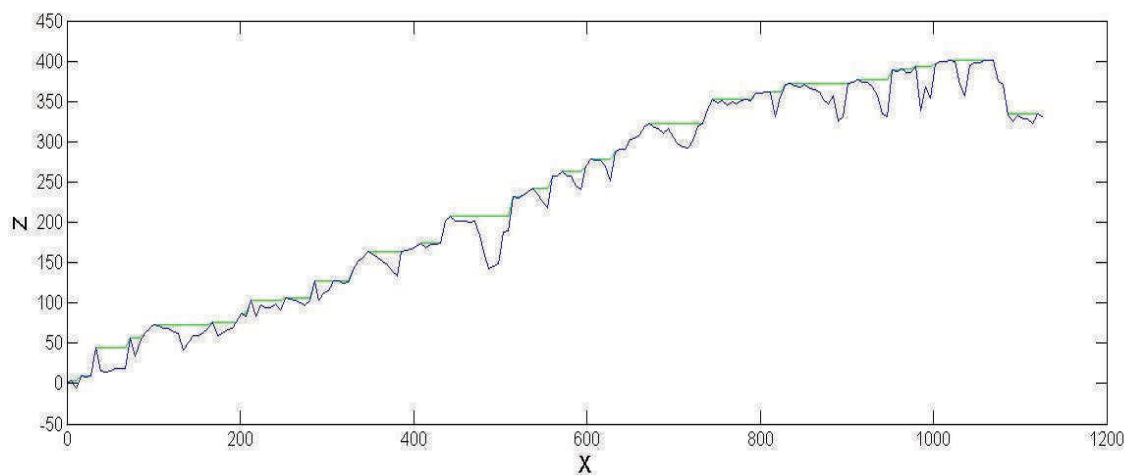
Figure 14. Measured profile in blue and envelope profile in green

Afterwards, the "x" values (longitudinal axis) were obtained for each 0.5 cm of height (z axis) by linear interpolation at each envelope profile. These values formed then the profile with which the recession will be calculated. Next, the recession was calculated by subtracting the "x" values of the profile of this step to the values of the initial profile (the one took before any wave step was run). Consequently, recession was obtained with a negative sign and accretion with a positive sign. The results were plotted in graphs like Figure 15.
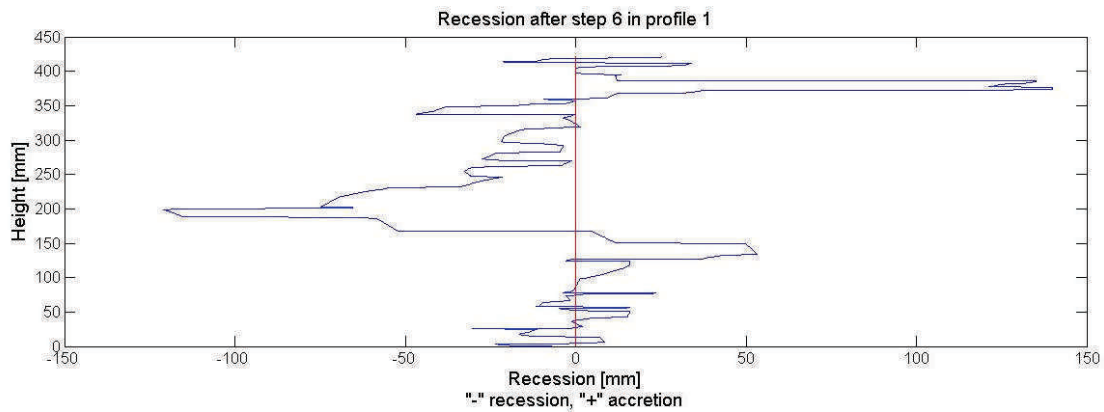
Figure 15. Example of a plot recession- height

The graph recession-height from the six profiles at all the models at different wave steps are illustrated in Appendix F.

At each of these plots, the maximum recession at each profile was measured. This value is the higher recession in within a peak of at least D_{n50}, as it is described in figure 16.
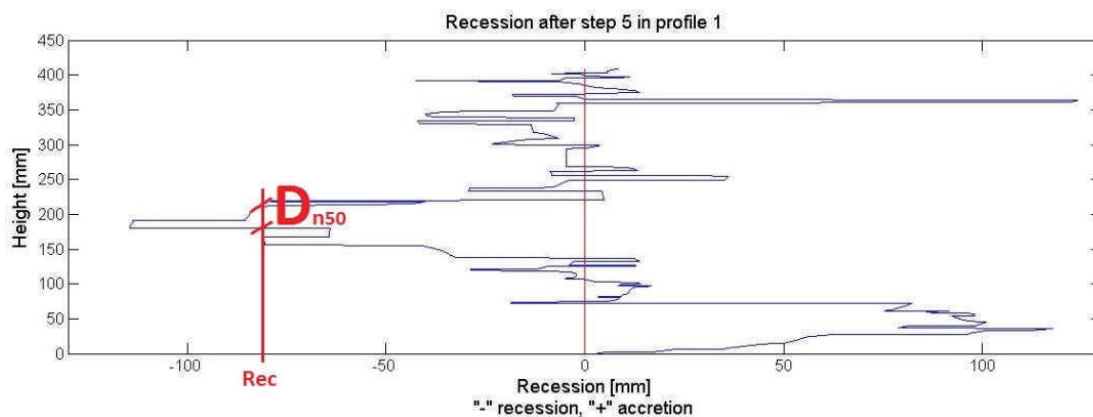
Figure 16. Example of the recession estimation method

The values of the recessions measured at each profile, step and model are listed in Appendix F.

This method of measuring the recession was used by Menze (2000), Myhra (2005) and Westeng (2011). The requirement for the recession to be at least D_{n50} was a step further from Tørum and Krogh (2000), where this type of diagram was first utilized in berm breakwater testing at SINTEF/NTNU (Westeng, 2011). The more general definition of recession is however that it should be measured at the top of the berm, as represented in the next figure:
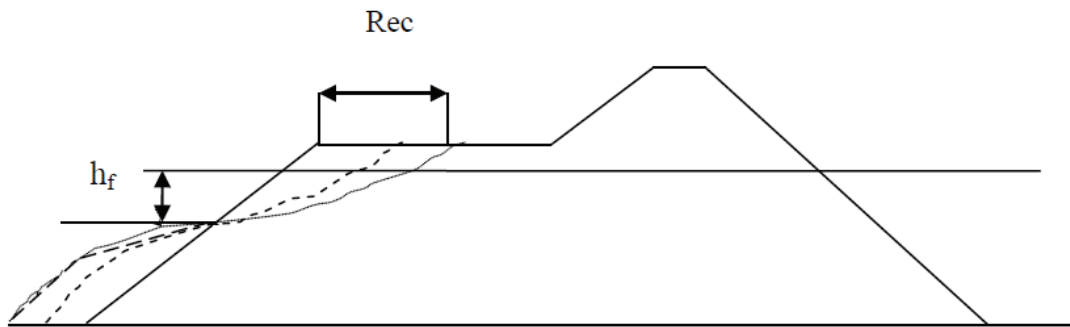
Figure 17. General definition of recession in berm breakwaters (Tørum 2011)

This method of calculating the recession is more objective than measuring it at the top of the berm. This is due to the pointy nature of the profile, because every profile has its own unique shape and to make objective guidelines for how to measure the recession at the top of the berm would be almost impossible. Furthermore, the berm of the models tested has not suffered the highest recessions, in general. As a consequence, the evaluation of the recessions at every high is unavoidable in order to know the real erosion in the breakwater.

An evaluation of the maximum erosion height is later developed at chapter 9.

8. REFLECTION

When a wave reaches an obstacle, as a beach structure, can be totally or partially reflected. All energy is dissipated, reflected or transmitted. The amount of energy reflected depends mainly on breakwater slope and wave steepness. If the slope is very gentle, energy is dissipated gradually due to friction with the bottom and to breakage. As the slope becomes steeper, the reflection increases. It is maximum for a vertical wall. If the slope is permeable, there is also dissipation due to friction and to transmission to the other side by flowing through the structure or overtopping.

The estimation of incident and reflected waves is a difficult problem that affects the physical results of laboratory experiments and the knowledge of the behaviour of marine structures. The main difficulty of the problem lies in the need to estimate the incident wave spectrum from the total wave field records that include the unknown reflection of the structure.

The methods that separate the incident and reflected waves in laboratory experiments with regular waves cannot be used with irregular waves because multireflection appears when using irregular waves. This happens because the wave packet reflected on the structure arrives to the wave paddle and reflected again on it as if it was another structure, adding difficulty to the problem.

The most of the analysis techniques are based on linear wave theory: they assume that an irregular wave packet can be represented by the superposition of a finite number of linear waves with different amplitude, phase and frequency, that impact at the structure and are reflected. Therefore, each linear wave can be treated separately with techniques developed for monochromatic packets.

The classical method for separating normal incident and reflected waves used in most laboratories is the two point method popularized by Goda and Suzuki (1976). The three point least squares method is the generalization by Mansard and Funke (1980) from the 2-point method when using three wave gauges. Goda and Suzuki (1976) built their work based on:

- Kajima (1969), who proposed a method using time series measurements at two points aligned in the direction of wave propagation. It assumes that the bottom is horizontal, and supports the validity of the linear theory. It expresses

the wave at each point as the sum of the different linear waves. Obtains the incident and reflected spectra from the spectra of each series and the cross-spectrum calculated with both signals.

- Thorton and Calhoun (1972). They performed a spectral analysis to obtain different wave components under the same assumptions as Kajima. They studied each linear wave separately and obtained the incident and reflected wave from the wave height at each point and the phase difference between the two signals. This method is not valid for frequencies whose wavelength L, verifies:

$$2\frac{\Delta l}{L} = n, n = 1,2,3 \ldots \qquad (21)$$

being Δl the separation between the wave gauges.

Goda and Suzuki (1976) introduced to the method of Thorton and Calhoun (1972) the algorithm of fast Fourier transform (FFT), to identify the two signals in each linear wave component.

The reflexion of each model was calculated using the tool WS Reflection Analysis from the software MIKE Zero. The data used as an input for the calculus was the one recorded by the five wave gauges situated in deep water. This software calculates incident and reflected wave spectra by frequency separation using at least squares fit approach. The calculus is based on the Goda and Suzuki method. The parameters calculated are:

- The average reflection coefficient:

$$C_R = \sqrt{\frac{\int_{f_{min}}^{f_{max}} S_R(f)df}{\int_{f_{min}}^{f_{max}} S_I(f)df}} \qquad (22)$$

Where $S_R(f)$ and $S_I(f)$ are reflected and incident spectrum, respectively.

- The significant wave height:

$$H_{m0} = 4\sqrt{m_0} \qquad (23)$$

- The mean wave periods:

$$T_{01} = \sqrt{\frac{m_0}{m_1}} \qquad (24)$$

Being

$$T_{02} \sim T_z T_{02} = \sqrt{\frac{m_0}{m_2}} \qquad (25)$$

- The spectral peak period:

$$T_p = \frac{1}{f_p} \qquad (26)$$

Where f_p is the frequency corresponding to the maximum spectral density.

- The spectral width or broadness parameter:

$$\varepsilon_4 = \sqrt{1 - \frac{m_2^2}{m_0 m_4}} \qquad (27)$$

The spectral moments (m_n) are defined as:

$$m_n = \int_{f_{min}}^{f_{max}} S_X(f) f^n df \qquad (28)$$

The reflection coefficients calculated for each model at each wave step are in table 8.

Table 8. Reflection coefficients

Step	Calibration without slope	Calibration with slope	Setup 1	Setup 2	Setup 3	Setup 4	Setup 5
1	0.078	0.103	0.288	0.179	0.282	0.233	0.267
2	0.084	0.115	0.313	0.215	0.306	0.286	0.299
3	0.091	0.126	0.344	0.267	0.352	0.317	0.294
4	0.121	0.106	0.351	0.319	0.376	0.33	0.296
5	0.165	0.113	0.333	0.337	0.37	0.317	0.318
6	0.152	0.117	0.299	0.32	0.35	0.278	0.31
7			0.211	0.261	0.239	0.191	0.246
			0.222	0.262	0.262	0.203	0.254
			0.244	0.267	0.295	0.211	0.272
			0.27	0.277	0.323	0.219	0.297
			0.294	0.291	0.342	0.223	0.318
			0.271	0.289	0.34	0.217	0.314
Average	0.115	0.113	0.287	0.274	0.320	0.252	0.290
Standard deviation	0.037	0.008	0.045	0.044	0.043	0.050	0.025

9. RESULTS

Five models were tested in total, three with concrete cubes in the armour layer and two with cubipods in the armour layer. Each model had a different profile and porosity, as is described in chapter 4.

9.1 VISUAL OBSERVATIONS

Pictures of the models after every wave step can be found in Appendix G.

Setup 1

- First wave step. Any movement can be seen neither in the concrete block nor in the rocks. The berm blocks have not got wet.
- Second wave step. Some stone and concrete blocks movement is registered. There is much more movements of rock II than of concrete blocks.
- Third wave step. The number of blocks moved is twice the number of blocks moved in the step before. The movement is more and less equal in the transversal axis.
- Forth step. The number of blocks moved keeps growing but with less intensity than in the step before. A gap is formed in the right side compared with the left side. That is, all the cubes located seawards from the berm on the right side are displaced, but most of them remain in their position on the left and centre parts. Almost any movement on the blocks of the berm is observed. Overtopping had started.
- Fifth step. The block's movement is higher in the centre part. The right side remains similar to the previous step, experiencing a few movements on the blocks of the first row of the berm. The left side suffer only minimal losses. Sixth step. The movement of concrete blocks highly increases compared with the class II rocks. Almost the totality of the cubes seawards the berm are displaced and an important amount of the first rows on the berm too. The recession is now more homogeneous at all the profiles. The blocks displaced are accumulated mostly on the low part of the front slope (from the centre of the slope to the bottom).
- Seventh step. No important changes can be seen. 12 more blocks are moved in this step.

Table 9. Blocks and rocks displaced during the test at setup 1

After step	Concrete blocks	Rock class II
1	0	0
2	6	25
3	20	50
4	37	65
5	49	70
6	76	85
7	88	97
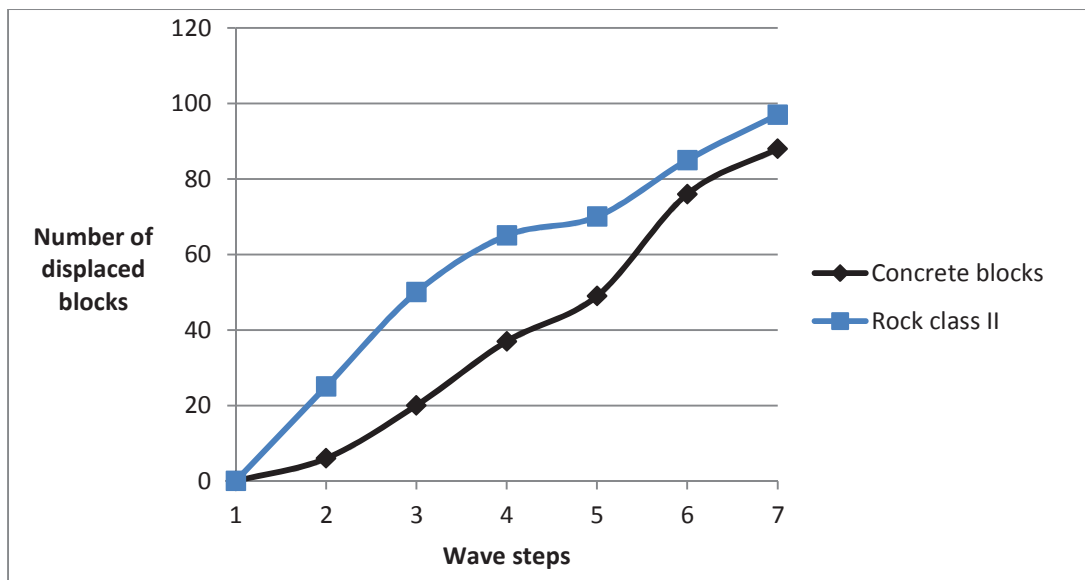
Figure 18. Blocks and rocks displaced during each wave step at setup 1

What we see in the graph is that the blocks displaced at each step are more and less constant, being at the earlier step a little higher. The rock class II follows more and less the same pattern.

Setup 2

- First wave step. 14 concrete blocks on the lower rows moved, probably due to instability in its placing.
- Second wave step. Only four more block are moved. The moved blocks are transported to the bottom.
- Third wave step. Seven more blocks are moved. The most of them are still from the lower rows. The movement are homogeneous in the transversal axis. Overtopping had occurred.
- Forth step. The number of blocks moved in this step is 10. Almost any movement at the blocks of the berm is observed. The most of the movements are still in the lower rows. Some rocks from the class II are

also moved. The erosion keeps being homogeneous in the transversal axis.

- Fifth step. The same erosion pattern is observed. In this step seven more blocks are moved.
- Sixth step. The number of blocks moved increases dramatically. In this step 55 concrete blocks are moved, making a total of 97 blocks in the 6 steps. The most of the new blocks displaced are from the upper layer of the lower slope. This upper layer is almost completely eroded. The blocks displaced are accumulated more and less homogenously over the lower slope. The erosion is lower in the columns closer to the left wall.
- Seventh step. No important movements are registered.

Table 10.Blocks and rocks displaced during the test at setup 2

After step	Concrete blocks	Rock III
1	14	0
2	18	0
3	25	0
4	35	15
5	42	20
6	97	28
7	101	28
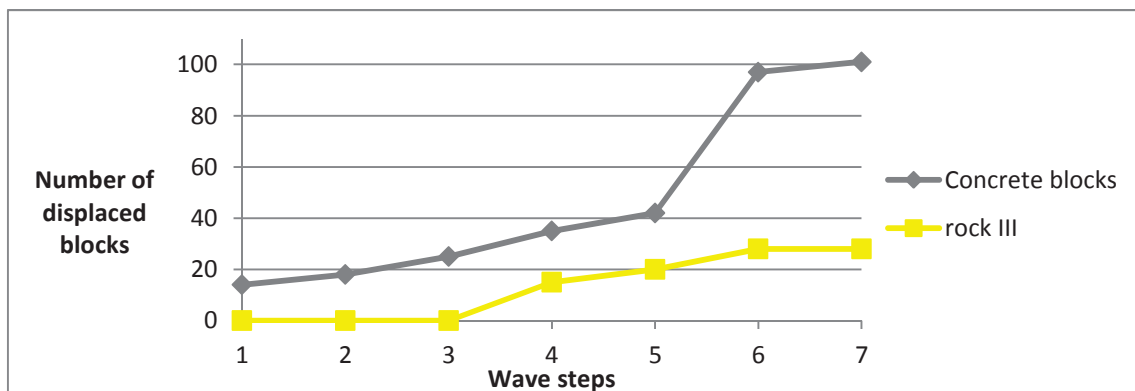
Figure 19. Blocks and rocks displaced during each wave step at setup 2

What we see in the graph is that the blocks displaced are more and less equal until the step 5. During the step 6 there is very high erosion and the amount of blocks increases dramatically. At the seventh step the erosion is minimal.

Setup 3

- First step: in the first 30 seconds, nearly all the movement are produced. 17 cubes from the first rows are moved, mostly from the first upper row.

This is due to instability in the placement of the cubes as this is the most fragile row because it does not have any support from the seaward side.

- Second step: the erosion is higher in the lower rows. This causes that the rocks on the slope slide resulting in the creation of some empty spaces in the slope. There are also 13 more blocks that are displaced from the slope.
- Third step: no much movement is observed. There are a few block sliding and only two more blocks are moved from the slope.
- Fourth step: the erosion starts to be more important in the higher rows of the slope, being more important in the right side. The left side does not undergo important changes. Therefore, the areas with more accumulation of blocks are the centre and right sides.
- Fifth step: the centre of the slope loses all the blocks of the upper layer, while the rest is not eroded as much. The moved blocks are displaced to the centre area of the lower berm. The first row of blocks of the berm is now exposed, but still any block has been significantly moved.
- Sixth step: the erosion of the upper layer continues being more important in the left side. 20 more blocks had been displaced. The blocks accumulated on the lower part are lifted by the waves during this test, but they are not displaced, they rest at the same spot when the wave leaves.
- Seventh step: almost no movement is observed. Any block of the berm has been displaced.

Table 11. Blocks displaced during the test at setup 3

After step	Concrete blocks
1	17
2	30
3	32
4	44
5	60
6	80
7	83
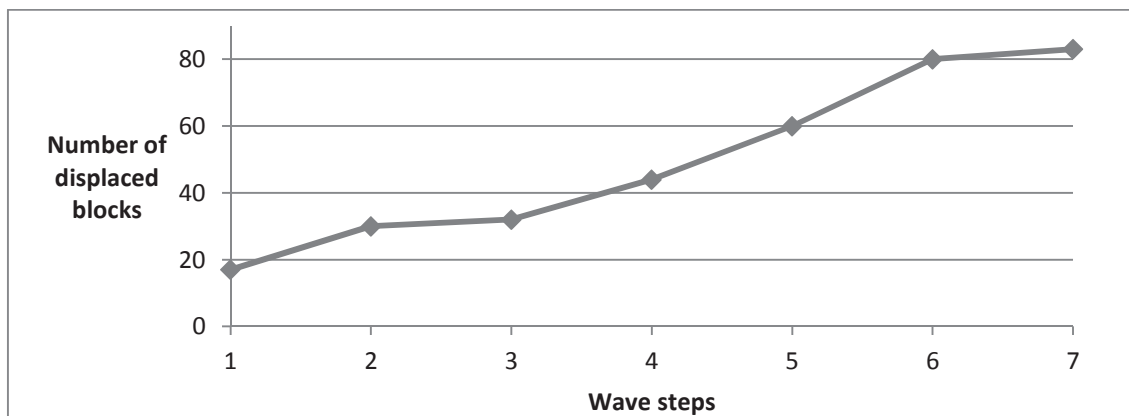
Figure 20. Blocks displaced during each wave step at setup 3

What we see in the graph is that the increase in blocks displaced is similar in the steps 3 to 6. In the step 3 and 7, there is almost no changes.

Setup 4

- First step: the most of the blocks displacément is done in the first minutes. Blocks from the first and second upper row are moved.
- Second step: the displaced blocks increase in 23. The most of them are from the upper layer. The erosion of this layer reaches the third row. It is slightly higher on the right side.
- Third step: large erosion on the right upper part of the slope. Almost all the upper layer blocks are displaced. Less erosion at the centre and left sides. 27 new blocks had been displaced, all of them from the upper layer.
- Forth step: the most of the erosion is this step occurs in the centre, where the rock layer below it is now visible. The upper layer of blocks of the slope is completely eroded in the right and centre parts. The berm blocks had not suffered any erosion yet. Overtopping is observed.
- Fifth step: the complete upper layer of blocks of the slope is displaced and most of the lower layer blocks of the upper part of the slope are also transported to the lower parts. There is still more erosion on the right side than on the left. Blocks from the upper layer of the berm are displaced for the first time (6 in total).
- Sixth step: the remaining upper blocks of the slope are displaced at the same time that the first rows of the berm (both layers). The rock below the blocks is now completely visible in the upper part. The blocks displaced are accumulated form the middle of the slope until the bottom.

Some very short rolling up and down of the already displaced blocks is observed.

- Seventh step: almost all the blocks of the berm are displaced now.

Green cubipods: upper layer of the front slope
Orange cubipods: upper layer of the berm
Grey cubipods: rest

Table 12. Blocks displaced during the test at setup 4

After step	Green cubipods	Grey cubipods	Orange cubipods	Total
1	12	1	0	13
2	30	6	0	36
3	57	6	0	63
4	72	18	0	90
5	117	43	6	166
6	127	100	24	251
7	127	120	64	311
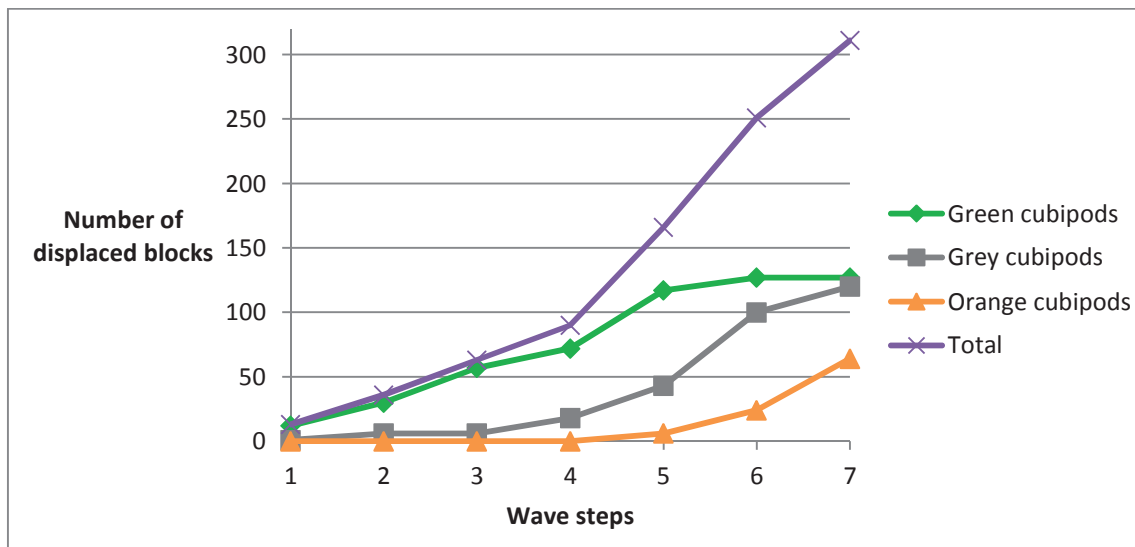
Figure 21. Blocks displaced during each wave step at setup 4

What we see in the graph is that the only blocks moved from the beginning are the green blocks, as they are the most exposed. The increase in green blocks moved is more and less constant until the fourth step. In the fifth step there is a higher increase and it is zero at the sixth and seventh step. The grey blocks start to have an important number of blocks displaced at the fourth step. The increase at each step after the fourth is higher than in the green blocks, reaching at the seventh step more and less the same number. The orange blocks do not suffer any movement until the fifth step, but the only important steps in

terms of number of displaced block are the sixth and seventh. Looking at the total blocks moved, there is and steady increase from step 1 to 4, and afterward the blocks displaced at each step rises to more that the double, being in the same range at the steps from 5 to 7.

Setup 5

- First step: only 6 blocks are displaced. All of them are from the first row. The displacement is produced in the first 30 seconds; therefore it is due to an instability placement during construction.
- Second step: 58 new blocks are displaced. The most of the movements are produced during the first 20 minutes. The erosion is higher on the right side, where most of the upper layer has been displaced.
- Third step: the erosion is higher in the left side now, being now more and less homogenous. The most of the upper layer blocks of the slope have been displaced, but only a few blocks from the lower layer.
- Fourth step: no much difference from the step before. Only 9 more blocks had been displaced, all of them from the upper layer. No movements of the blocks of the berm.
- Fifth step: Three blocks from the upper layer of the berm had been displaced. In addition to them, the last blocks from the upper layer of the slope had been displaced. During the tests, the blocks tend to be lifted by the waves and then lay on the same spot, without rolling up.
- Sixth step: only three new blocks from the lower layer of the slope are displaced. During the tests, the blocks tend to be lifted by the waves and a few of them are rolled, but in the same placed.
- Seventh step: only 3 more blocks are displaced.

Table 13. Blocks displaced during the test at setup 5

Step	Green cubipods	Grey cubipods	Orange cubipods	Total
1	5	1	0	6
2	50	14	0	64
3	90	18	0	108
4	101	18	0	119
5	117	18	3	138
6	117	20	3	140
7	120	20	3	143
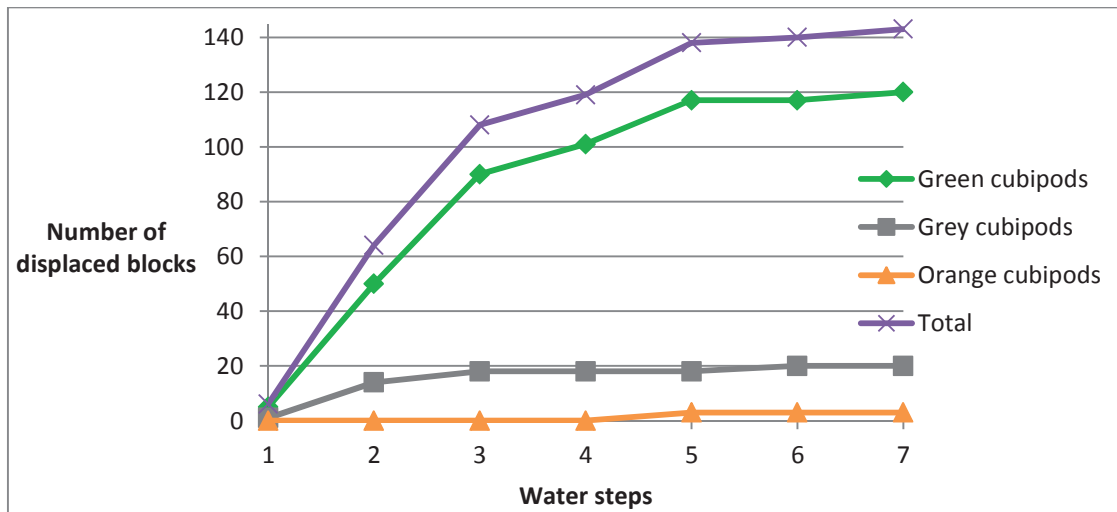
Figure 22. Blocks displaced during each wave step at setup 5

What we see in the graph is that the green blocks are the only ones with important displacement. The grey blocks only suffer and important displaced at the second step, and only three orange blocks are displaced at the fifth step. Therefore the total follows a similar path to the green blocks. This is important at steps 2 and 3 and relaxes at 4 and 5. After 5 the blocks displaced are almost 0.

9.2 WAVE MEASUREMENTS

The wave steps are supposed to be equal at the different setups, as they have the same inputs. Nevertheless there are small deviations in the values. All the values of the waves acting during the test are in Appendix E. The average values of the deep water wave height from the incident wave spectrum and the standard deviation for each wave step is shown in the table below.

Table 14. Average incident wave height at deep water and standard deviation, at model and prototype scale

Step	1	2	3	4	5	6
Average H_S [m], model scale	0.049	0.062	0.080	0.098	0.111	0.119
Average H_S [m], prototype scale	3.455	4.369	5.599	6.892	7.774	8.343
S^2	4E-06	1E-06	3E-06	1E-05	3E-06	1E-05

Table 15. Average incident wave mean period at deep water and standard deviation, at model and prototype scale

Step	1	2	3	4	5	6
Average T_z [s], model scale	1.03	1.13	1.23	1.34	1.45	1.45
Average T_z [s], prototype scale	8.65	9.46	10.33	11.22	12.14	12.17
S^2	4E-06	1 E-06	3E-06	1E-05	3E-06	1 E-05

The wave conditions correspondents to the 100 years recurrent period are approximately reproduced in the step 4 and the 1000 years recurrent period are approximately reproduced in the step 6.

9.3 RECESSION RESULTS

The recession calculation method has been explained in chapter 6. The recession-height graphs and all the recession values measured can be found in appendix F.

With the aim of compare equitably the different performances of all the models, their recessions have to be compared in the same terms of wave action, and block resistance capacity. With this purpose, the recession is plotted against the stability number (Ho), the period stability number (HoTo) and the square root period stability number (Ho√To). These parameters take into account the wave action, through the significant wave height and the mean period, and the characteristics of the armour blocks, through the density and the nominal diameter. The recessions of each profile and the averages at each wave step are plotted against the parameters previously mentioned.

Setup 1

Figure 23. Non-dimensional recession against stability number in setup 1. Profile values and average value at each wave step

Figure 24. Non-dimensional recession against period stability number in setup 1. Profile values and average value at each wave step

Figure 25. Non-dimensional recession against root square period stability number in setup 1. Profile values and average value at each wave step

We can see in the results that, as it has been mentioned before, the wave parameter of the step 6 (with an orange average point) does not follow the increasing tendency. This is corrected in the following setups by increasing the peak period at the step 6. This incoherence does not affect significantly to the calculation of the trend line that will be shown afterwards.

Setup 2

Figure 26. Non-dimensional recession against stability number in setup 2. Profile values and average value at each wave step.

Figure 27. Non-dimensional recession against period stability number in setup 2. Profile values and average value at each wave step

Figure 28. Non-dimensional recession against root square period stability number in setup 2. Profile values and average value at each wave step

The results obtained in this setup do not follow the same behaviour that the other models. An explanation is that the underwater berm is a weak point and made the waves break in this point, producing higher erosion in this area. This model experiment helped to develop a better profile, nevertheless, the results

of this setup are not going to be further analysed because they do not have relevance on the study.
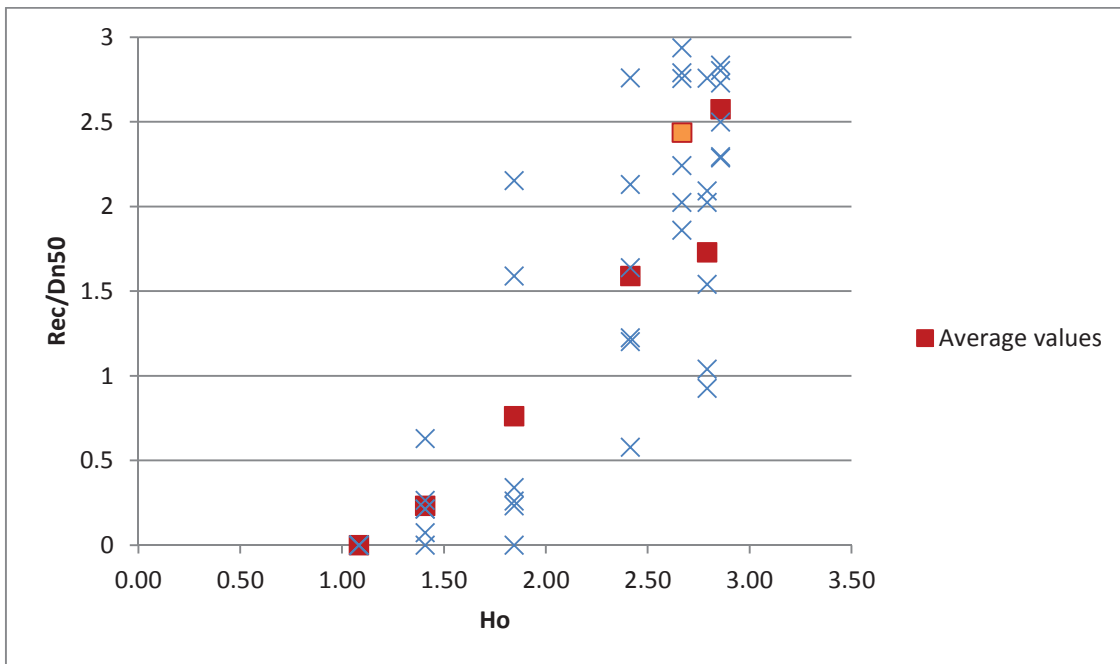
Setup 3

Figure 29. Non-dimensional recession against stability number in setup 3. Profile values and average value at each wave step
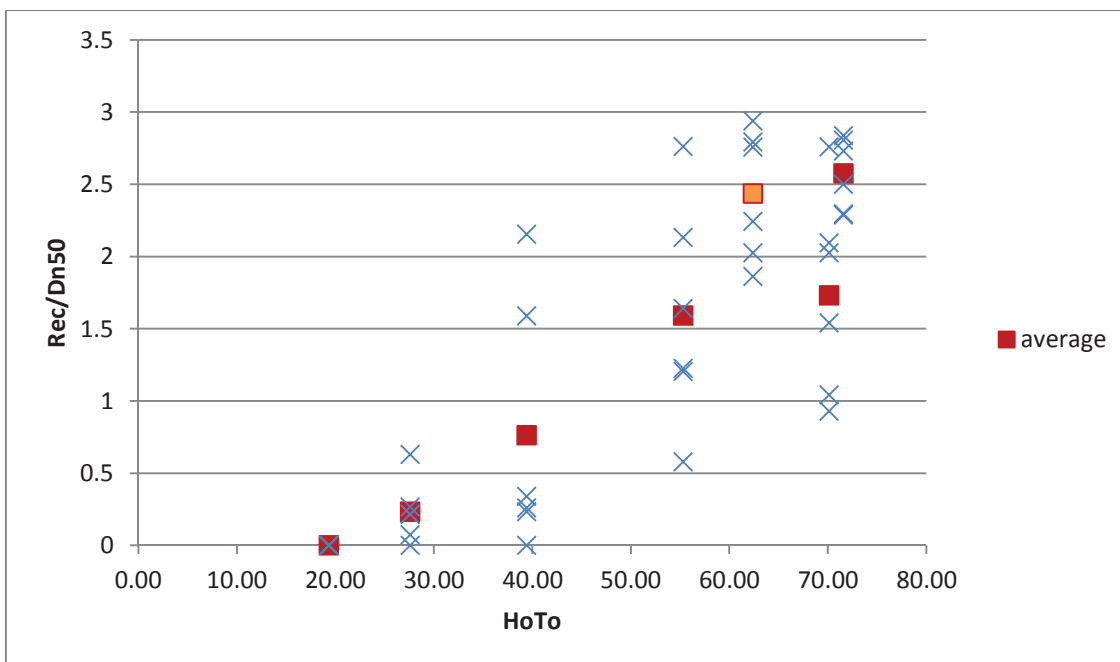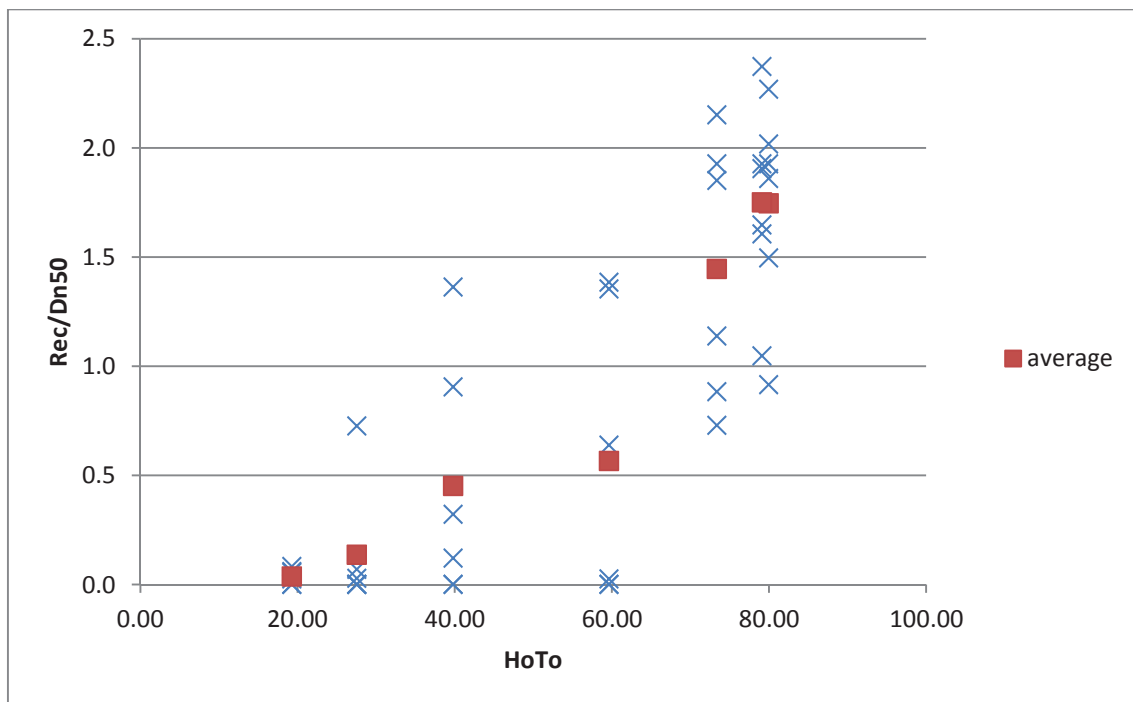

Figure 30. Non-dimensional recession against period stability number in setup 3. Profile values and average value at each wave step
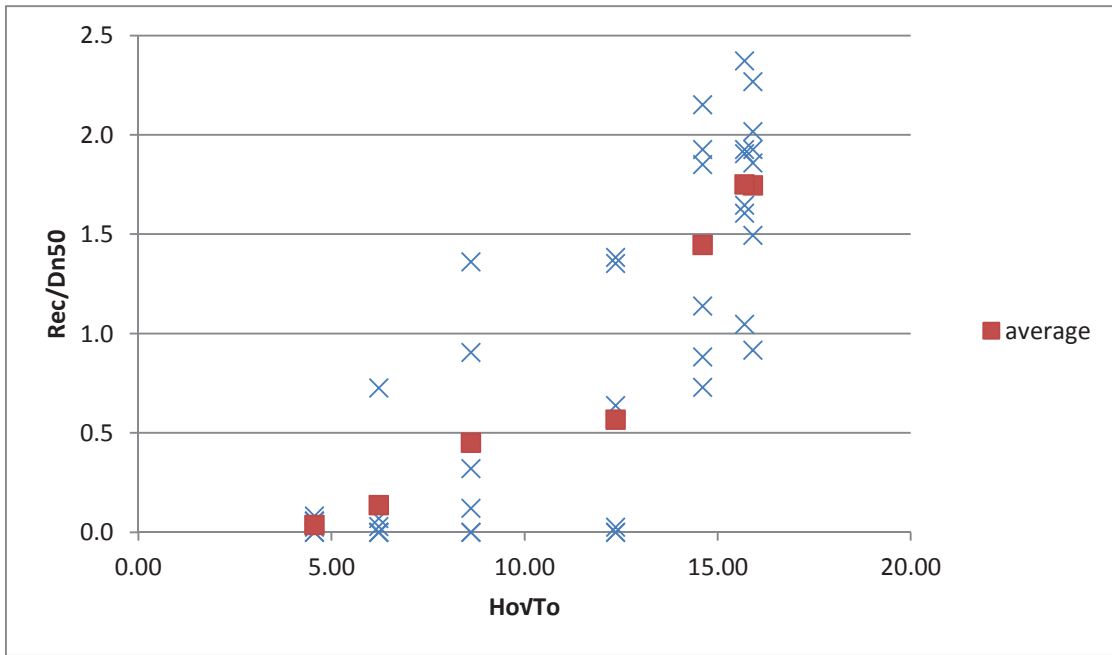
Figure 31. Non-dimensional recession against root square period stability number in setup 3. Profile values and average value at each wave step

The graphs show an approximately steady increment of the recession, except for step 4 and 7. At these steps the increment of recession is very small.

Setup 4
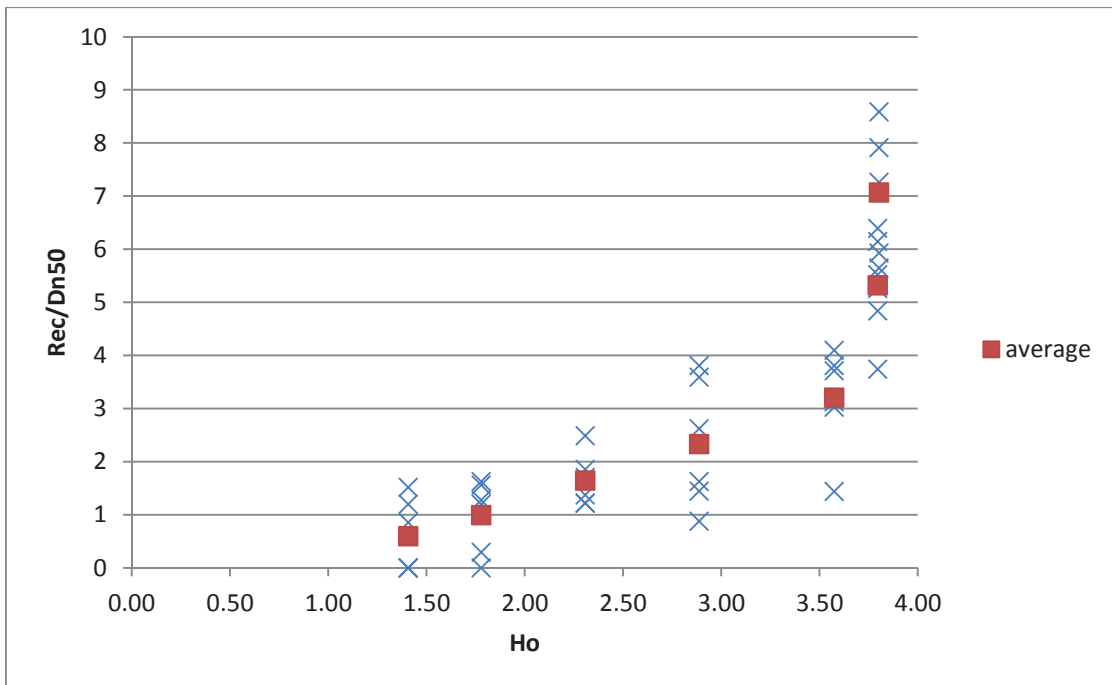
Figure 32. Non-dimensional recession against stability number in setup 4. Profile values and average value at each wave step
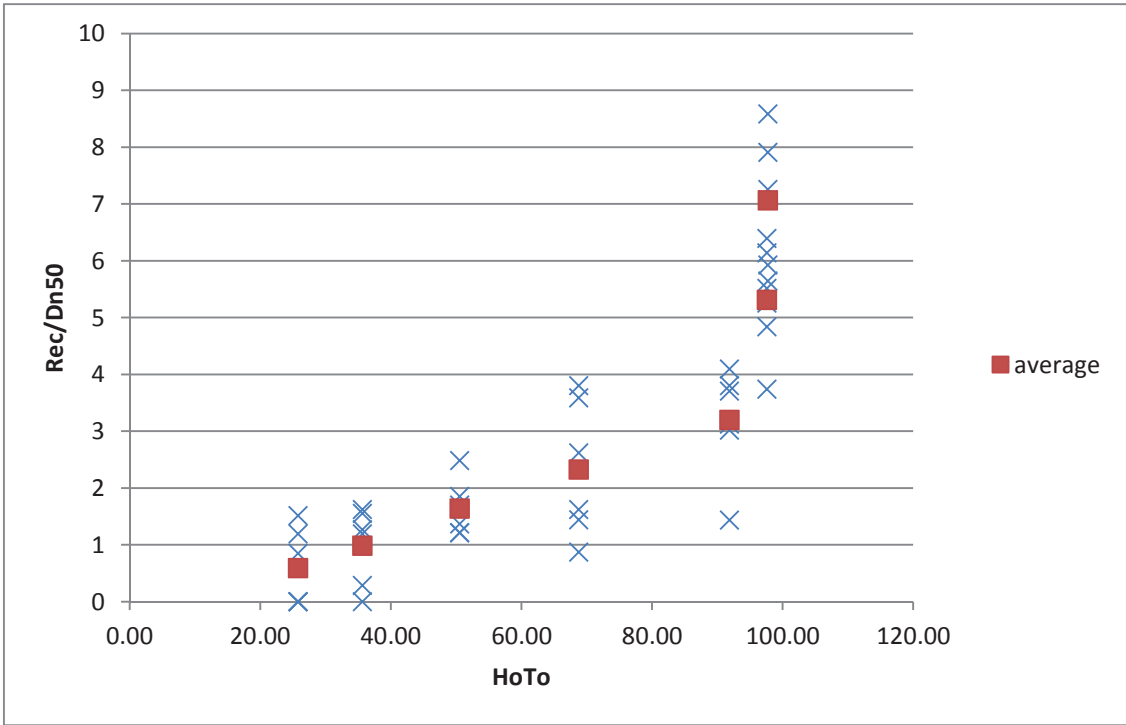
Figure 33. Non-dimensional recession against period stability number in setup 4. Profile values and average value at each wave step
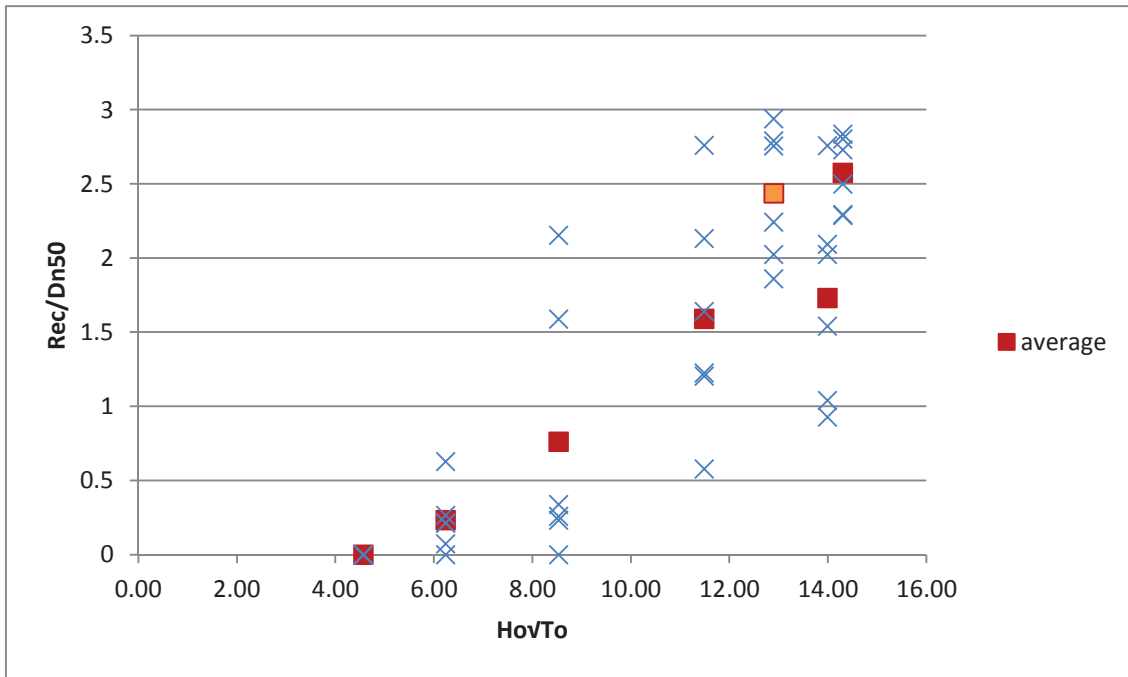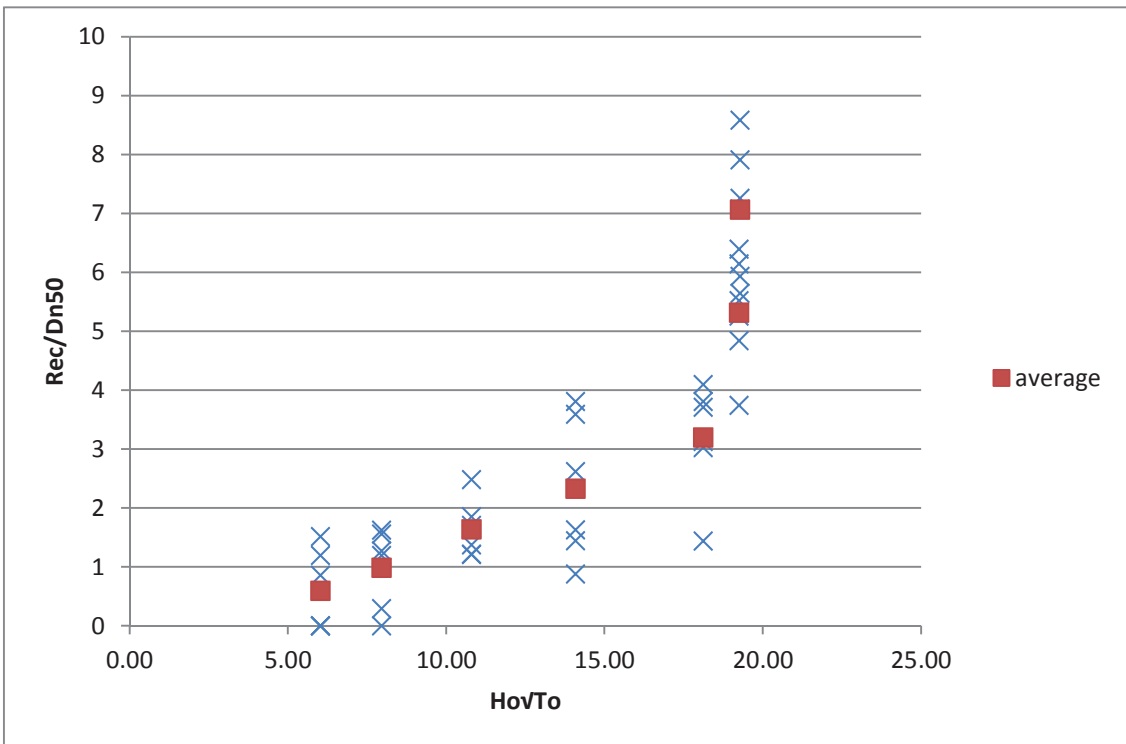

Figure 34. Non-dimensional recession against root square period stability number in setup 4. Profile values and average value at each wave step

We can see that there is and steady increase from step 1 to 5. At steps 6 and 7, with a lower increment of wave height and period, the model experience a much higher recession (more than double) than at the steps before.
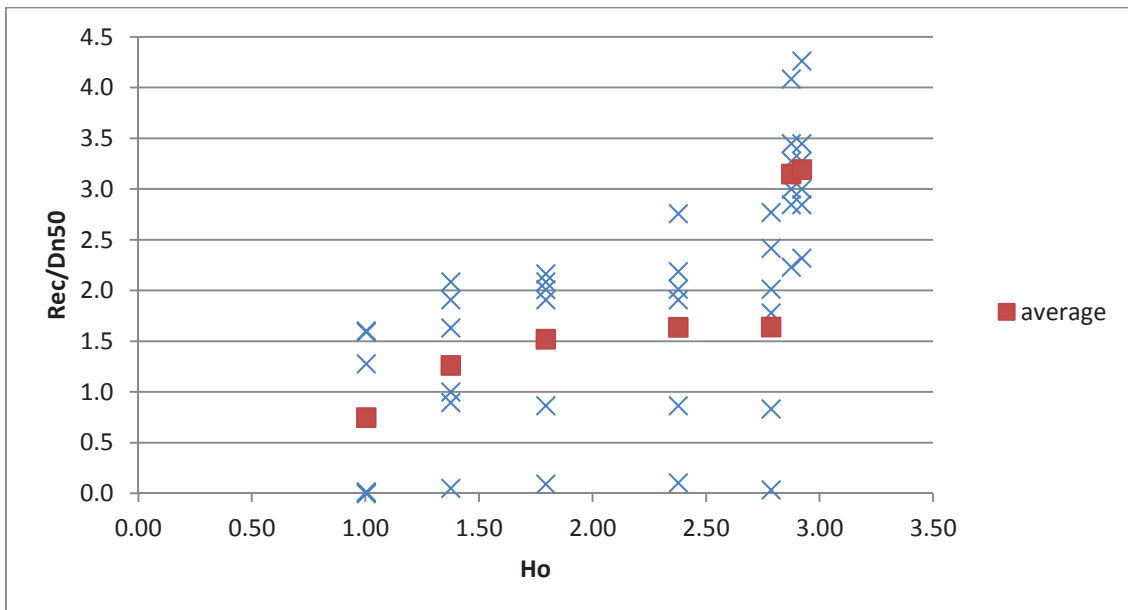
Setup 5
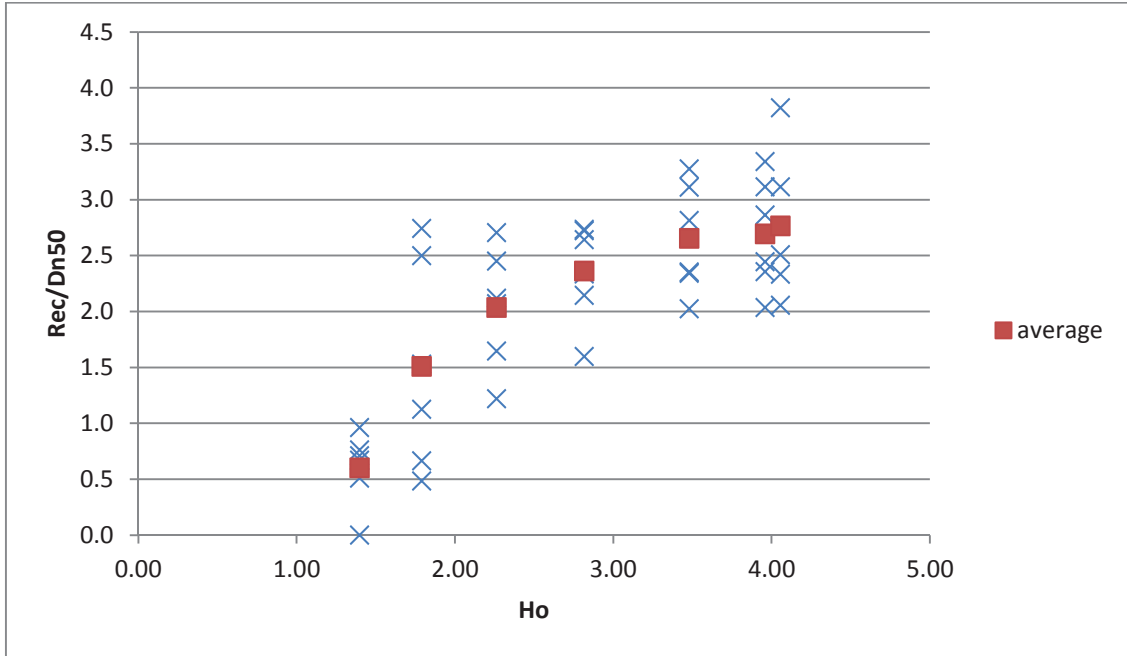
Figure 35. Non-dimensional recession against stability number in setup 5. Profile values and average value at each wave step
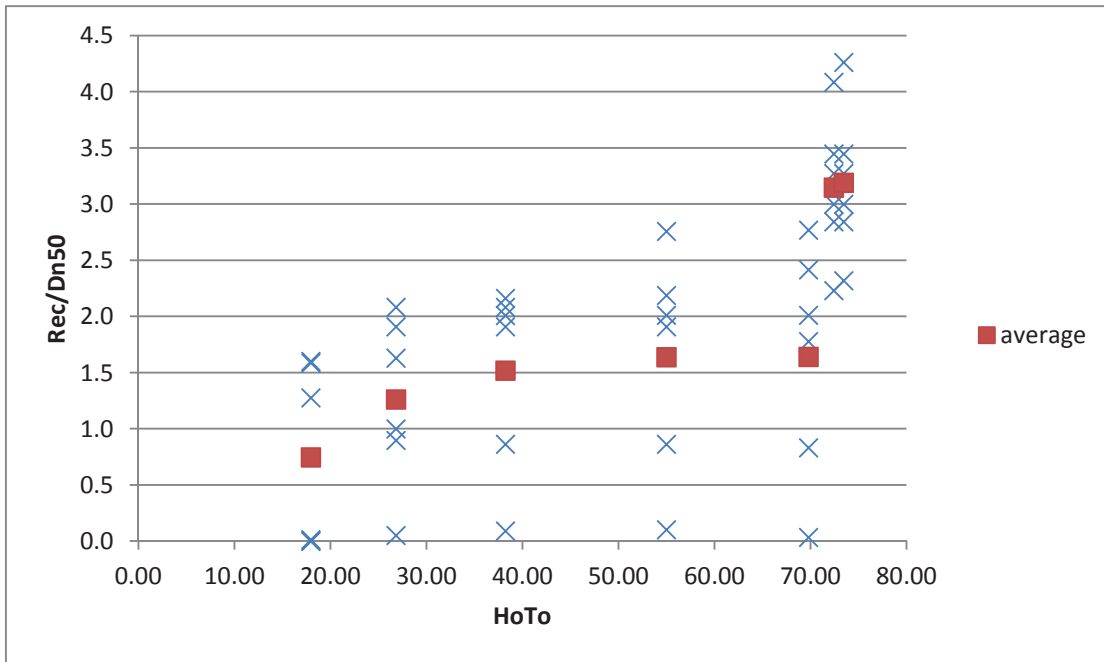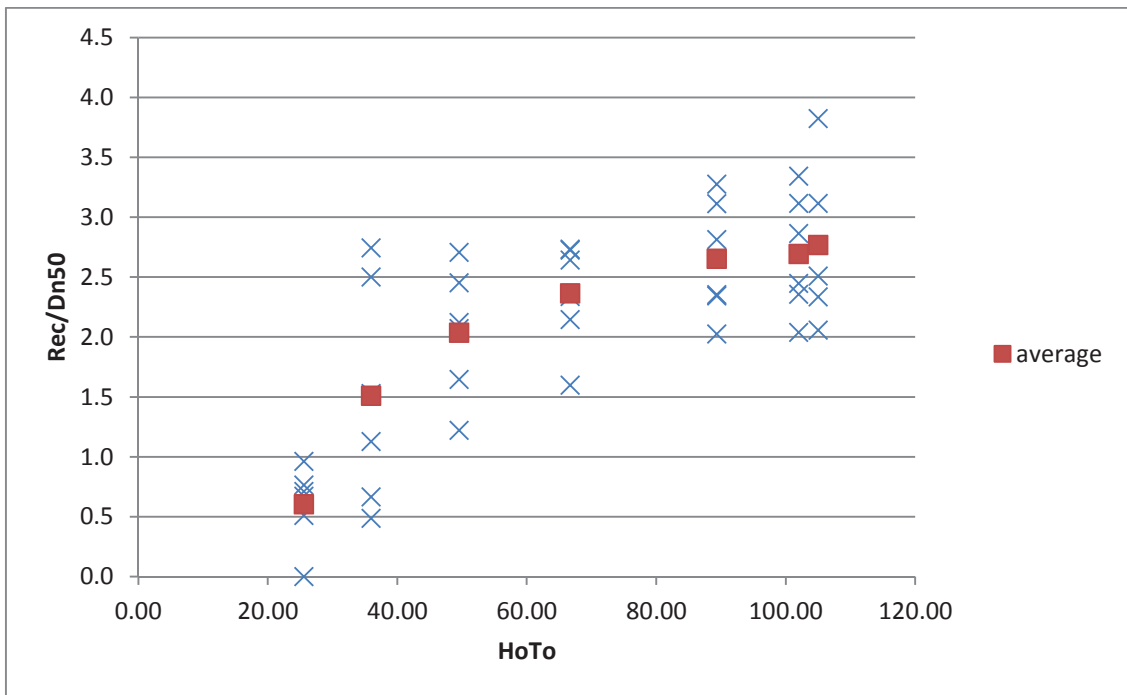

Figure 36. Non-dimensional recession against period stability number in setup 5. Profile values and average value at each wave step
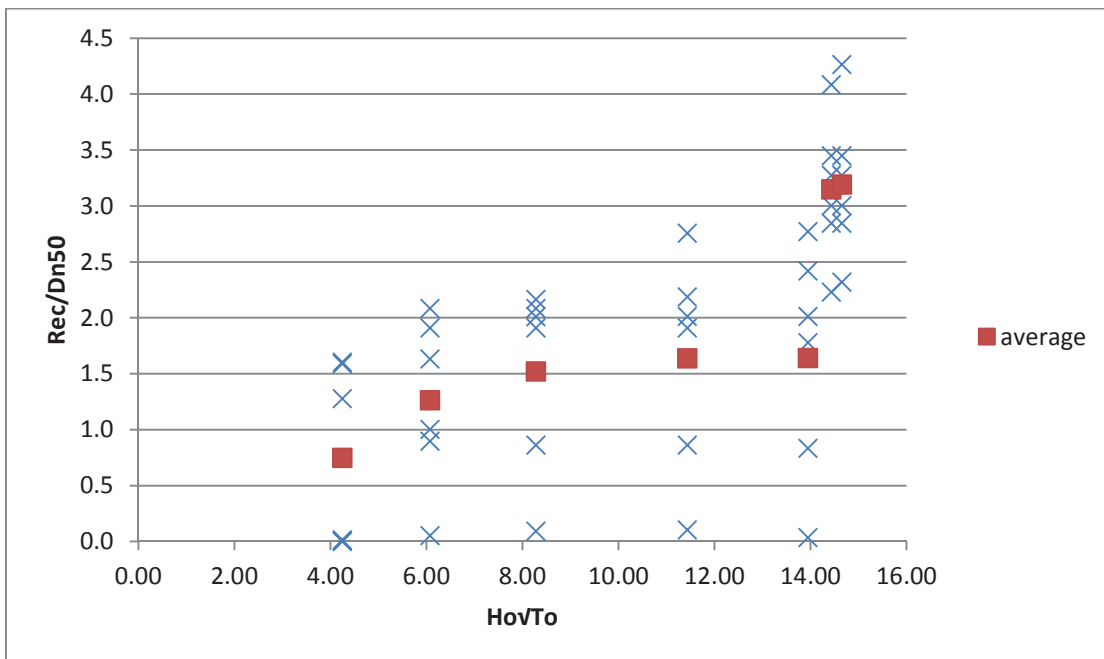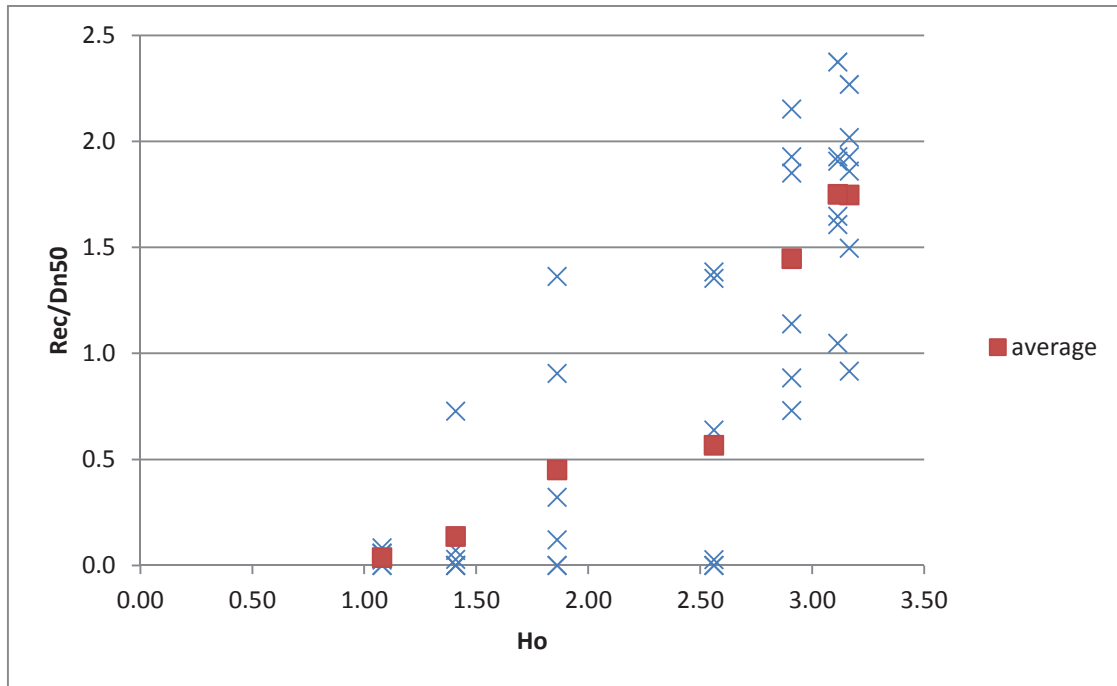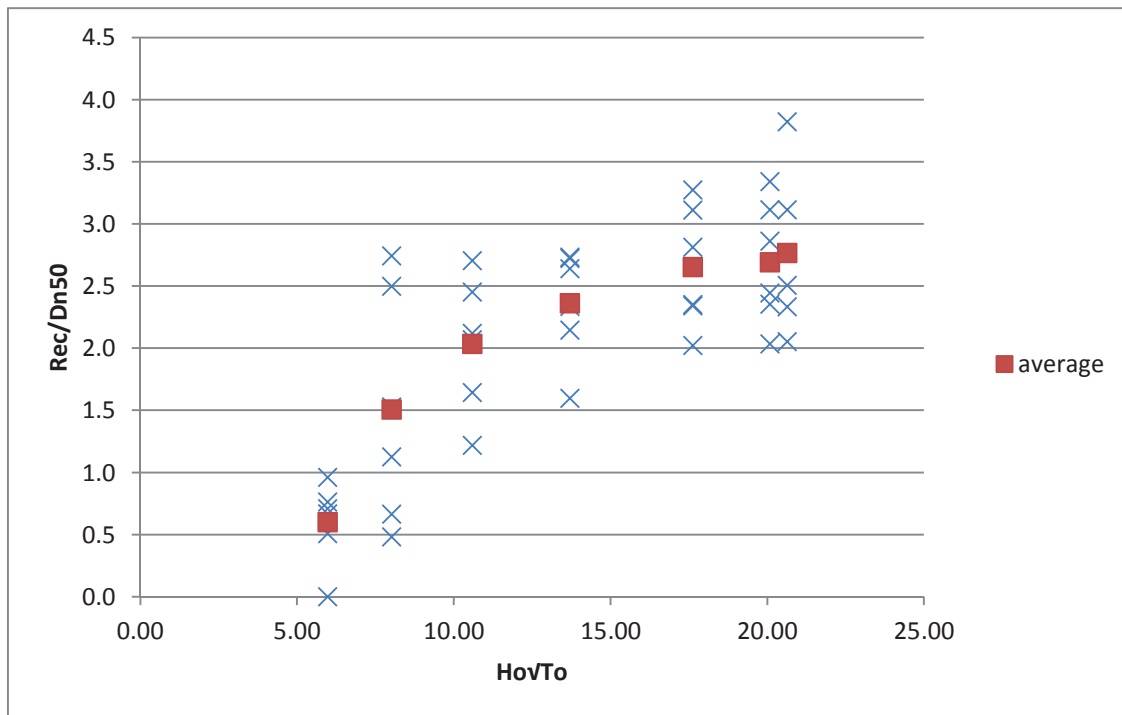
Figure 37. Non-dimensional recession against root square period stability number in setup 5. Profile values and average value at each wave step

We can see on the graphs that the recession is higher at the first steps, being lower as the wave steps are growing. After step 5, the model seems to have reached equilibrium because there is almost not more recession, even when the wave steps are more aggressive.

9.3.1 TRENDLINES

Originally it was planned to build second order polynomial trend lines, but they do not fairly represent the behaviour of the recession. The cause of this is that the curves have an inflexion point after which the ratio Rec/D_{n50} is reduced for a growing Ho. This reduction in recession when the waves are growing is not a behaviour that has been observed in the models. Owing to it, a different function was used. This is increasing for all the values of x.

The function used is:

$$y=K1*(x-K2)^{K3}$$ (29)

Where y= Rec/D_{n50}

x= Ho, HoTo or HoVTo

K1, K2 and K3 = constants
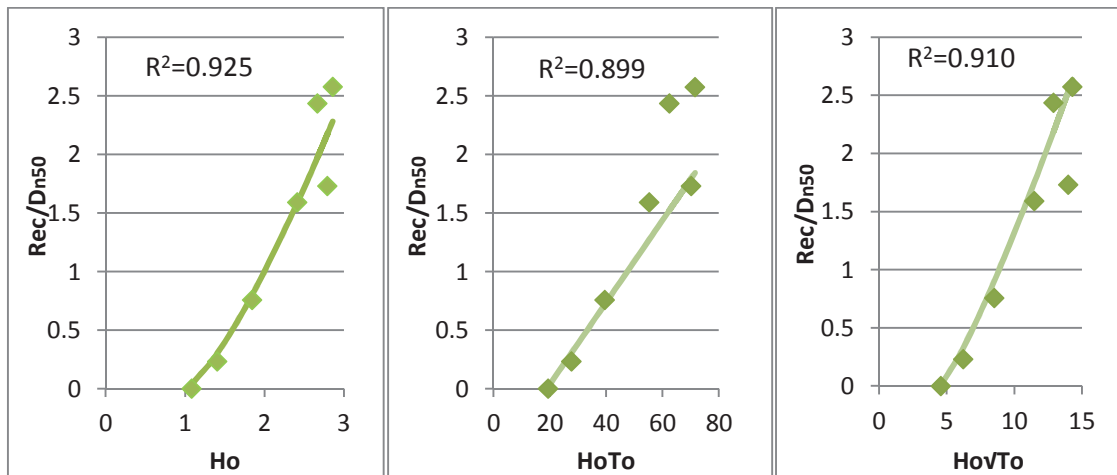
Figure 38. Average values of recession over nominal diameter against different stability parameters at each wave step and their trend lines. Setup 1

$$\frac{Rec}{D_{n50}} = (Ho - 1)^{1.33} \tag{30}$$

$$\frac{Rec}{D_{n50}} = 0.035(HoTo - 19) \tag{31}$$

$$\frac{Rec}{D_{n50}} = 0.17(Ho\sqrt{To} - 4.5)^{1.2} \tag{32}$$

These funtions represent very close the behaviour of a berm breakwater with this profile and material properties. They are convex increasing continuous in the interval from the lower value of x (Ho, HoTo or Ho√To) until the positive infinitive. For lower values of x, the value Rec/D_{n50} is negligible. The HoTo and Rec/D_{n50} have a linear relation. Is important to say that the incoherence of the point of the sixth step were the "x" is lower, does not affect significantly to the calculation of the trend line.

Setup 3
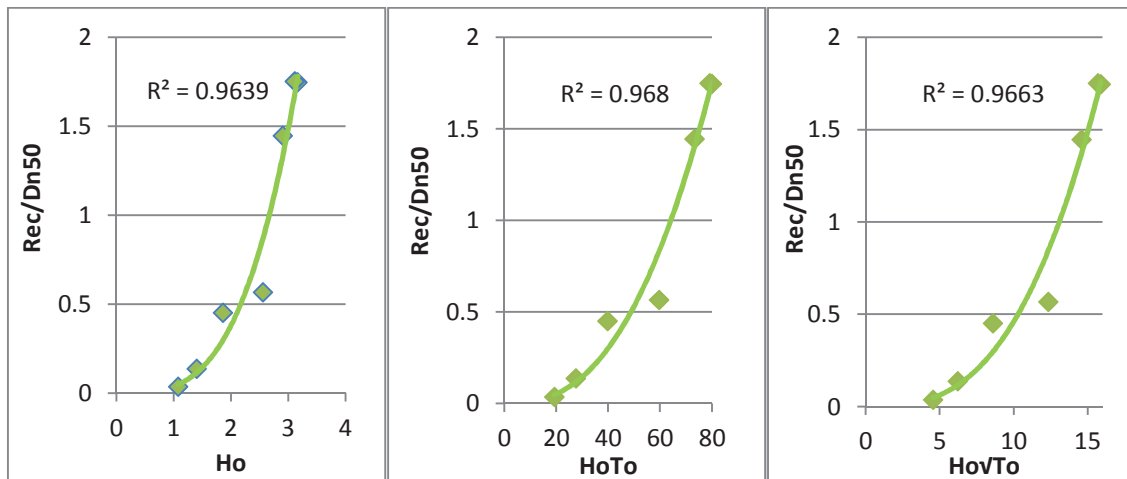
Figure 39.Average values of recession over nominal diameter against different stability parameters at each wave step and their trend lines. Setup 3

$$\frac{Rec}{D_{n50}} = 0.037(Ho)^{3.37} \tag{33}$$

$$\frac{Rec}{D_{n50}} = 0.00003(HoTo)^{2.54} \tag{34}$$

$$\frac{Rec}{D_{n50}} = 0.0006(Ho\sqrt{To})^{2.9} \tag{35}$$

These functions represent almost exactly the behaviour of a berm breakwater with this profile and material properties. They are convex increasing continuous to every positive value of x (Ho, HoTo or HovTo).

Setup 4
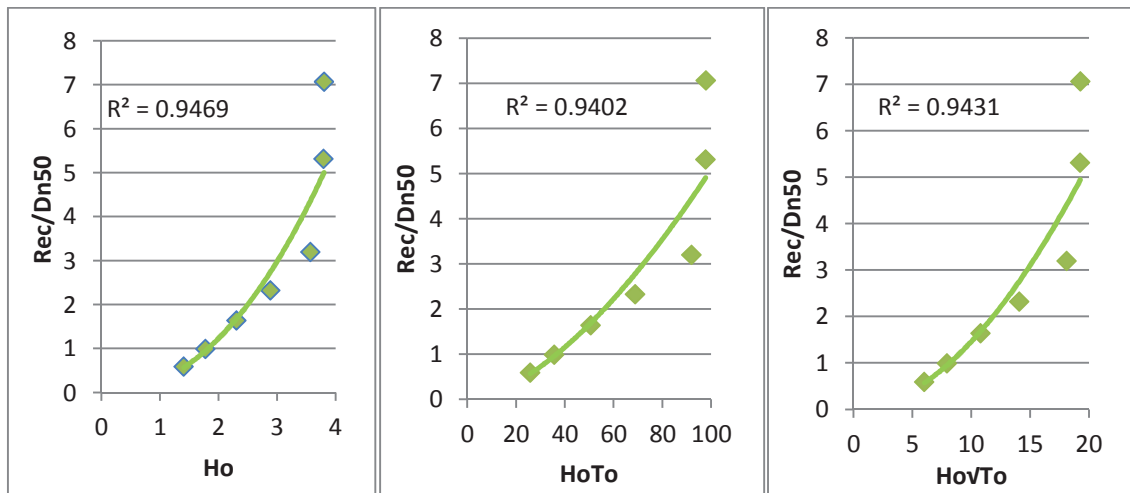
Figure 40.Average values of recession over nominal diameter against different stability parameters at each wave step and their trend lines. Setup 4

$$\frac{Rec}{D_{n50}} = 0.27(Ho)^{2.2} \tag{36}$$

$$\frac{Rec}{D_{n50}} = 0.003(HoTo)^{1.6} \tag{37}$$

$$\frac{Rec}{D_{n50}} = 0.02(Ho\sqrt{To})^{1.86} \tag{38}$$

These functions represent very close the behaviour of a berm breakwater with this profile and material properties. They are convex increasing continuous to every positive value of x (Ho, HoTo or HoVTo).

Setup 5
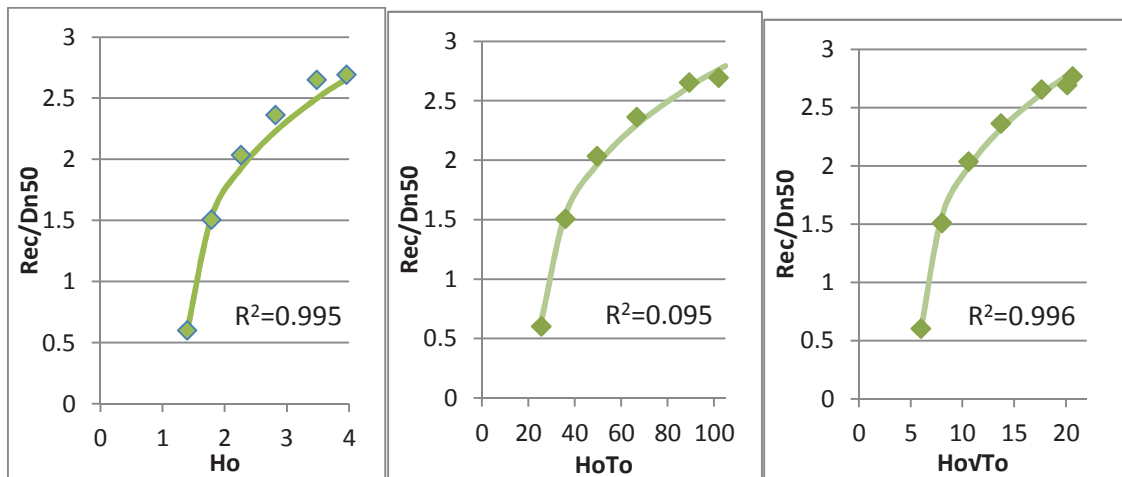
Figure 41. Average values of recession over nominal diameter against different stability parameters at each wave step and their trend lines. Setup 5

$$\frac{Rec}{D_{n50}} = 2(Ho - 1.38)^{0.3} \qquad (39)$$

$$\frac{Rec}{D_{n50}} = 0.75(HoTo - 25)^{0.3} \qquad (40)$$

$$\frac{Rec}{D_{n50}} = 1.25(Ho\sqrt{To} \qquad (41)$$
$$- 5.9)^{0.3}$$

These functions represent exactly the behaviour of a berm breakwater with this profile and material properties. They are concave increasing continuous in the interval from the lower value of x (Ho, HoTo or HoVTo) until the positive infinitive. For lower values of x, the value Rec/D_{n50} is negligible. Moreover we can see that the exponent is the same in all the relations.

9.3.2 RECESSION HEIGHT

The height of the maximum recession at each profile has been measured (the value of the height corresponds to the centre of the peak in which the recession is measured). The complete list of the values can be read in the appendix F. The objective of this measurement is to find the area that had been more eroded and therefore that was more vulnerable. As said before, erosion on the berm was generally not important in the tests performed. Some of the models did not even experiment movements on the berm blocks.
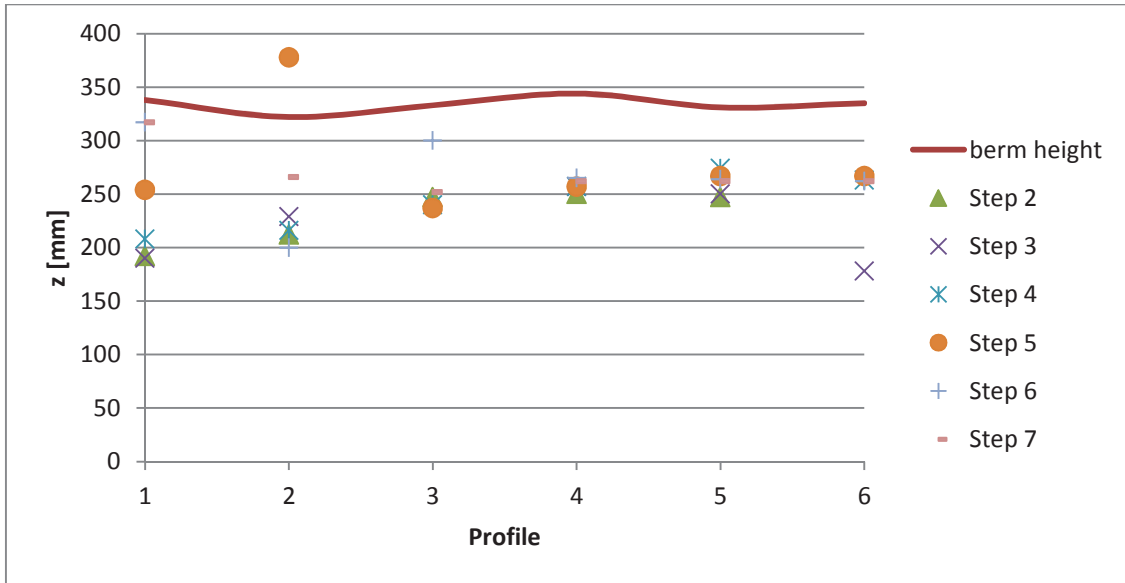
Figure 42. Height of the maximum recession at each profile and wave step. Setup 1
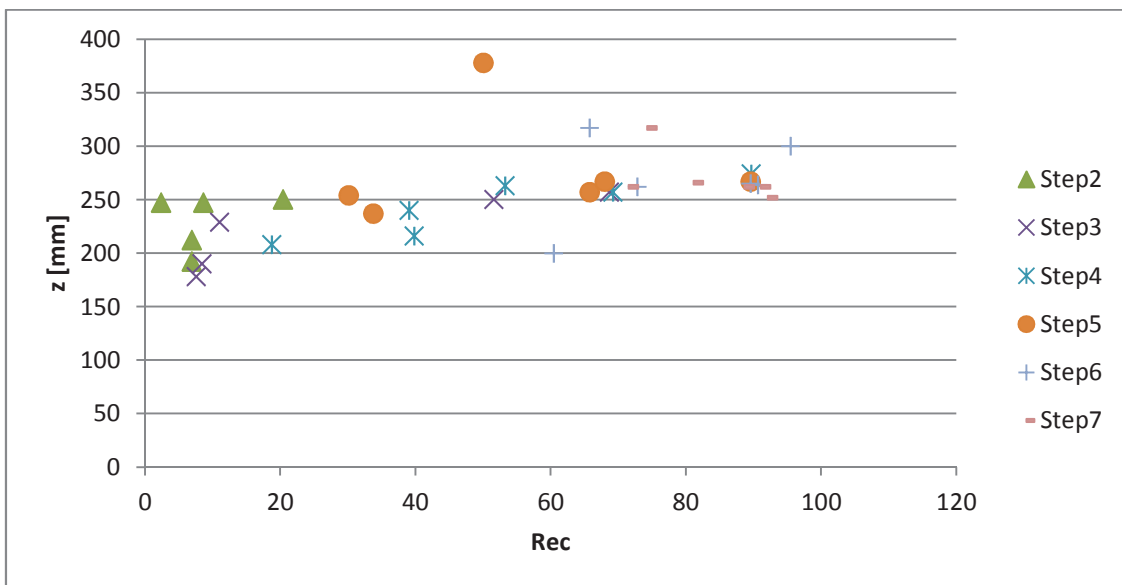
Figure 43. Height of the maximum recession of each profile at each step against its recession value. Setup 1

The graph show that the most of the higher recessions were located around 250 mm of height. This corresponds with the mean water level.

There is only one point over the berm height. This means that the maximum recession was on the berm only in one profile at the fifth wave step.
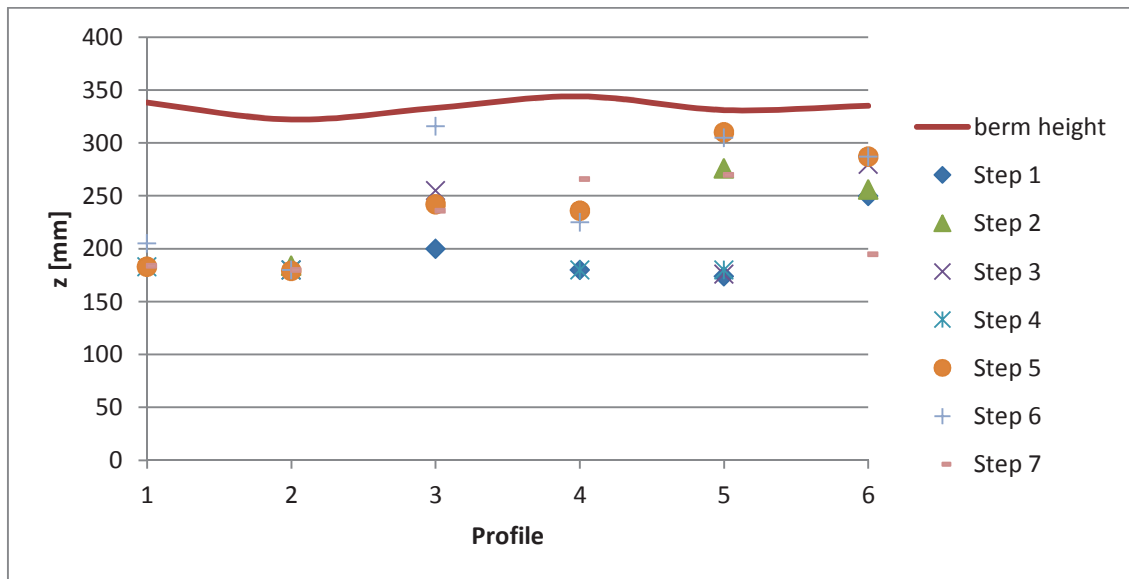
Figure 44. Height of the maximum recession at each profile and wave step. Setup 3
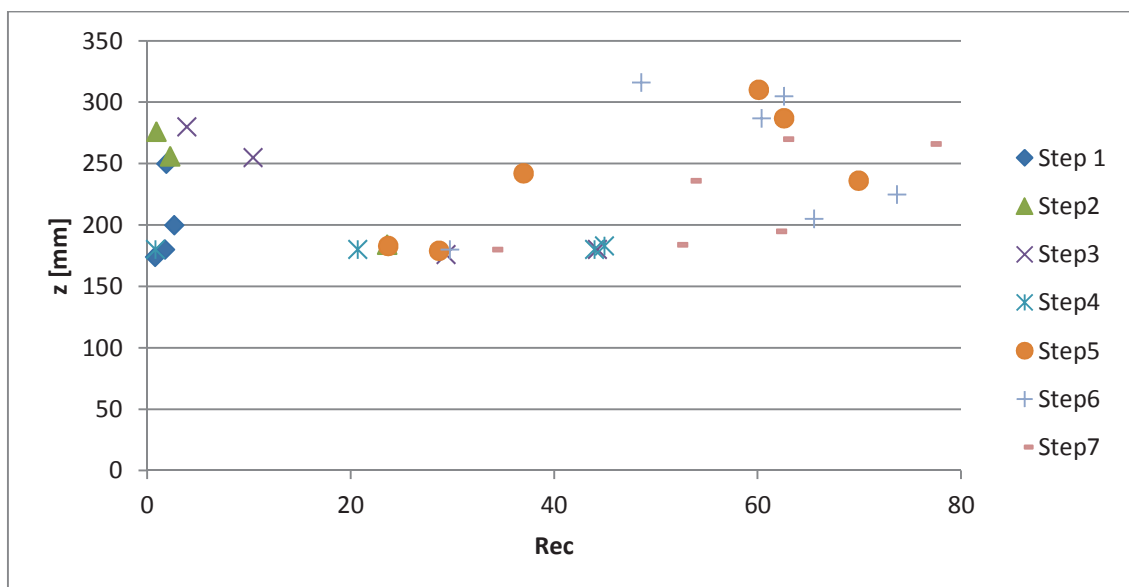
Figure 45. Height of the maximum recession of each profile at each step against its recession value. Setup 3

We can see in these graphs that any of the higher recessions was in the berm. Actually this model did not suffer significant movements in the blocks of the berm.

We can also see that the recessions were in a height interval of 150 mm and 300 mm approximately. This interval corresponds to the area between the lower row of blocks and 50 mm over the mean water level.
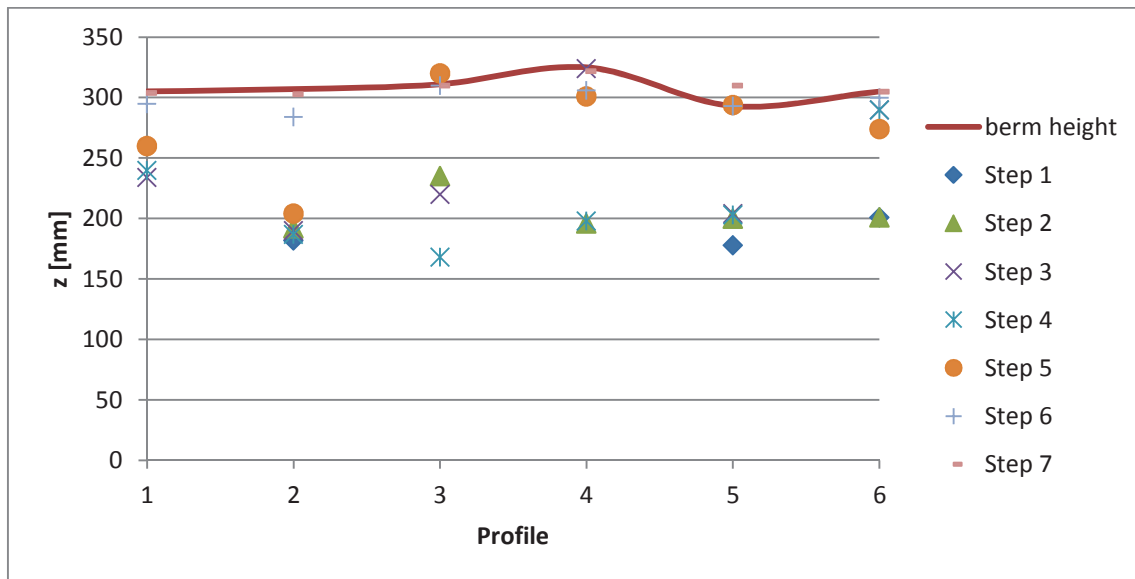
Figure 46. . Height of the maximum recession at each profile and wave step. Setup 4
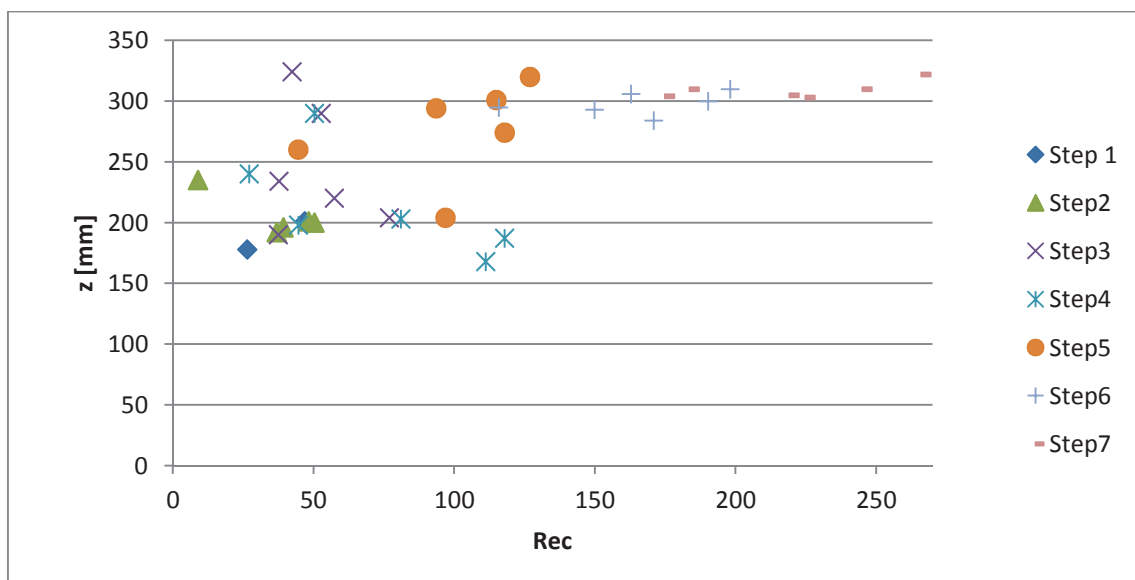
Figure 47. Height of the maximum recession of each profile at each step against its recession value. Setup 4

We can see in these graphs that the berm experienced some recessions, mostly during the steps 5, 6 and 7. We can see how at the earlier step, the recession was low and concentrated around 200mm. At the intermediate step the erosion was dispersed and at the last step it was concentrated at the berm. The recession values of the berm were higher because there were more blocks accumulated in horizontal and, when they were displaced, the horizontal "emptiness" was higher than in the slope, where there were only 2 blocks in horizontal.

The interval of recessions in this model was between the heights 150 mm and 325 mm approximately. This interval corresponds to the area between the lower row of blocks and the berm.

Setup 5
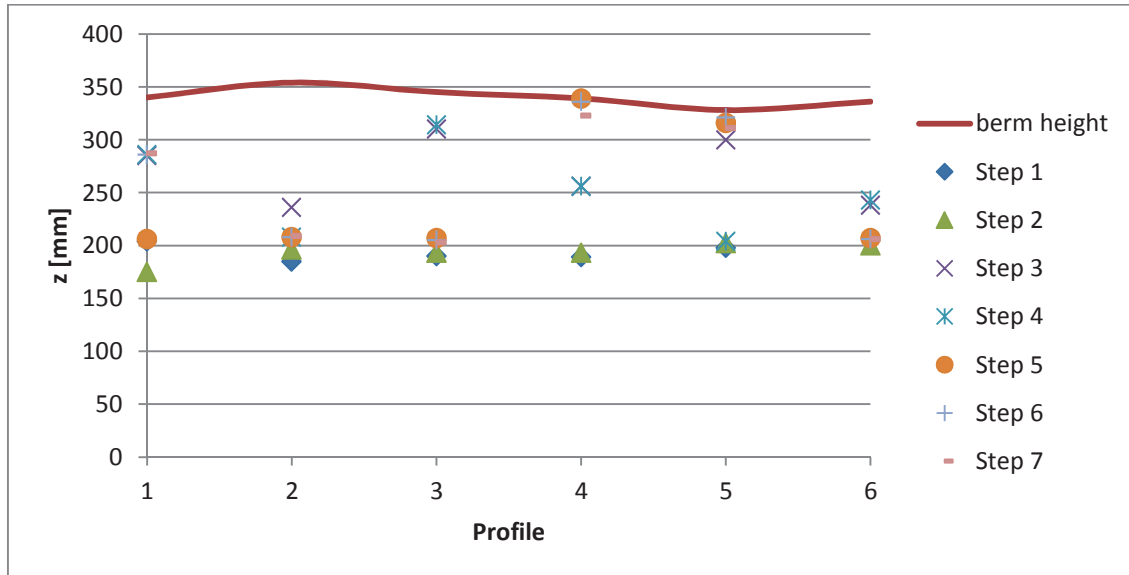
Figure 48. Height of the maximum recession at each profile and wave step. Setup 5
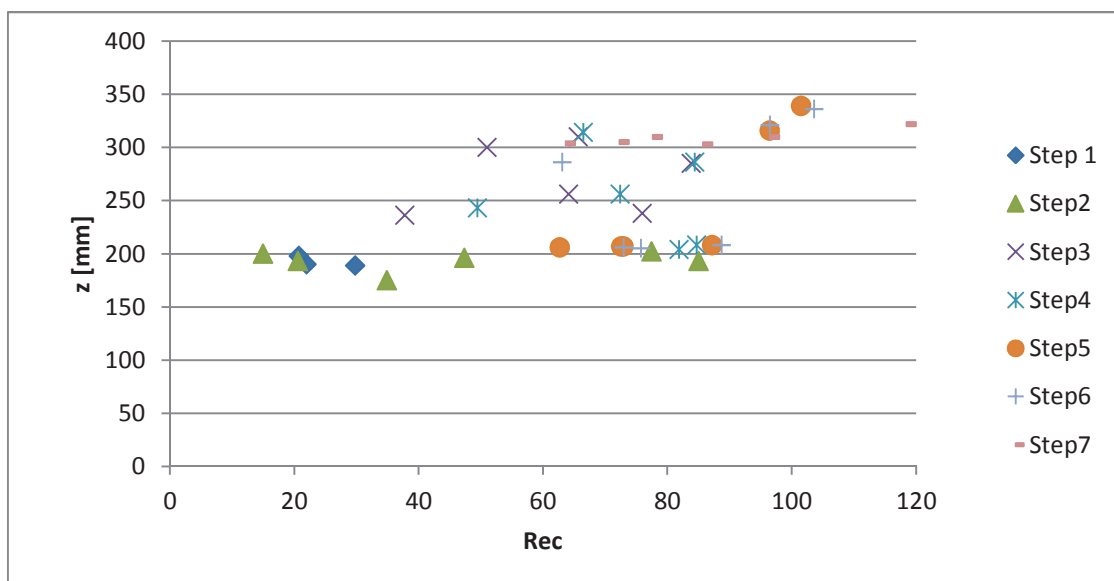
Figure 49. Height of the maximum recession of each profile at each step against its recession value. Setup 5

We can see in these graphs that the berm experienced some recessions mostly during the steps 5, 6 and 7, but it is lower than in setup 5. We can see how at the earlier step, the recession was concentrated around 200mm. Afterwards, the erosion kept growing in this area but also in upper levels. Finally at the last

step, all the higher recessions were at the berm. The interval of recessions in this model was more and less the same than in the previous one.

Summary

The maximum recessions at the beginning were located at the lower rows of blocks. This erosion made easier the displacement of the blocks at the mean water level that would be the ones displacing afterwards. With the increase of the wave height, the berm was more exposed and it started to erode. In addition, the recession at the berm, when was reached, was much higher that on the slope.

Therefore, with a normal wave climate, the berm breakwater is only reshaped at its lower rows of the armour layer. Giving more stability to these rows will significantly increase the stability of the whole structure, making it tougher. This is discussed at chapter 11, conclusions and further investigations.

10. ANALYSIS AND DISCUSSIONS

10.1 MOVEMENTS, COMPARATIVE BETWEEN THE DIFFERENT MODELS
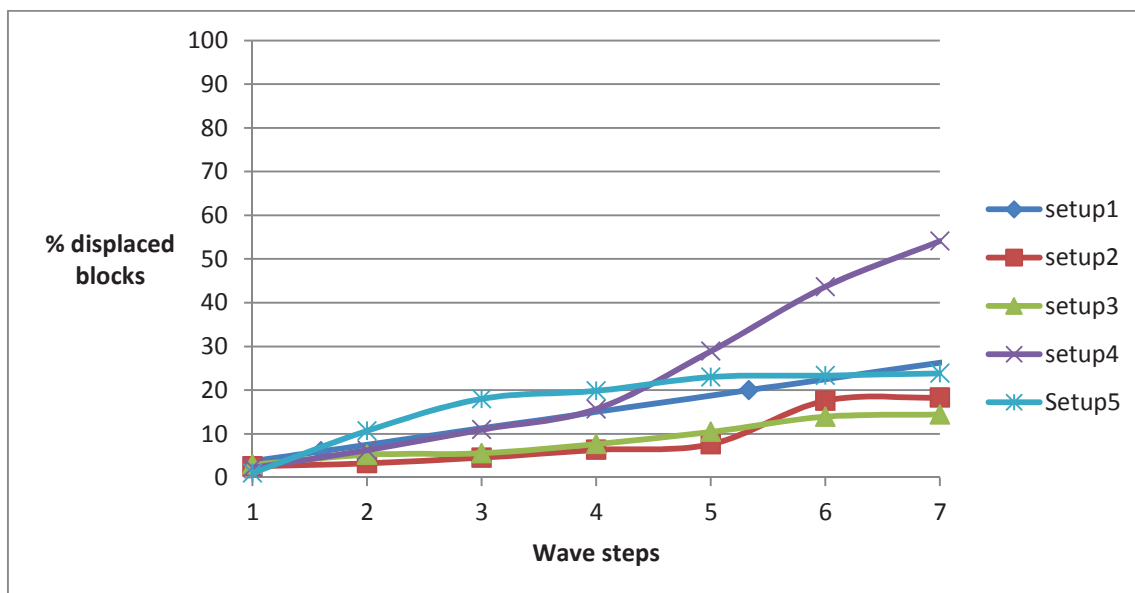
Figure 50. Percentage of concrete blocks moved at each wave step at the different models

If we compare all the models, at the setups 4 and 5 the amount of blocks displaced was higher. This is due to the lower density of the concrete of this blocks and the lower nominal diameter. Therefore, the models should not be compared between them in terms of blocks moved. The comparative has to be in equal term of stability number or period stability number, which takes into account these material differences.

In figure 51, we can see the comparative between the models built with concrete cubes. We see that the setup 1 was the one with fewer displacements at the beginning. That is because the rock displaced is not taken into account in this graph, and the rock was located in an area where models 2 and 3 had cubes, being the movements of these cubes took into account in the graph. For this reason, the comparison between models with so different profiles in terms of displaced blocks is not relevant. The analysis in terms of recession that would be done after is more reasonable. However, we can see in this graph that the behaviour of the setup 2 was completely different from the other two models, as it was pointed previously. This topic would be discussed in the recession analysis.
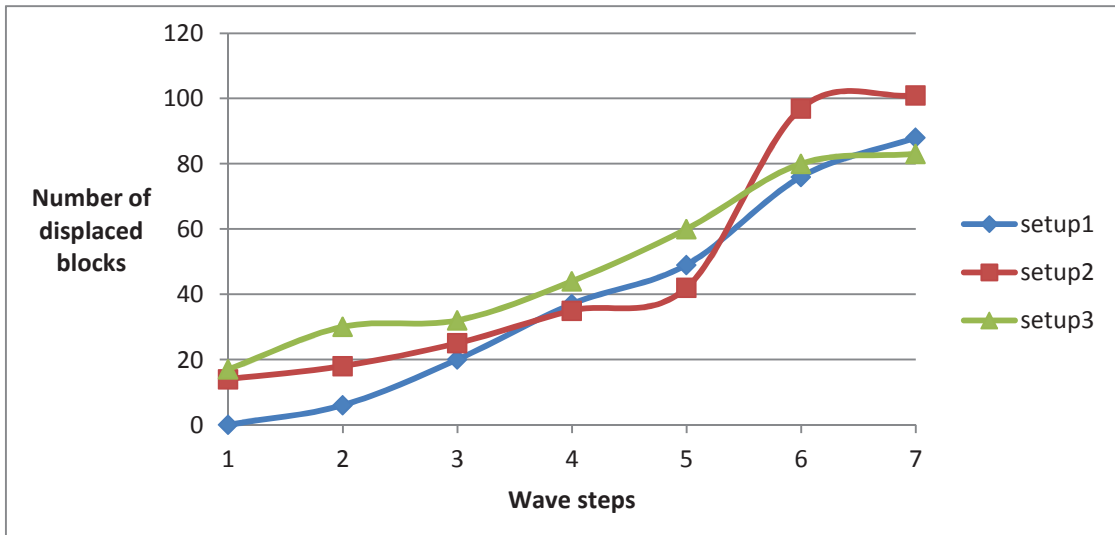
Figure 51. Concrete blocks moved at each wave step at the models with concrete cubes

The two models with cubipods had the same profile, for this reason they can be compared in term of displaced blocks. We can see in figure 52 that setup 5 had higher erosion at the beginning, but from the third step on, the erosion became very low and there was almost not increase in the moved blocks. On the other hand, the setup 4 experienced a slower growth of displaced blocks, but it did not stop, becoming steeper from the fifth step on. At the end, the number of displaced blocks at the setup 5 was more than double of the blocks displaced in setup 4.

Summing up, the recession in setup 4 was higher than in setup 5 after wave step 5 and setup 5 reached some point of equilibrium after wave step 5. Therefore, setup 5 was much more "tough" than setup 4.
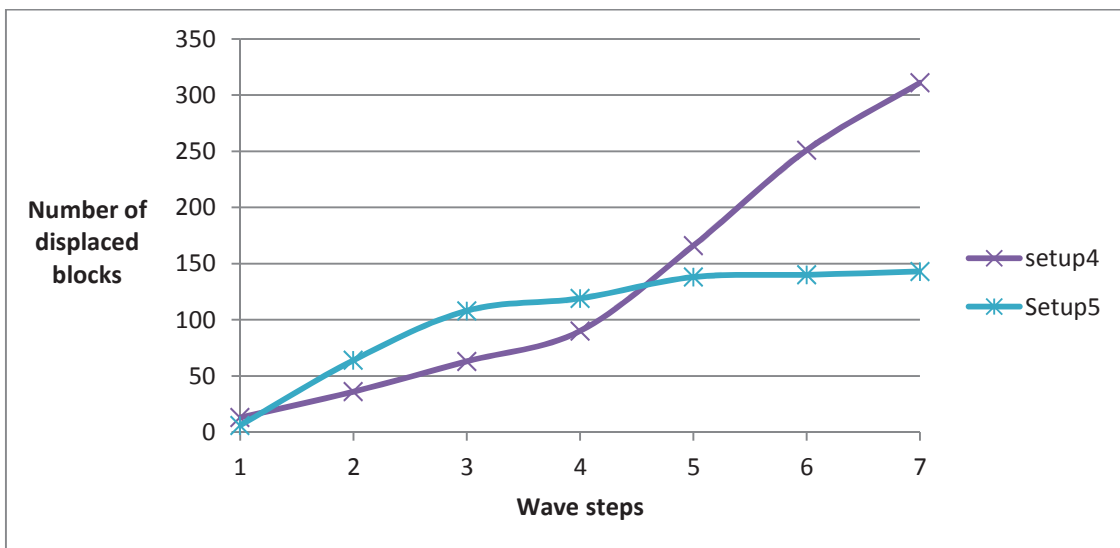
Figure 52. Concrete blocks moved at each wave step at the models with concrete cubipods.

10.2 RECESSION

10.2.1 COMPARARISON BETWEEN MODELS

First, a comparison between the two models built with concrete cubes will be done (setup 1, 2 and 3). As it can be seen in the graphs below, the setup 1 experienced higher recession than the setup 3. The difference between the two models is that the concrete cubes layer in the first model starts at level -1.0 m while in the second starts at -7.0 m. Therefore, it seems that the elongation of the armour layer to lower level under water is beneficial for the structure.

A similar test was developed by Myhra (2005). He tested two profiles with different rock armour layer, one down to level -1.0 m and the other to -7.0 m. He also found the model with the larger layer experienced less recession that the original.

Furthermore, the test of the setup 2 gives more details to the subject. This model has also the armour layer starting at level -7.0m, but its recession is higher than in step 1 and 3, as can be seen in figure 53. As it has been said before, this is probably due to the underwater berm that produces a discontinuity on the front slope, creating a weak point where the waves break.

The conclusion is that the continuity of the armour layer until level -7.0 is beneficial to the structure because reduces the recession, but it is important to maintain a continuous front slope until a certain depth.

In rubble mound breakwaters is recommended that in case of building a toe or intermediate berm, it should be at a depth higher than 1.5 times the significant wave height.

$$h_s \geq 1.5 \, H_s \qquad\qquad (42)$$

At this case, h_s has to be higher than 10.5 m at prototype scale. At setup 2 the depth of the berm was -2.5 m. It evidently does not fulfil the recommendation.
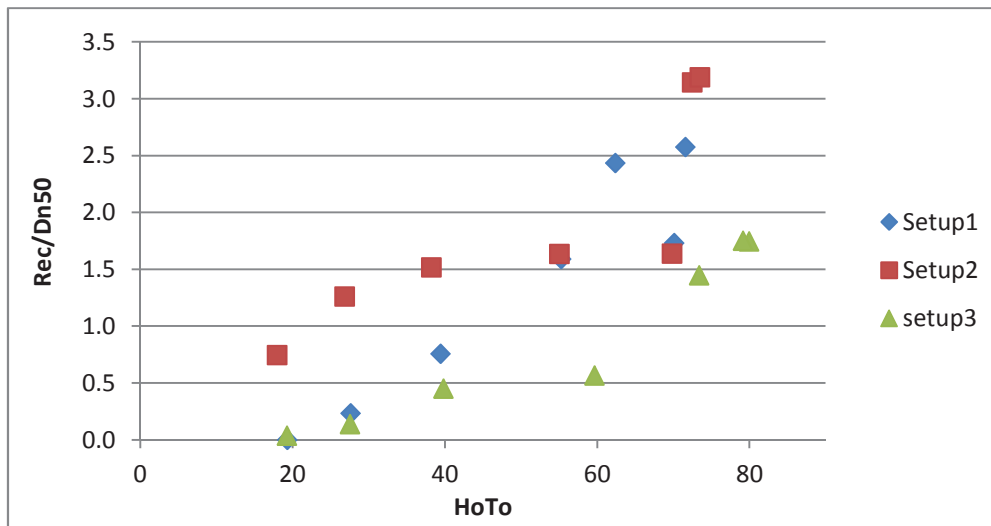
Figure 53. Average non-dimensional recession against the period stability number of each step. Comparison between setups 1,2 and3

Secondly, a comparison between the models with cubipods will be made. The difference between setup 4 and 5 is the armour porosity. Model 4 has a layer porosity of 0.44 while model 5 has 0.39. That means that the setup 5 has more cubipods per area. Looking at figures 55, 56 and 57 we can see a large difference between the two curves. But if we look at the points, we can see not large differences until step 6, when model 4 suffered very high erosion while model 5 almost did not increase the recession. An explanation to this difference is that at step 5, model 4 lost almost all the first layer of cubipods form the slope while in model 5 the lower layer did not suffer significant loses of blocks. This is a very important factor because if the lower layer is stable and does not loose pieces, the structure could stop reshaping finding an equilibrium profile. Therefore the recession will be lower and the structure more resistant towards future reshaping. The location of the displaced blocks can help to maintain the stability of the lower layer. If they are accumulated right next to the lower rows, they would help stabilize the whole layer. On the other hand, if they are displaced to the bottom, the lower layer will be easier to erode.

The conclusion is that the layer porosity is a critical factor in cubipods layers. If there is not enough friction between the blocks they cannot work as a group and the resistance against the wave action is much lower. However, if they have good contact, they can build a very strong layer, with higher hydraulic stability, that will lead to a reduction in recession and a stable profile. It is also important the stability of the lower rows of blocks, as they are the support of the rows of the slope.

Armour porosity is also a critical factor in cubes layers, but this fact has not been verified in this thesis.

Before doing a comparison between all the setups, it is important to discuss the different behaviour of the models build with cubes and cubipods. The same model (same profile and armour porosity) built with cubipods (setup 5) experienced more recession that the one built with cubes (setup 3). This is an unexpected result, as the cubipods have been tested to be more hydraulic stable that the cubes in rubble-mounded breakwaters (Gómez-Martin, 2007). An explanation to this behaviour could be the different density of cubes and cubipods.

Although this difference is represented in Ho, the value of the density of the cubipods is very low, lower than the recommended value (2.2 t/m^3). This may lead to behaviours of the cubipods "out from the ordinary". Perhaps, when we are working with values of density under normal, the effect of the density is over the recession is more importance that what is represented in Ho. This is just an idea that should be further tested to be confirmed or denied.

Menze (2000) tested the Sirevåg breakwater with two different rock densities, 2.7 t/m^3 and 3.1 t/m^3. He found out that the two models had very similar behaviours. Therefore, this experiment proved than the recession at berm breakwater built with rock armour layer with densities higher than 2.7 t/m^3 do not strongly depend on this density. Nevertheless, neither the behaviour with lower densities nor the effect in concrete unit is tested, and consequently it could be possible that the behaviour of berm breakwater with lower density armour layers depends on the density.

Some studies about the influence of density in concrete units armour layers in rubble mounded breakwater have been done. Zwamborn (1978) investigated the effect of relative density of the stability of Dolos armour units. This investigation was further extended by Scholtz and Zwamborn (1982). They concluded that on steep slopes of 1:1.5 the positive influence of increasing density is overestimated by the current design formula of the stability number Ns (Hs/ΔD_n). Zwicht et al. (2009) investigated the effect of the concrete density on the stability of Xbloc armour units and expressed that the assumption of dominance of lift, drag and gravity forces in which the stability number is based, does not hold for steeper slopes and/or interlocking armour units. This could be the case of cubipods. After their experiments, they concluded that the stability number formula tends to underestimate the influence of the specific weight for

a slope with cotα=1.33 (the slope used in setup 4 and 5 in our experiments). This results in light concrete elements having less hydraulic stability than according to the stability number.

After taking this into account, we can start with the comparison between all the models. When looking into figures 55, 56 and 57, we can see that the performance of setup 3 is the best one, with the lower recession. We also see that setup 1 and 4 have a similar behaviour in the interval that setup 1 has been tested. In general, the models with cubes experience less recession than the models with cubipods. We can see that while setups 1, 3 and 4 have a convex recession evolution, in setup 5 is concave. This is perhaps due to the reduction on the recession pace after the upper layer was displaced in setup 5, because the lower layer proved to be much more stable in this model than in the models before (even when it had the same armour porosity than setups 1 and 3). Setups 3 and 5 have the same profile and very similar layer porosities, but its behaviour was very different. Setup 3 experimented a lower recession in general (more than half of the recession in some parts), but it had a different growing ratio than in setup 5. In setup 5, the most of the recession occurred during the second step, where the most of the upper layer blocks of the slope were displaced. After that, the erosion rate was reduced at each step, as it can be seen at figure 54 where the increment over the total in percentage is plotted against HoTo. On the other hand, setup 3 alternated between increments and reductions of recession rate. Looking at the pictures (Appendix G), we see that both structures started losing their lower rows, and this destabilized the whole armour layer. Then, giving more stability two this layers should be a priority if we want to improve the behaviour and reduce the recession.
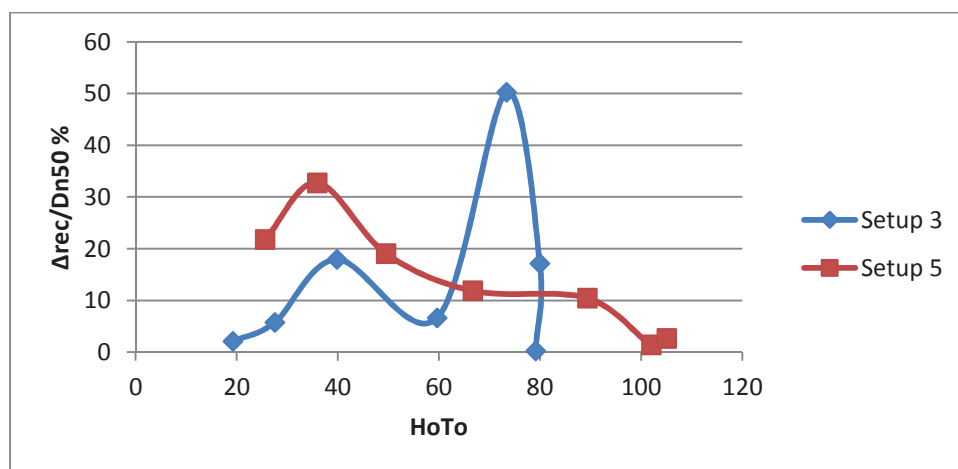
Figure 54. Increment of non-dimensional recession at each step over the total in percentage against HoTo

As a result, in this investigation has been proved that the concrete cubes have a very good behaviour in berm breakwater structures and that starting the armour layer at level -7.0 m beneficiate the structure by reducing the recession. The models with concrete cubipods in this investigation, experienced more recession than the one with cubes under the same Ho, HoTo and HoVTo circumstances. Another important conclusion from these tests is that the layer porosity is a critical factor in the behaviour of concrete block layers. To finish, the improvement of stability of the first rows at any of the models will probably lead to a dramatically improvement in the recession ratio.
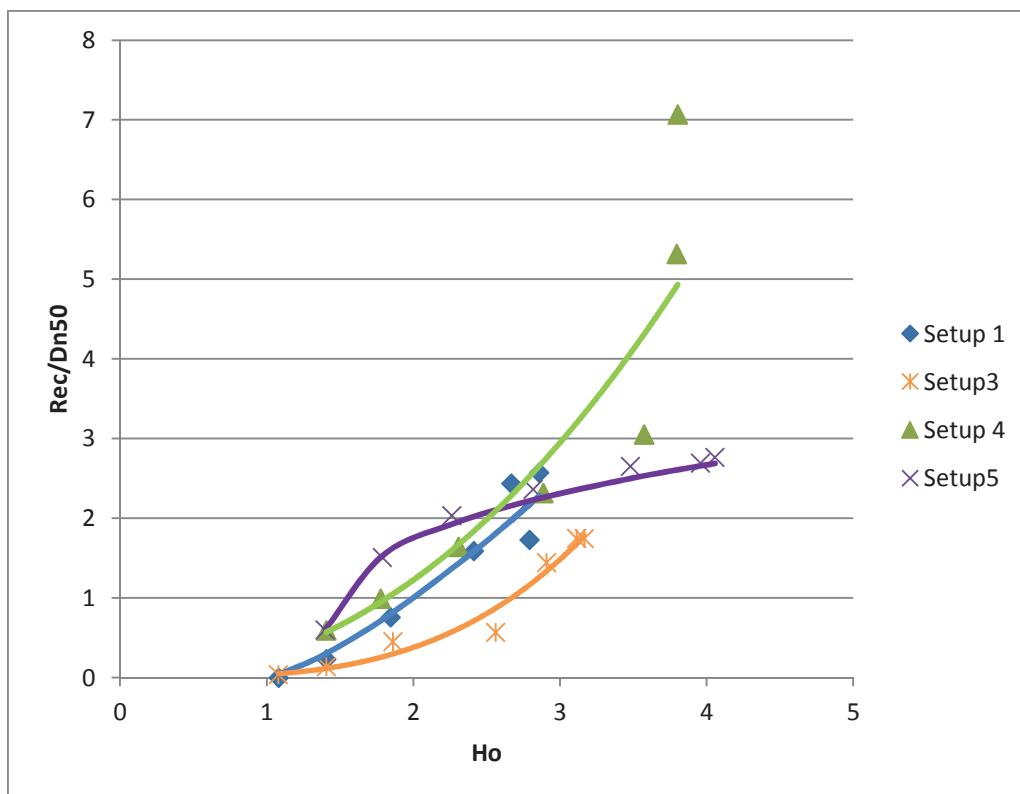
Figure 55. Comparative of non-dimensional recession against stability number of the different setups
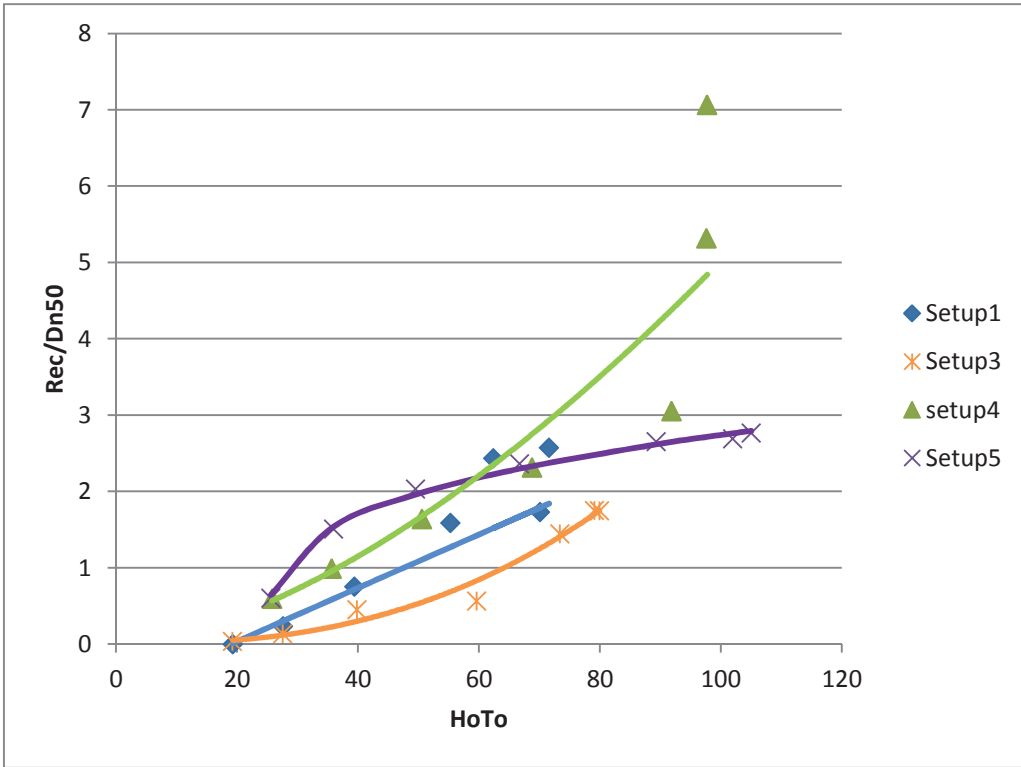
Figure 56.Comparative of non-dimensional recession against period stability number of the different setups
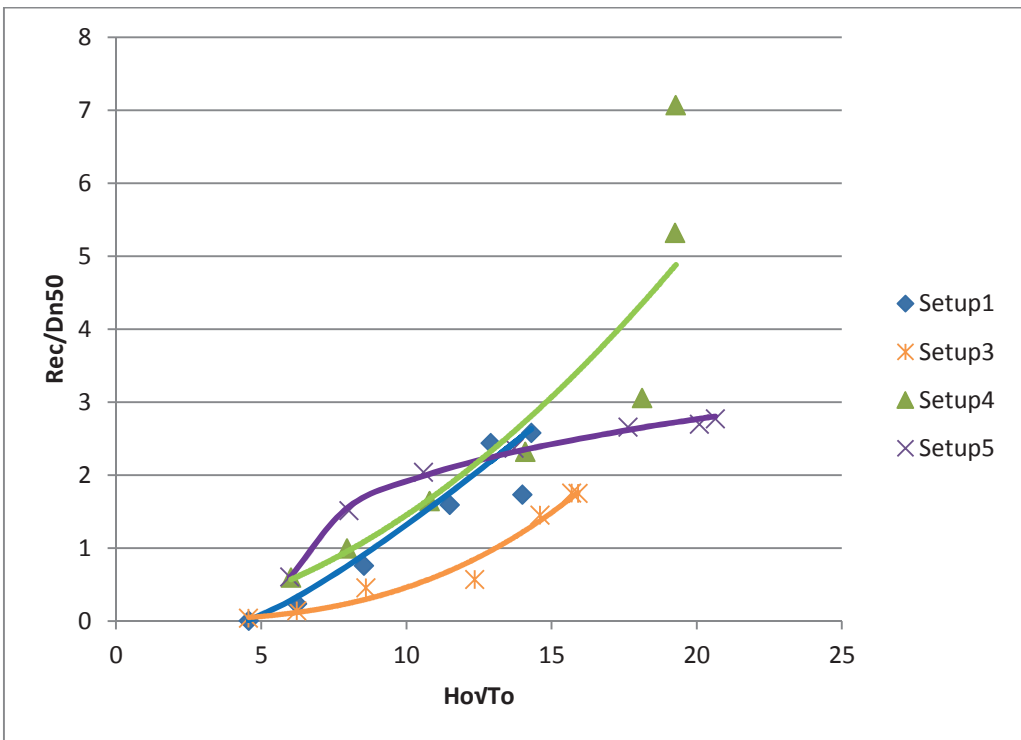
Figure 57. Comparative of non-dimensional recession against HovTo of the different setups

10.2.2 COMPARATION WITH MYHRA (2005)

Myhra (2005) investigated the recession of two berm breakwaters with different construction design, in two models, one from the Sirevåg breakwater and an Alternative model with narrower and higher berm and class I rock placed down to level -7.0m. This profile is similar to the one used in setups 3, 4 and 5, because in all of them the armour layer starts at level -7.0m. He tested both profiles with pell-mell and orderly placed rocks; the data represented here is from the pell-mell models. The results from his test are plotted in figure 58 with the results of the tests from this thesis.

Menze (2000) and Westeng (2011) tested also the Sirevåg berm breakwater and modifications of it. Menze (2000) studied the behaviour of multilayer berm breakwaters, testing two stone densities in two different set-ups, with three dimensional tests. Westeng (2011) studied the recession of two different berm breakwaters, a model of the Sirevåg breakwater and a similar one with class II armour at the upper front of the berm. However, they both did their tests in a 3D wave flume while Myhra (2005) did them in the same 2D flume that the tests of this thesis were made in. Myhra (2005) compared his results with Menze's on the Sirevåg breakwater and he found a significant difference in results (see Appendix H). Therefore, the results from Menze (2000) and Westeng (2011) are not going to be compared with the experiments done in this thesis.

Setup 1 and Myhra Sirevåg have the same profile. The difference is that Setup 1 uses concrete cubes in the armour layer and Myhra Sirevåg rocks. We can see in the graph below that at the beginning the behaviour is the same, but after step 3 (in setup 1) the recession in Myhra Sirevåg starts growing more that in setup 1. At values of HoTo around 55, the difference in non-dimensional recession is 0.8. Myhra Alternative and Setup 3 have a similar profile, again with the difference on the armour units. The difference in behaviour is similar than in the previous comparison. They have the same behaviour until step 3 and afterward the recession in Myhra Alternative starts growing at a higher rate. This change in behaviour appears with larger waves when the armour layer starts at lower levels (setup 3 and Myhra Alternative) than in the previous comparison. This mean that the reduction in recession in setup 3 compared with the original Sirevåg breakwater until values of HoTo around 50, is due to the fact of starting the armour layer at level -7.0m. Afterwards, the benefits come from the use of concrete cubes in the armour layer instead of rock.

Therefore, the used of concrete blocks in berm breakwater seems to be beneficial with large waves, and have the same behaviour as rock with lower waves. In this comparison we found also the important benefit of longer armour layers that continue further under water.

The performance of the models with cubipods follows a very different path as it has been mentioned before. The same interpretations commented previously are applicable at this comparison.
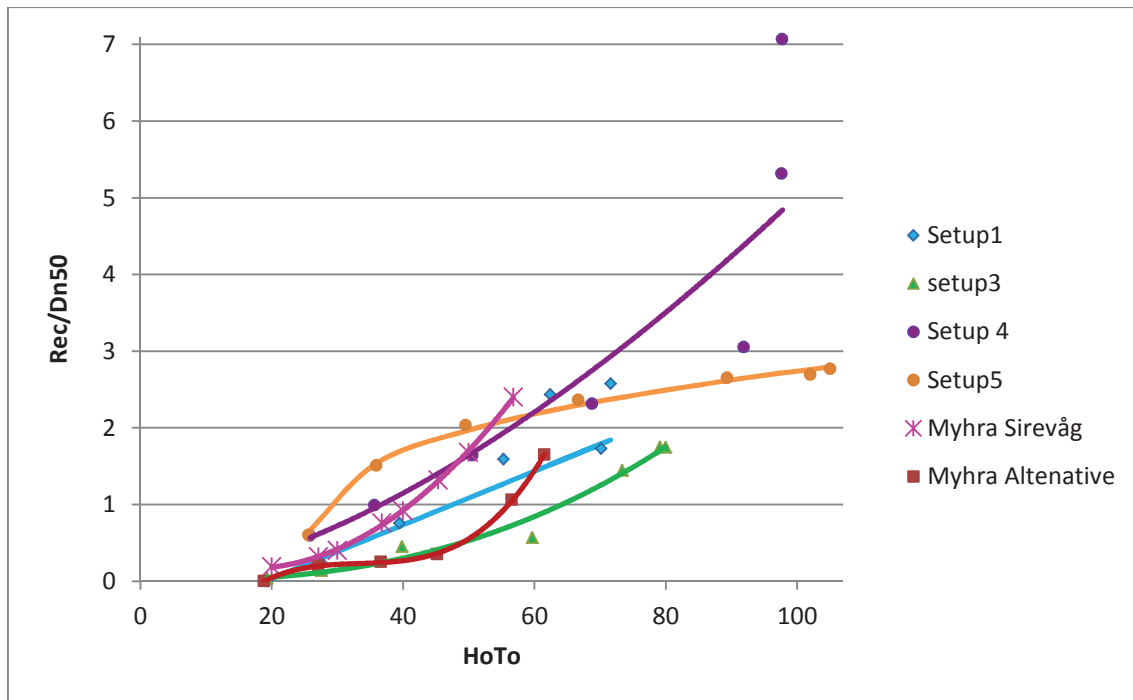
Figure 58. Comparative analysis of non-dimensional recession against HoTo of the setups from this thesis and other authors.

10.2.3 COMPARATION WITH FORMULA

Figure 59 shows the recession parameter for setups 1,3,4 and 5 compared to Tørum's revised formula. This formula is:

$$\frac{Rec}{D_{n50}} = 0.0000027(HoTo)^3 + 0.000009(HoTo)^2 + 0.11(HoTo)$$
$$- \left(f_{Dn}(f_g)\right) + f_d(\frac{d}{D_{n50}})) \frac{HoTo}{120}$$

(7)

where,

Dn50 is the average between Dn50 of cubes and cubipods,
fg= 1 and
d=0.258 m

Therefore the function of the curve is:

$$\frac{Rec}{D_{n50}} = 0.0000027(HoTo)^3 + 0.000009(HoTo)^2 + 0.0583(HoTo) \qquad (43)$$
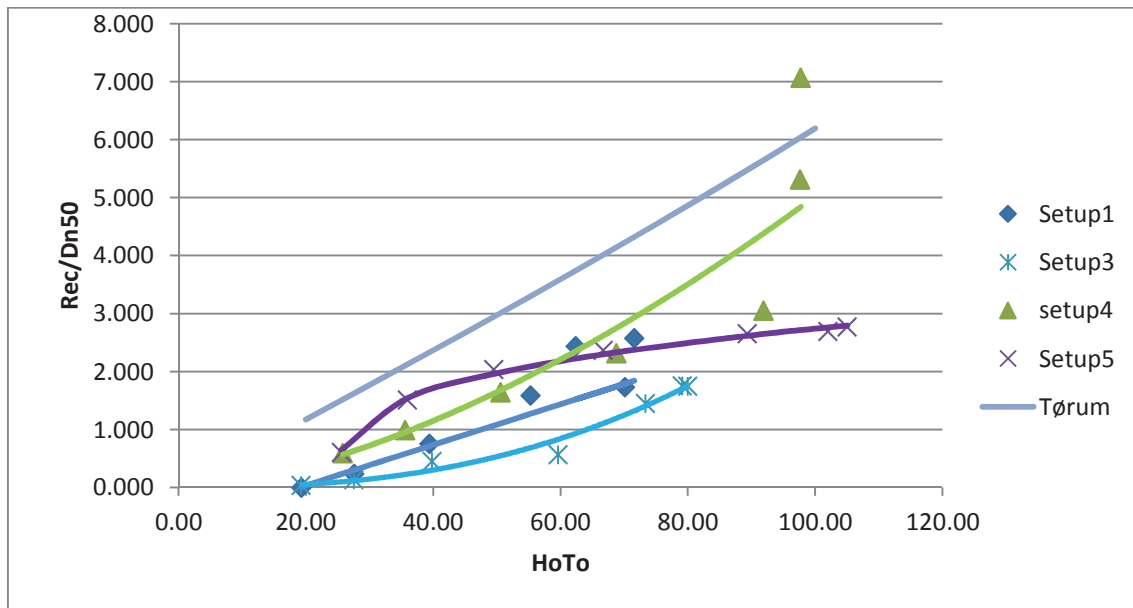
Figure 59. Comparative analysis of non-dimensional recession against HoTo of the setups from this thesis and the formula developed by Tørum.

We can see that the values obtained with Tørum's formula are more conservative than the obtained. When looking at the tendency, setup 4 tendency is more and less parallel to the formula and setup 1 is also close. On the other hand, setup 3 and 5 trend lines are completely different. Consequently, it can be said that Tørum's formula does not reflect the behaviour of these berm breakwaters with concrete blocks.

10.3 REFLECTION

Several investigations about the reflection coefficient have been performed and many empirical laws have been developed in order to get a best fit for the data. The value of the reflection coefficient is often in the range 0.10 − 0.50 (PIANC, 2003), and a mean value of 0.30 is often experienced in tests.

During these tests a mean value of the reflection coefficient was about 0.28, with all the values in the range 0.18 − 0.38.

Table 16. Average values of refection coefficient at each setup

	Setup 1	Setup 2	Setup 3	Setup 4	Setup 5
Average	0.287	0.274	0.320	0.252	0.290
Standard deviation	0.045	0.044	0.043	0.050	0.025

The slope angle was 1:1.5 over the mean water level in setup 1 and 1:1.3 under the mean water level, and 1:1.3 at the whole front slope in the rest of the models. The slope angle changed during the test runs, getting more irregular with the erosion of the front slope, and maintaining more and less the steepness over the water level (as the lower layer was not removed generally until the last steps). Under the water level the steep was flatter due to the accumulation of the blocks displaced by the waves.

In a study of Lissev (1993) it was concluded that the reflection coefficient shows a tendency to increase with increasing wave period and wave height (Myhra, 2005). This is in correspondence with the observations in the tests performed here. The exception appears at the highest wave steps, where the reflection coefficient decreases due to a flatter slope (see figure 60).

We can also see that the values of the reflection coefficient at the seventh wave step (see figure 61) were lower than in the steps before. The wave conditions at the six subtesps that form step 7 are the same wave conditions that at the 6 steps before. That means that the reshaped breakwater had a lower reflection coefficient that the original, due to a decrease on the slope steepness.

Looking at the table 16 we can see that the model with higher reflection was setup 4 and the one with lower reflection coefficient was setup 3.
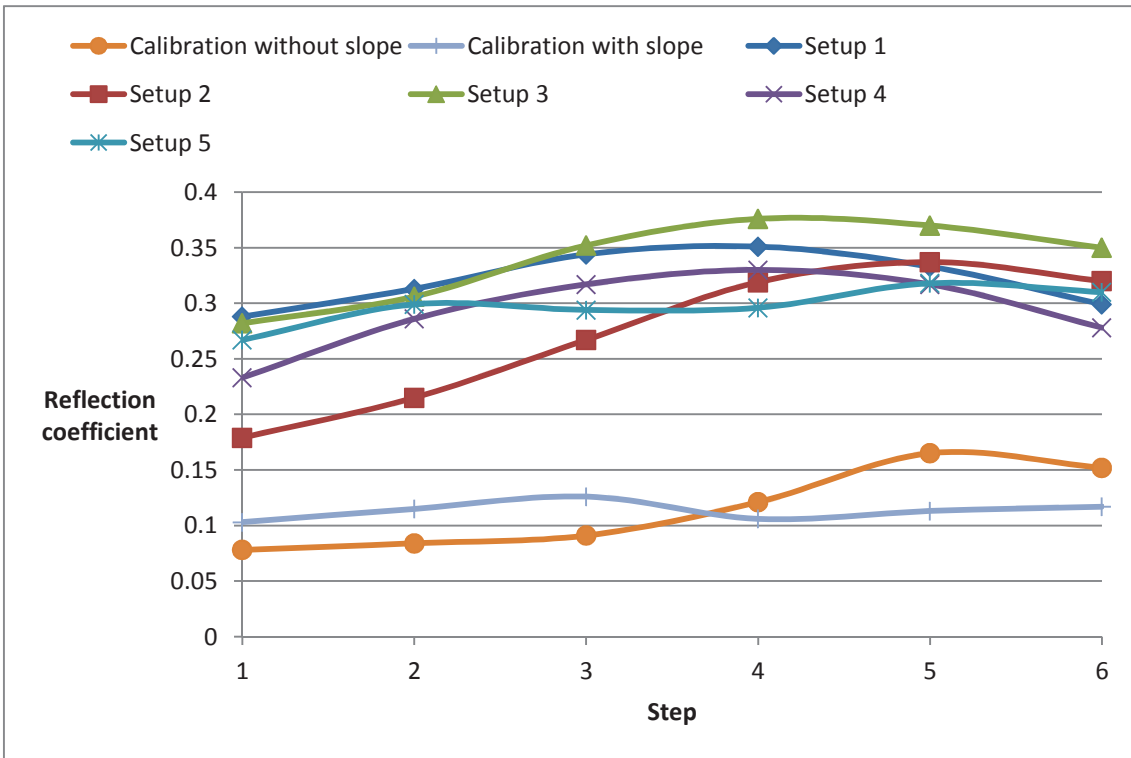
Figure 60. Reflection coefficients from step 1 to 6 at each model
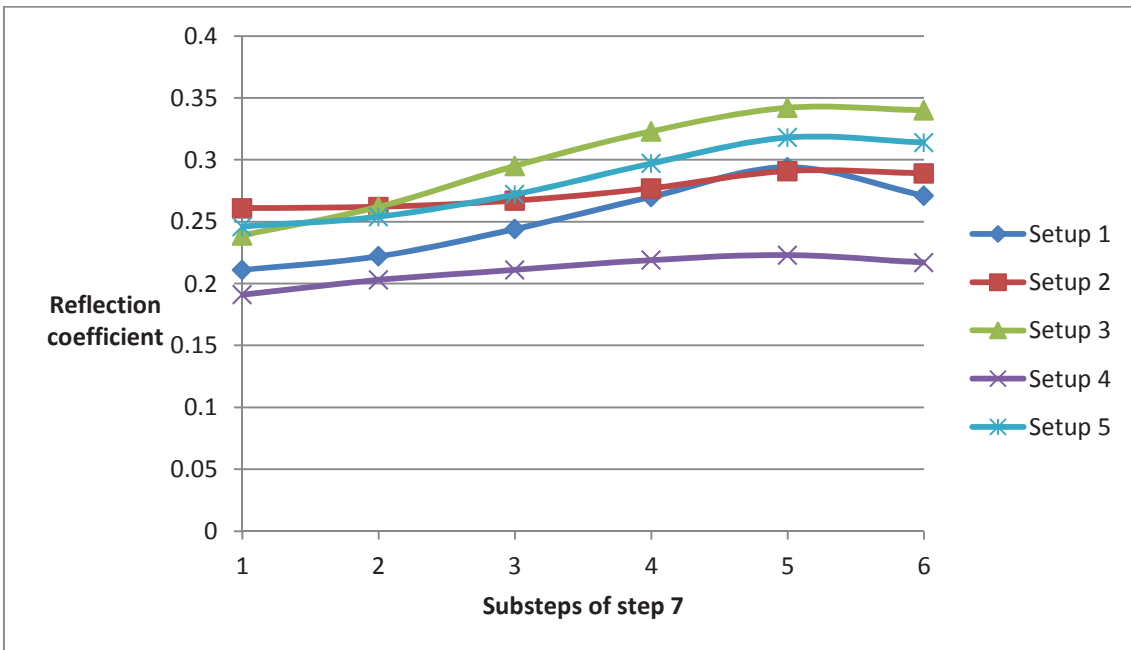
Figure 61. Reflection coefficient at step 7 in the different models

| Master Thesis, spring 2013   Altea Cámara Aguilera   NTNU

10.4 STABILITY INTERVAL

The stability criterion used to divide the categories of berm breakwaters with rock armour layer shown in Table 2, cannot be applied in these models without deeper investigation on the issue. However, based on the observations during these tests, it can be said that the intervals applicable to berm breakwater with concrete armour will not differ much from the original ones.

In these tests seem that the non-reshaping berm breakwater category will be with values of HoTo lower than 30. That corresponds approximately to steps 1 and 2, where the blocks were displaced mostly because of instabilities in the placement of the blocks. Nevertheless, if a system to reduce the movement due to this effect was utilized, the intervals will probably change dramatically. It also seems that the reshaping dynamic stable berm breakwater will take place with values of HoTo higher than 100. It is observed that at values of HoTo around 80 the blocks started to be lifted by the waves, although they did not roll up. This was the start of the rolling up and down movement characteristic of this category.

10.5 ULTIMATED LIMIT STATE

PIANC 2003 proposes some guidelines about the Ultimate Limit States (ULS), based on Tørum (1999). It has to be checked for a sea state with a 100 year recurrence period. The requirement that the structure has to accomplish is that the residual berm width should not be less than $4*D_{n50}$.

The 100 year recurrence period wave state is reached more and less in step 5. The residual berm requirement of $4*D_{n50}$, is equivalent to a recession on the berm equal to approximately 15 cm in model scale (there is small difference between different profiles). This value was only reached in the setup 4, but in the wave step 6, being the wave step 4 the one that had more and less the characteristics of the 100 year recurrence period wave conditions. Therefore, all the model tests achieved this requirement of the ultimate limit state.

Another requirement is that after reshaping, the distance from the reshaped profile to the lower layer with smaller stones, possibly a filter layer, should be larger than $1.5*D_{n50}$ or at least 2 m.

In our models, in model scale, this value was 4.88 cm with cubes, and 4.65cm with cubipods. The lower layer with smaller stones corresponded to the rock

class IV. The recession needed to have the minimum required is 15.7 cm. This was also reached in the step 6 on the setup 4, but not before. Therefore, this requirement was also achieved in all the models.

The last requirement is that the armour stones should be able to withstand the reshaping without splitting, which reduces D_{n50} due to the motion of the stones.

Any damage was observed in the concrete blocks during the tests. Nevertheless, this fact does not prove that the blocks are strong enough to achieve the requirement. A separate study should be done in order to reach a conclusion about this topic.

Tørum and Krogh (2000) investigated the rock strength in field drop tests, and they founded it lower that the strength of the model pieces.

11. CONCLUSIONS AND FURTHER INVESTIGATIONS

The Sirevåg berm breakwater has been tested to be a tough structure, its design being very conservative compared to the demands. This behaviour is amplified with the use of concrete cubes in the armour layer.

Several conclusions were reached during this investigation. The most important conclusion is that concrete cubes have a very good behaviour in berm breakwater structures. It was proved here that the models built with concrete cubes in the armour layer experienced the same recession as the same model built with rock when they were exposed to low waves (HoTo lower that 50 at setup 3). When they were exposed to values of HoTo higher that 50, the model with concrete cubes experienced lower recession than the one with rock. This value is representative of a berm breakwater with an armour layer starting at level -7.0 m as at setup 3.

The second conclusion was that the continuity of the armour layer until level -7.0 reduced the recession, if the front slope is continuous until a certain depth. This confirmed that the conclusion reached by Myhra (2005) about the same issue in berm breakwater with rock can be applied to structures with concrete units.

In addition, it was found that the layer porosity is a critical factor in cubipods layers. If there is not enough friction between the blocks they cannot work as a group and the resistance against the wave action is much lower. However, if they have good contact, they can build a very strong layer, with higher hydraulic stability, that will lead to a reduction in recession and a stable profile.

The models with concrete cubipods in this investigation experienced more recession than the one with cubes under the same Ho, HoTo and HoVTo circumstances. This result contradicts other tests made with cubipods that proved that cubipods have more hydraulic stability than cubes. A reason for this difference could be the lower density of the cubipod units, as some experiments had proved that light concrete elements have less hydraulic stability than according to the stability number.

Therefore, further experiments with concrete cubipods with concrete densities closer to the values used in prototype construction (around 2.4 t/m3) should be conducted to clarify this issue.

In regard to the ability of the Tørum formula to describe the reshaping process in the structures tested in this thesis, the values obtained with Tørum's formula are more conservative than the ones obtained in the experiments. Therefore, it does not represent the process at these structures closely.

It was observed that the lower rows of concrete blocks, which were displaced at the very beginning of the tests, are the most unstable. Giving more stability to these rows will significantly increase the stability of the whole structure, making it tougher and probably reducing dramatically the recession. A way to improve the structure's behaviour would be to build a toe berm were the concrete units' layer starts. This is a technique used at rubble mounded breakwater. This underwater berm has a few design restrictions. In the Coastal Engineering Manual (2002) we find the stability of the toe berm design method. For a two layer armour stone toe berm for exposed sides of rubble-mound breakwaters and jetties the figure below was found.

Two layer armor stone toe berm for exposed sides
of rubble-mound breakwaters and jetties
(CERC 1986)

$B = 3t$ for (W_{50}) berm
where $t = (W_{50}/\gamma)^{1/3}$
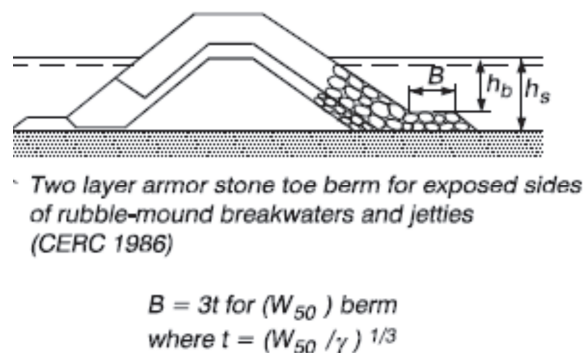
Figure 62. Two layer armour stone toe berm for exposed sides of rubble-mound breakwaters and jetties (CEM, 2002)

And the following equation:

$$N_s = \frac{H_s}{\Delta D_{n50}} = \left(0.4\frac{h_b}{\Delta D_{n50}} + 1.6\right) N_{od}^{0.15} \qquad (44)$$

Another recommendation is that the top of the toe berm has to be at the depth equal or higher than 1.5*H$_s$.

Based more and less in these calculations, a toe berm on the Sirevåg berm breakwater profile as the one shown on the following figure is proposed:
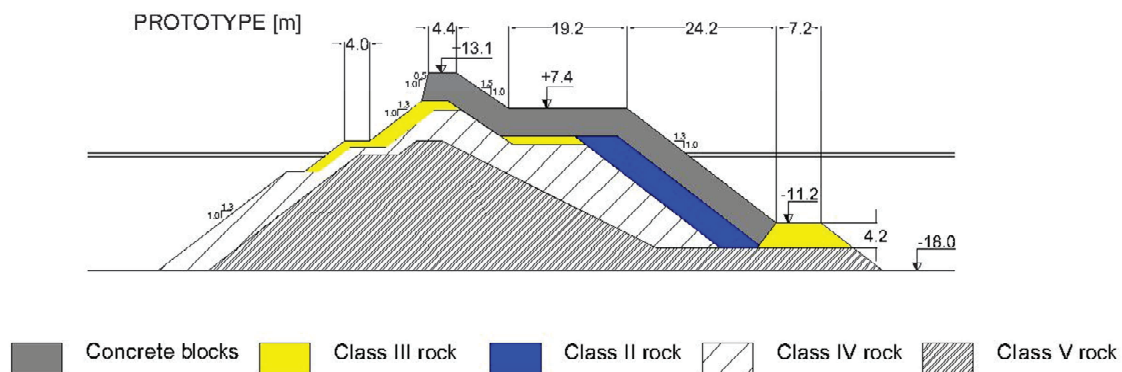
Figure 63. Alternative profile with a toe berm

Further investigations could also test profiles in which the concrete units are lying over rock with lower Dn50. This way the rocks will fit better between the units, increasing the friction of the armour layer with the underlying rock layer and therefore increasing the stability. During the construction process of the models in this thesis, it sometimes seemed that the class II rock, over which the concrete units were placed, was a slippery surface to lay the concrete units on.

As the most of the models tested in this thesis did not suffer displacement of the upper layer of concrete unit for the 100 year return period waves, it could be interesting to try replacing the class II and III stones under the armour layer by the class IV rock, as it is sketched at the following figure:
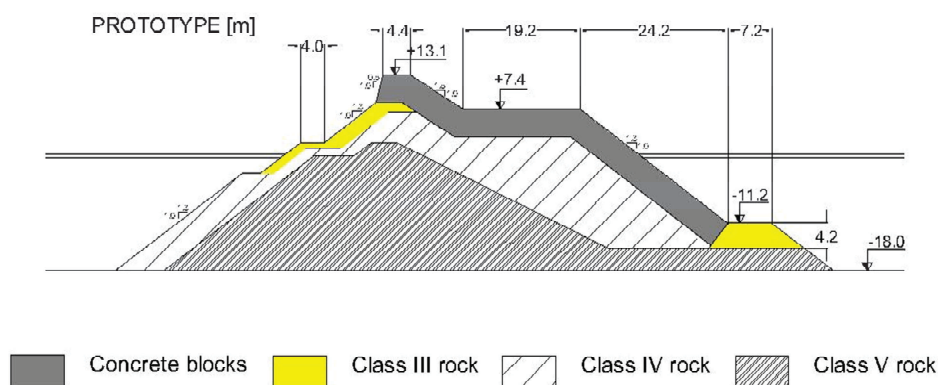
Figure 64. Alternative profile with class IV rock under the concrete units

If the class IV rock layer from the previous profile was finally exposed when tested, it would be better to test a model with class III rock all under the armour layer, as shown in the following figure:
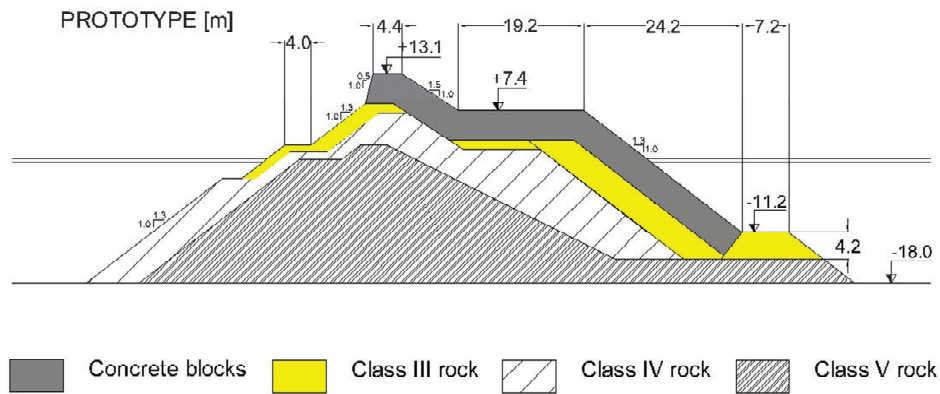
Figure 65. Alternative profile with class III rock under the concrete units

If the breakwater is built in very deep water, the berm could be placed at the middle of the front slope. This way, the construction of the armour layer at high depths would be avoided.

Another issue that could be investigated is the influence of the storm length in this type of berm breakwaters. Subba Rao et al. (2012) concluded that the stability of the berm breakwater with concrete cubes that they tested was largely influenced by the storm duration. They found that after a certain number of waves and for a specific wave height, the model was stable.

The action of ice in berm breakwater with concrete units is also an important topic of investigation, due to the possibility of building these structures at locations where this action is significant.

An analysis of cost would, of course, be needed in order to entirely know the viability of these structures.

12. REFERENCES

Baird, W. and K. Woodrow (1987). The development of a design for a breakwater at Keflavik, Iceland. In D. Willis, W. Braid, and O. Maggon (Eds.), *Berm Breakwaters: Unconventional Rubble-Mound Breakwaters,* pp.138-146. ASCE.

B.N.M. van Zwicht, H.J. Verhagen, P.B. Bakker (2010). "Effect of the concrete density on the stability of Xbloc armour units". 32nd International Conference on Coastal Engineering, Shanghai

CUBIPOD. "The idea: the evolution from cube to cubipod" (2013). From http://www.cubipod.com

"CUBÍPODO" (2013b). From http://www.lpc.upv.es/index.php?id=64

Frigaard, P., Jensen, M.S., and Hald, T. (1996). Berm Breakwater Design – influence of rock shape. Berm Breakwater Structures, MAS2 – CT94 – 0087. Hydraulics & Coastal Eng. Lab., Aalborg University, October 1996.

Goda, Y. (1994). On the Uncertainties of Wave Heights and the Design Load for Maritime Structures. *Proceeding of the International Workshop on "Wave Barriers in Deepwaters"*, Port and Harbour Research Institute, Yokosuka, Japan, January 10-14, 1994

Goda, Y. (2000). *Random Seas and Design of Maritime Structures* (2n ed.). World Scientific.

Goda, Y. and Suzuki, Y. (1976): "Estimation of incident and reflected waves in random wave experiments. Proceedings, *15th International Conference of Coastal Engineering*, Honolulu, HI, Vol.1, pp.828-845.

Gómez-Martín, M.E., J.R. Medina (2007). "Cubipod concrete armour unit and heterogeneous packing". Coastal Structures.

Gómez-Martín, M.E (2013). Ingeniería Marítima y Costera, lecture notes. University of Alicante, Internal Note.

Klopman, G., Jentsje W. and Van der Meer (1999) "Random Wave Measurements in Front of Refrective Structures". Journal of Waterway, Port, Coastal, and Ocean Engineering.

Mansard, E. and Funke, E. (1980): The measurement of incident and reflected spectra using a least squares method. Proceedings, 17th International Conference on Coastal Engineering, Sydney, Vol. 1, pp. 154-172.Kajima (1969),

Medina, J.R., M.E. Gómez-Martín, and A. Corredor. 2010. "Influence of armor unit placement on armor porosity and hydraulic stability". *Proc. 32nd International Conference on Coastal Engineering*, ASCE, Paper No. 255/structures.41.

Pardo, V., M.P. Herrera, J. Molines and J. R. Medina (2012). "Placement grids, porosity and randomness of armor layers". Coastal Engineering 2012

Menze, A. (2000). *Stability of multilayer berm breakwaters*. Master Thesis, NTNU.

Myhra, H. (2005). *Berm breakwaters. Influence of construction method and storm duration on stability ice ride-up*. Master Thesis, NTNU.

Newberry, S., J. Latham, T. Stewart, and J. Simm (2002). "The effect of rock shape and construction methods on rock armour layer". *Proc. International Coference on Coastal Engineering*, UK.

Lissev, N. (1993): Influence of the core configuration on the stability of berm breakwaters. Experimental model investigation. Report No. R-6-93. Department of Structural Engineering, Norwegian Institute of Technology, Norway.

Rauw, C.I. (1987). "Berm type armor protection for a runway extension at Unalaska, Alaska". In *Berm Breakwaters*. Edited by D.H.Wills, W.F.Baird and O.T.Magoon. Published by ASCE.

Scholtz , D.J.P., Zwamborn, J.A.(1982) "Dolosse stability. Effect of block density and waist thickness". *Proceedings of the 18th ICCE 1982*, Cape Town, South Africa pp. 2026-2046

Sigurdarson, S., Viggosson, G., Benediktsson, S., Einarsson, S., & Smarason, O. (2001). "Berm Breakwaters, Fifteen Years Experience". Coastal Engineering Proceedings, 1(26). doi:10.9753/icce.v26.

Sigurdarson, S., Jacobsen, Smarason, Bjordal, Viggosson, Urrang and Tørum, (2003). "Sirevåg Berm Breakwater, design, construction and experience after design storm". *Proc. Coastal Structures 2003*, Portland, USA, ASCE.

Sigurdarson, S., O.B. Smarason and G. Viggosson (2006). "Appendix II: Berm Breakwaters" at Per Bruun, *Port Engineering*, 5th edition, Chapter 3.

Sigurdarson, S., O.B. Smarason, G. Viggosson and S. Bjørdal (2006b). Wave height limits for the statically stable Icelandic-type Berm Breakwater, ICCE, ASCE

Subba Rao, Kiran G. Shirlal, Balakrshna Rao K. and Prashanth J. (2012). "Berm Breakwater Study with Concrete Cubes – An Experimental Approach". *8th International conference on Coastal and Port Engineering in Developing Countries.* COPEDEC 2012, IIT Madras, Chennai, INDIA. 20-24 February 2012.

Tørum, A. (1997). "Berm breakwaters – EC MAST II Berm Breakwater Structures. Technical Report, SINTEF.

Tørum, A., Krogh, S.R. Bjørdal, S., Fjeld, S., Archetti, R. and Jacobsen, A. (1999): Design criteria and design procedures for berm breakwaters. Proceedings of the international conference "Coastal Structures'99", Santander, Spain. Editor I.Losada.. A.A Balkema/Rotterdam/ Brookfield /2000.

Tørum, A. and Krogh, S.R. (2000): Berm breakwaters. Stone quality. SINTEF Report STF22 A00207, July 2000.

Tørum, A., Kuhnen, F. and Menze, A. (2003): On berm breakwaters. Stability, scour, overtopping. Coastal Engineering, Vol. 49 (2003) pp 209 – 238.

Tørum, A. (2007b): Berm beakwaters revisited. Internal note, Dept. of Civil and Transport Engineering, Norwegian University of Science and Technology, Trondheim, Norway.

Tørum, A. (2011). Coastal Structures, lecture notes. NTNU, Internal Note.

Tørum, A., M. N. Moghim, K. Westeng, N. Hidayati and Ø. Arntsen (2012). "On berm breakwaters: Recession, crown wall wave forces, reliability". Coastal Engineering 60.

US Army Corps of Engineers (2002). Coastal Engineering Manual, EM 1110-2-1100 (Part VI), Change 3 (28 Sep 11). Chapter 5.

Westeng (2011). *Berm Breakwaters – A Modified Version.* Master Thesis, NTNU.

PIANC (2003). Working Group 40 of the Maritime Navigation Commission. "State-Of-The-Art of Designing and Constructing Berm Breakwaters". International Navigation Association.

Thornton, E.B. and R.J. Calhoun (1972), "Spectral Resolution of Breakwater Reflected Waves", *Journal ASCE Waterways Harbour and Coastal Engineering*, WW4.

Zwamborn, J.A. (1978) "Dolos packing density and effect of relative Block density". *Proceedings of the 16th ICCE 1978*, Hamburg, Germany. pp 2285-2304

13. LIST OF SIMBOLS

A_t = total area where the blocks are placed

C_R = average reflection coefficient

D_n = nominal diameter

D_{n50} = equivalent cube length

D_{n15} = 15% of the stones have a smaller diameter than D_{n15}

D_{n85} = 85% of the stones have a smaller diameter than D_{n85}

f_g = gradation factor

f_p = frequency corresponding to the maximum spectral density

g = acceleration of gravity

H_s = significant wave height

h_s = height of a single stone

H = wave height impacting at the breakwater

H_{m0} = significant wave height

Ho = stability number

$HoTo$ = period stability number

$Ho\sqrt{To}$ = square root period stability number

h_f = water depth in front of the berm breakwater with no recession or accretion

K_s = shoaling coefficient

$K1, K2\ and\ K3$ = constants

k = volume reduction factor

L_0 = wave length at deep water

l_s = length of a single stone

m = scaling factor

m_0 = zero moment of the original variance spectrum

m_1 = first moment of the original variance spectrum

m_2 = second moment of the original variance spectrum

m_4 = fourth moment of the original variance spectrum

m_n = spectral moments

m_s = mass of a single stone

N = number of blocks placed in an area A_t in one layer

N_s = stability number

n = number armour unit's layers

p = layer porosity

R^2 = coefficient of determination

Rec = recession

S^2 = standard deviation

$S_R(f)$ = reflected spectrum

$S_I(f)$ = incident spectrum

T_p = peak period

T_z = mean wave period, or zero up-crossing period

T_{01} = mean wave period

W = mass

W_{50} = median stone mass, i.e. 50% of the stones are larger (or smaller) than W_{50}

w_s = width of a single stone

z = distance to the bottom of the flume

$$\Delta = \frac{\rho_s}{\rho_w} - 1$$

Δl = distance between wave gauges

γ = peak enhance factor

ε_4 = spectral width or broadness parameter

ϕ = packing density

φ = placing density

ρ_s = density of stone

ρ_w = density of water

APPENDIX A. STONE GRADING CURVES

The curves presented below are extracted from Westeng (2011), as the rock used in this investigation was the same used by him. He measured 3 samples of each class of rock, with 200 individual stones at each sample.
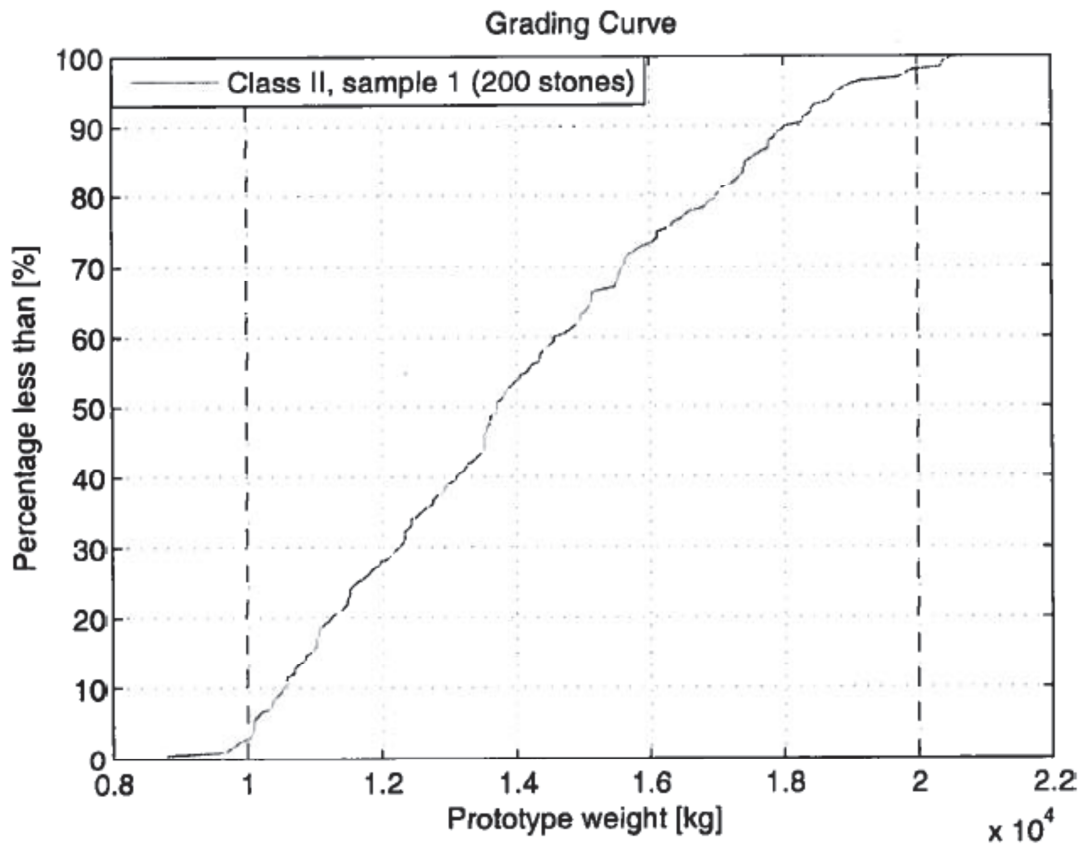
Figure 1. Grading curve for class II, sample 1.
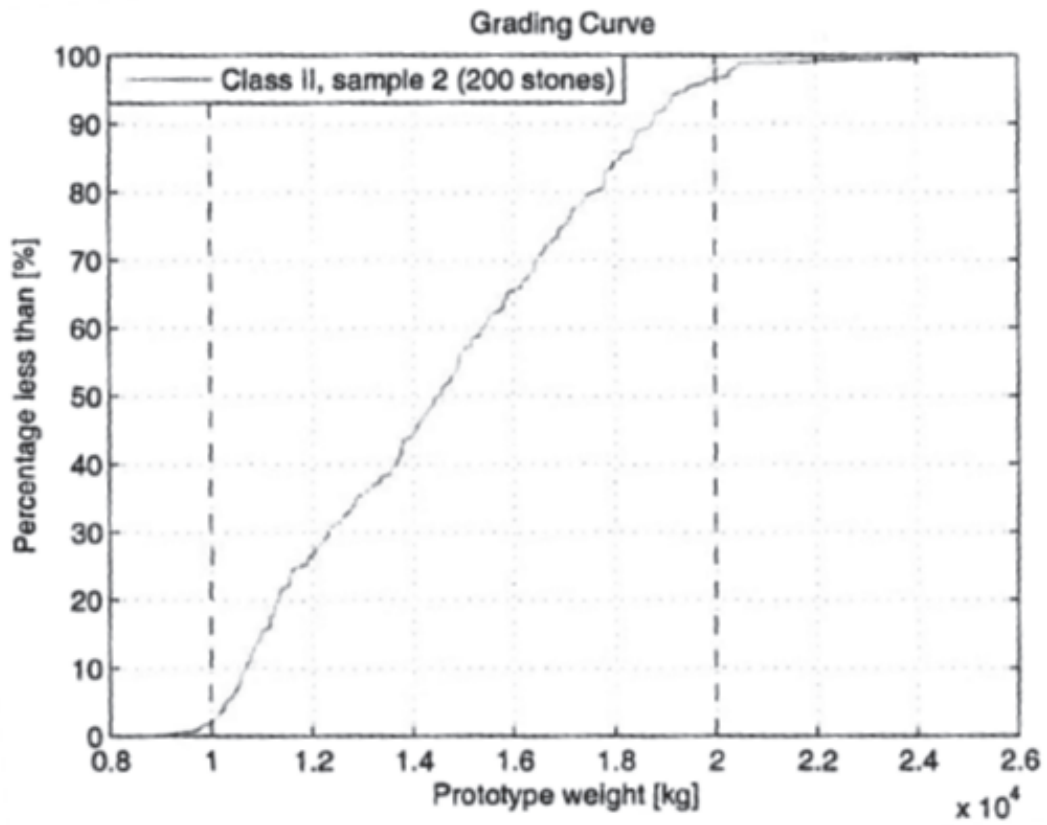
Figure 2. Grading curve for class II, sample 2.
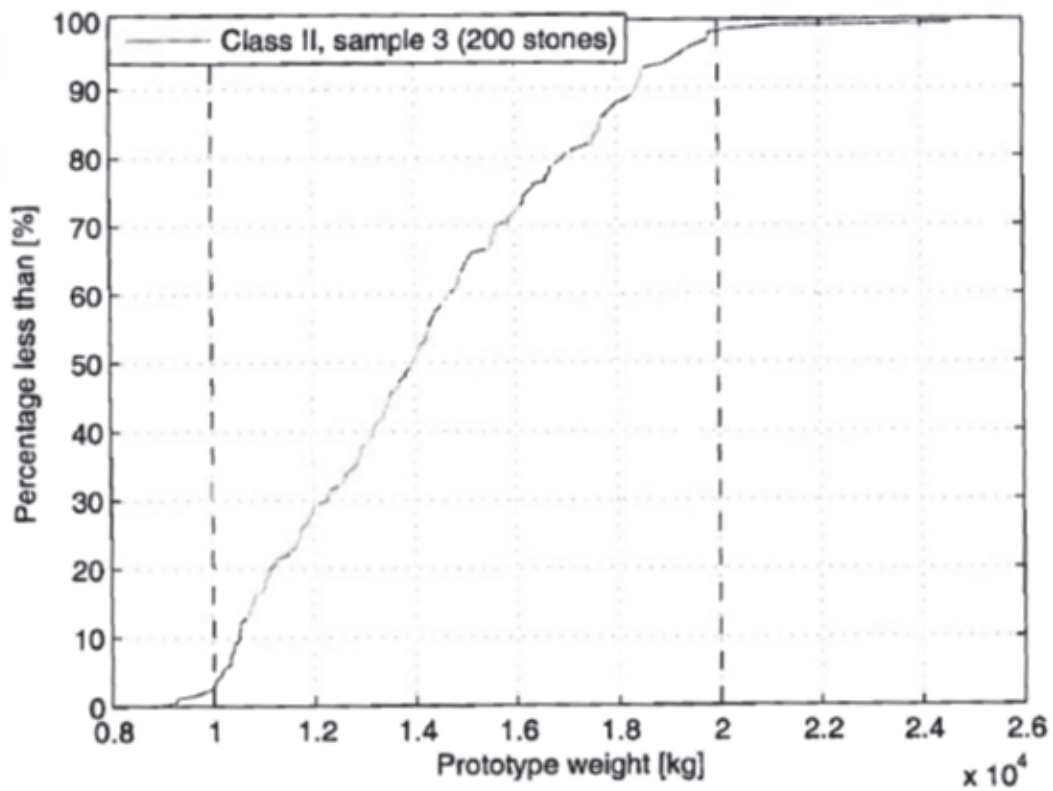
Figure 3. Grading curve for class II, sample 3.

Master Thesis, spring 2013   Altea Cámara Aguilera   NTNU
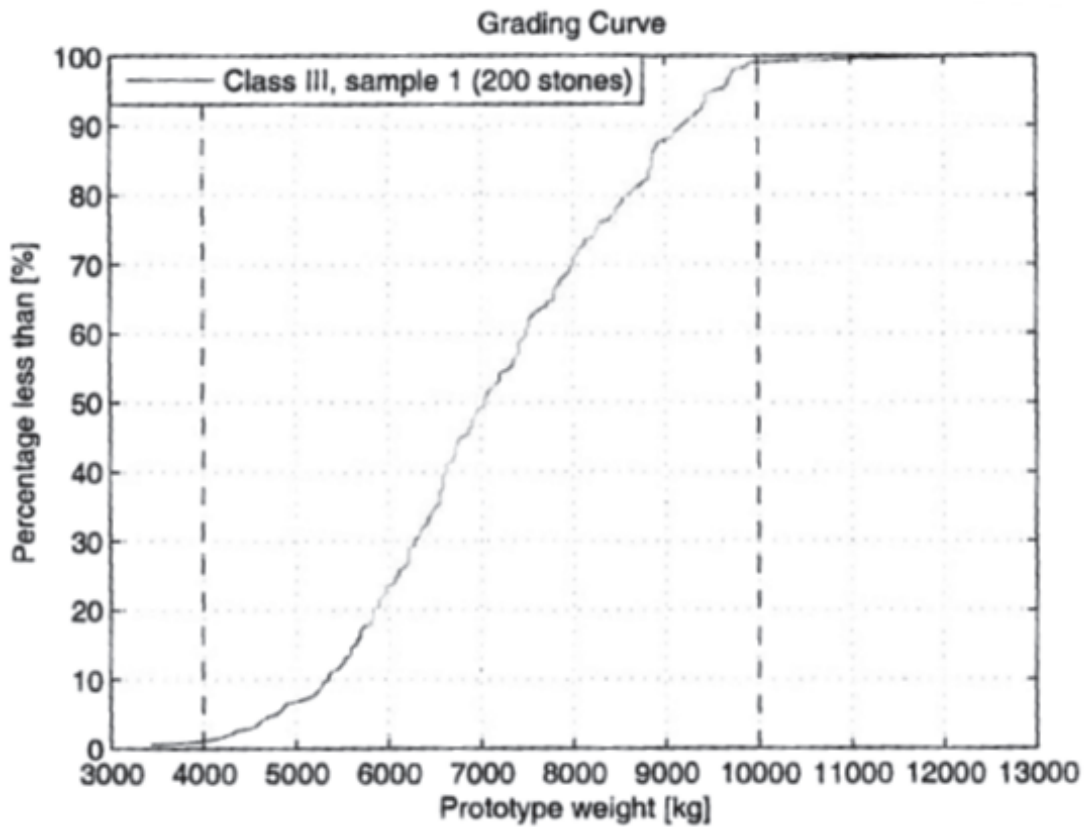
Figure 4. Grading curve for class III, sample 1.
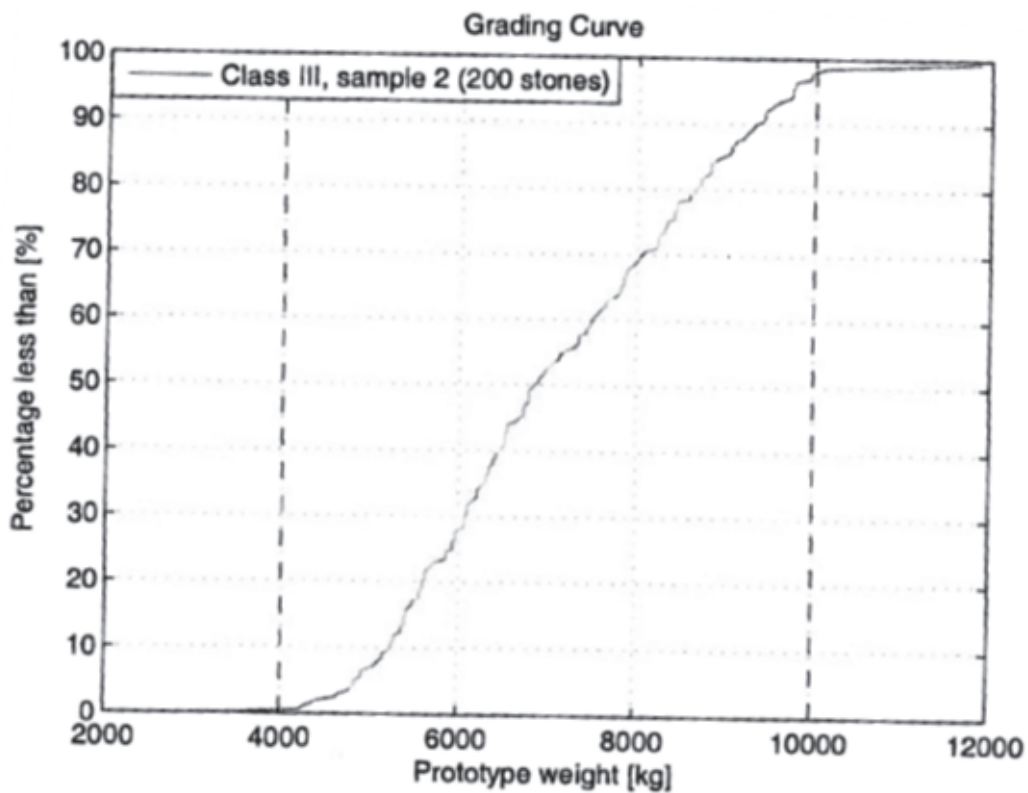
Figure 5. Grading curve for class III, sample 2.
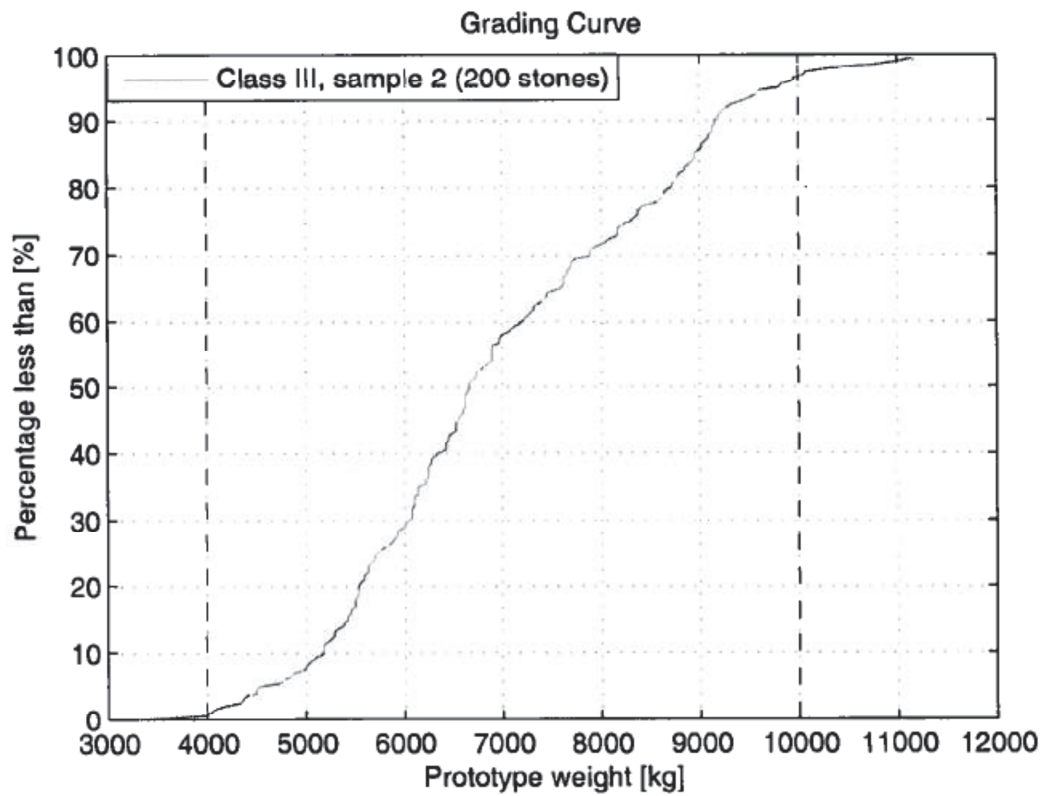
Figure 6. Grading curve for class III, sample 3.

APPENDIX B. CONCRETE BLOCKS CHARACTERISTICS

The density and volume of the concrete cubes and cubipods used to build the models was calculated by measuring the dry and submerged weight of a sample of the blocks. Ten concrete cubes and 20 concrete cubipods were measured. The values obtained and the averages calculated are shown in the tables below.

Table B.1. Concrete cubes measurement
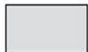
Sample	Model values					Prototype values		
	Dry weight [g]	Submerged weight [g]	Volume [cm3]	Dn [cm]	Density [g/cm3]	W [t]	Dn [m]	Density [kg/m3]
1	79.9	46.4	33.5	3.22	2.385	27.41	2.257	2385
2	78.4	44.7	33.7	3.23	2.326	26.89	2.261	2326
3	81.3	46.4	34.9	3.27	2.330	27.89	2.288	2329
4	80.4	45.4	35	3.27	2.297	27.58	2.290	2297
5	79.9	45.8	34.1	3.24	2.343	27.41	2.270	2343
6	79.7	45.8	33.9	3.24	2.351	27.34	2.266	2351
7	79.8	45.4	34.4	3.25	2.320	27.37	2.277	2319
8	79.7	45.6	34.1	3.24	2.337	27.34	2.270	2337
9	81	46.7	34.3	3.25	2.362	27.78	2.274	2361
10	79.8	44.5	35.3	3.28	2.261	27.37	2.296	2260
Average	**79.99**	45.67	34.32	**3.25**	**2.331**	**27.44**	**2.275**	**2331**
Standard Deviation	0.795	0.717	0.587	0.018	0.034			
Variance	0.632	0.513	0.344	0.000	0.001			

Table B.2. Concrete cubipods measurement

Sample	Model values					Prototype values		
	Dry weight [g]	Submerged weight [g]	Volume [cm3]	Density [g/cm3]	Dn [cm]	W [t]	Dn [m]	Density [kg/m3]
1	64.9	34.8	30.1	2.156	3.111	22.26	2.177	2156
2	61.7	32.5	29.2	2.113	3.079	21.16	2.156	2113
3	58.3	30	28.3	2.06	3.047	20.00	2.133	2060
4	64.4	34.6	29.8	2.161	3.1	22.09	2.17	2161
5	58.8	32.4	26.4	2.227	2.978	20.17	2.084	2227
6	62.5	32.4	30.1	2.076	3.111	21.44	2.177	2076
7	60.2	30.4	29.8	2.02	3.1	20.65	2.17	2020
8	62.2	31.7	30.5	2.039	3.124	21.34	2.187	2039
9	56.2	25.9	30.3	1.855	3.118	19.28	2.182	1855
10	62.1	31.9	30.2	2.056	3.114	21.30	2.18	2056
11	62.2	32.3	29.9	2.08	3.104	21.34	2.173	2080
12	62.7	32.8	29.9	2.097	3.104	21.51	2.173	2097
13	64.8	33.4	31.4	2.064	3.155	22.23	2.208	2064
14	65.6	35.1	30.5	2.151	3.124	22.50	2.187	2151
15	65.5	35.1	30.4	2.155	3.121	22.47	2.185	2155
16	58.3	28.1	30.2	1.93	3.114	20.00	2.18	1930
17	61.1	30.7	30.4	2.01	3.121	20.96	2.185	2010
18	58.9	29.6	29.3	2.01	3.083	20.20	2.158	2010
19	62.5	32.5	30	2.083	3.107	21.44	2.175	2083
20	62	31.9	30.1	2.06	3.111	21.27	2.177	2060
Average	**61.75**	31.905	29.84	**2.07**	**3.101**	**21.18**	**2.171**	**2070**
Standard Deviation	2.745	2.536	1.254	0.101	0.045			
Variance	7.533	6.432	1.573	0.01	0.002			

APPENDIX C. BREAKWATER PROFILES

KEY:

	Cubipods
	Concrete blocks
	Class II rock
	Class III rock
	Class IV rock
	Class V rock

SETUP 1

PROTOTYPE [m]
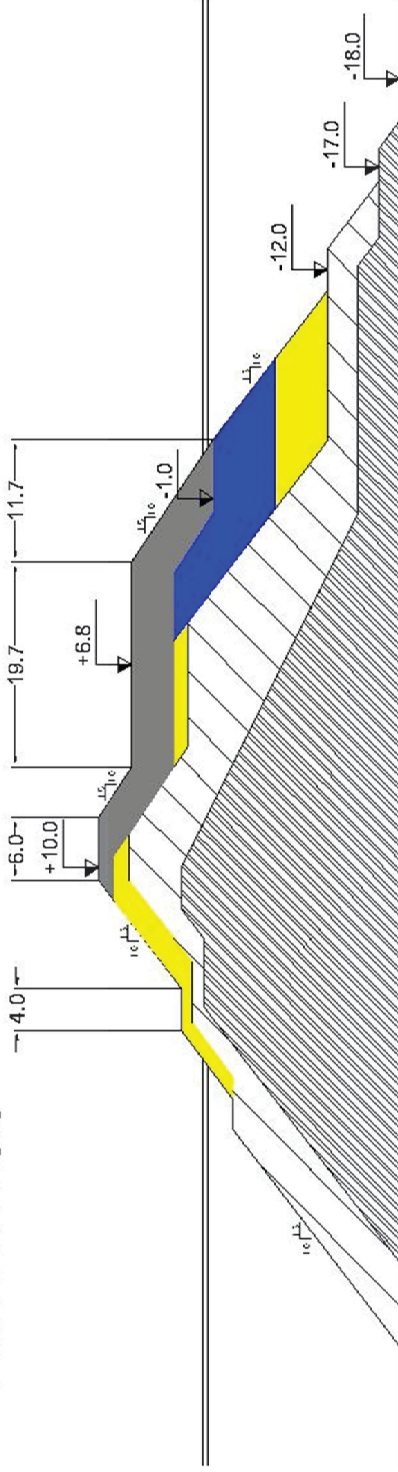
MODEL [cm]
1:70
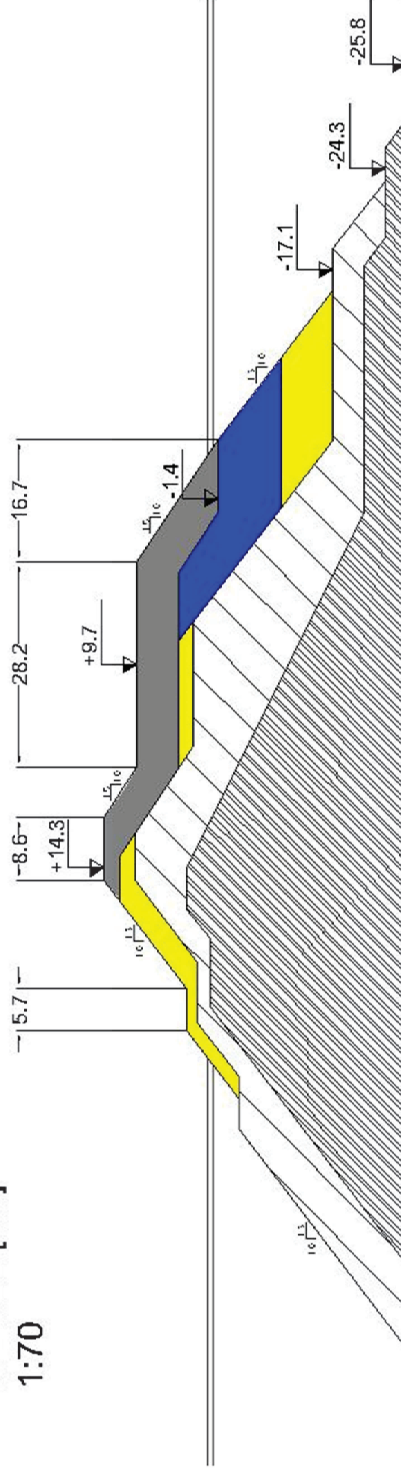
Figure C.1. Prototype and model cross section of the breakwater in the setup 1.

Master Thesis, spring 2013   Altea Cámara Aguilera   NTNU
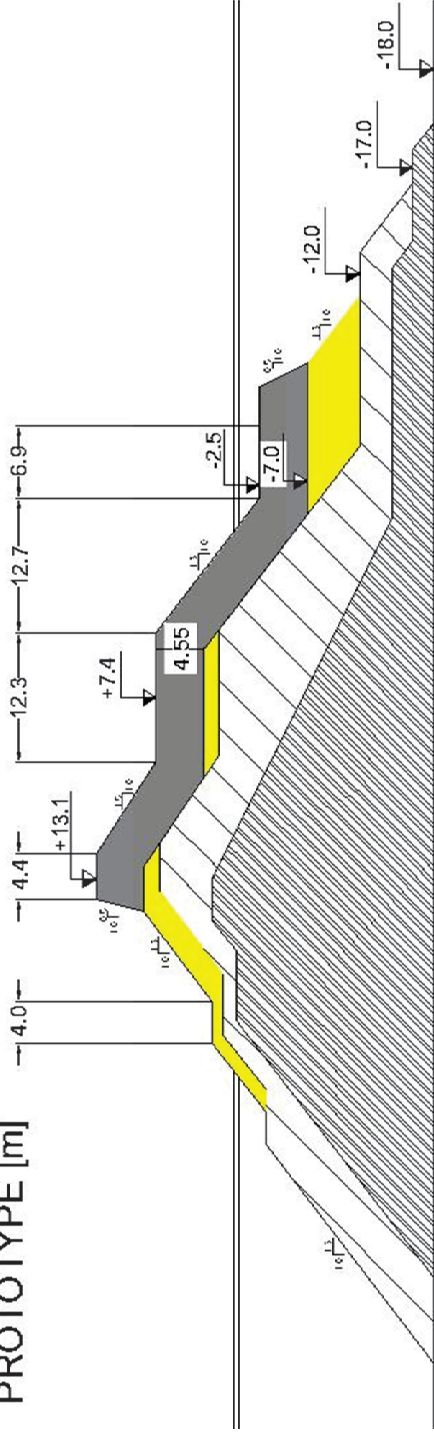
PROTOTYPE [m]
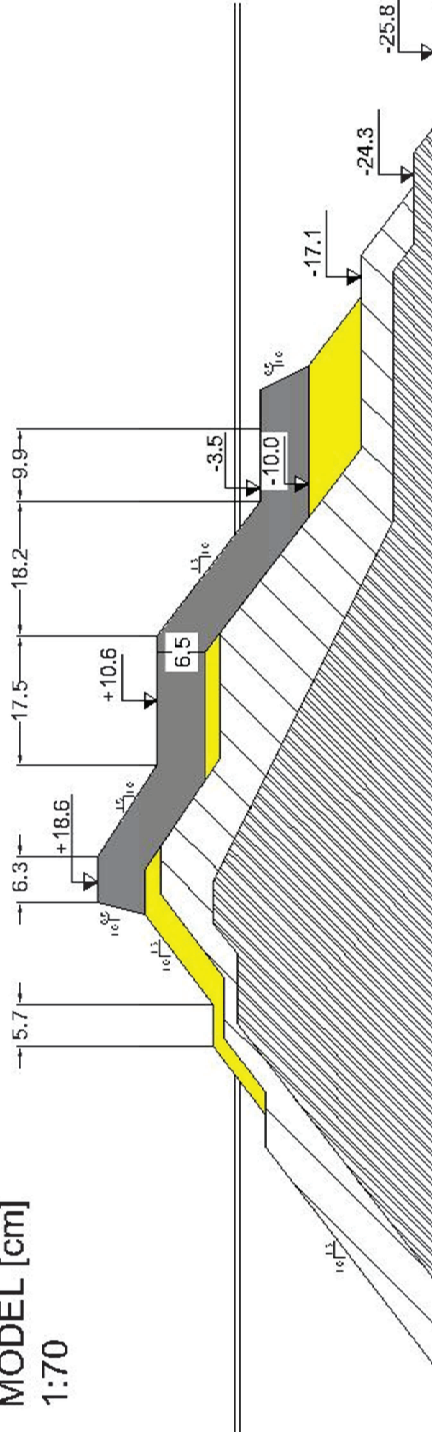
MODEL [cm]
1:70

Figure C.2. Prototype and model cross section of the breakwater in the setup 2.

SETUP 3

PROTOTYPE [m]
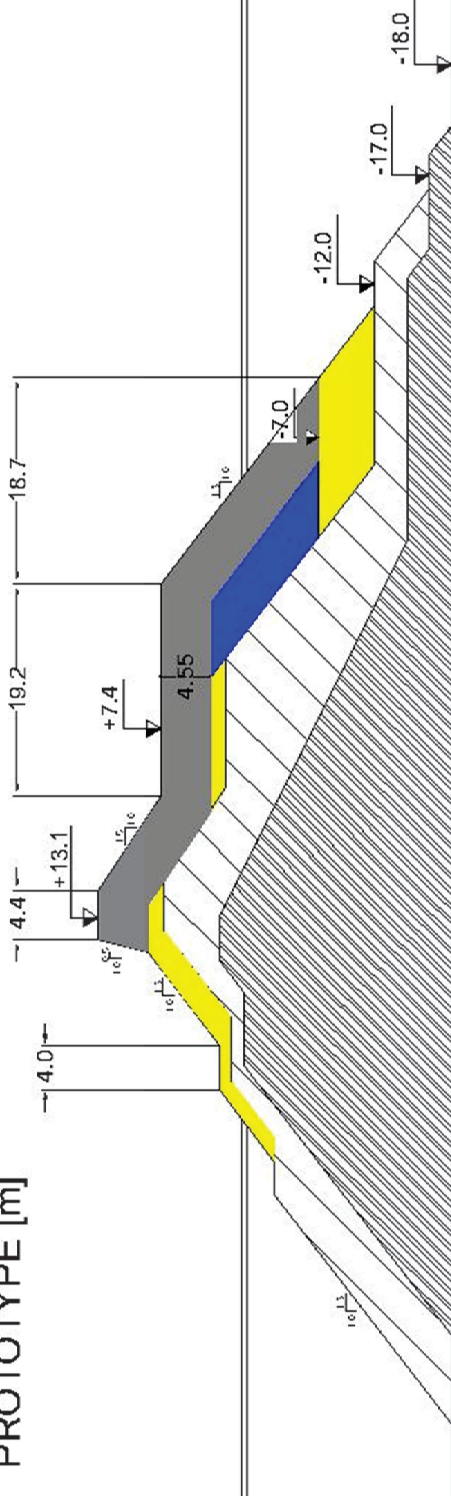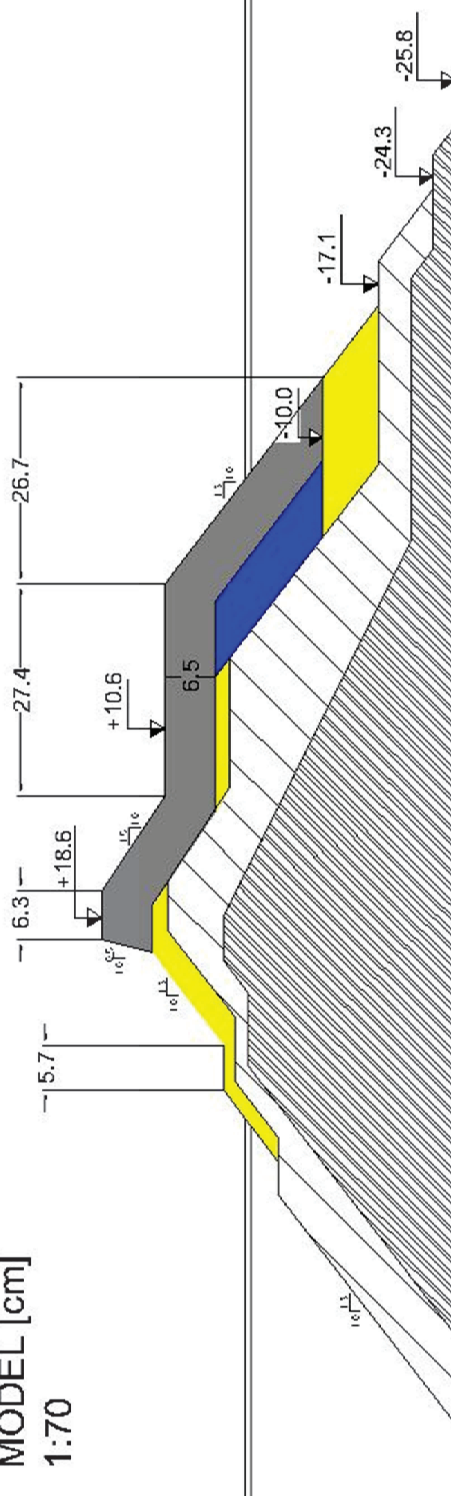
MODEL [cm]
1:70

Figure C.3. Prototype and model cross section of the breakwater in the setup 3.
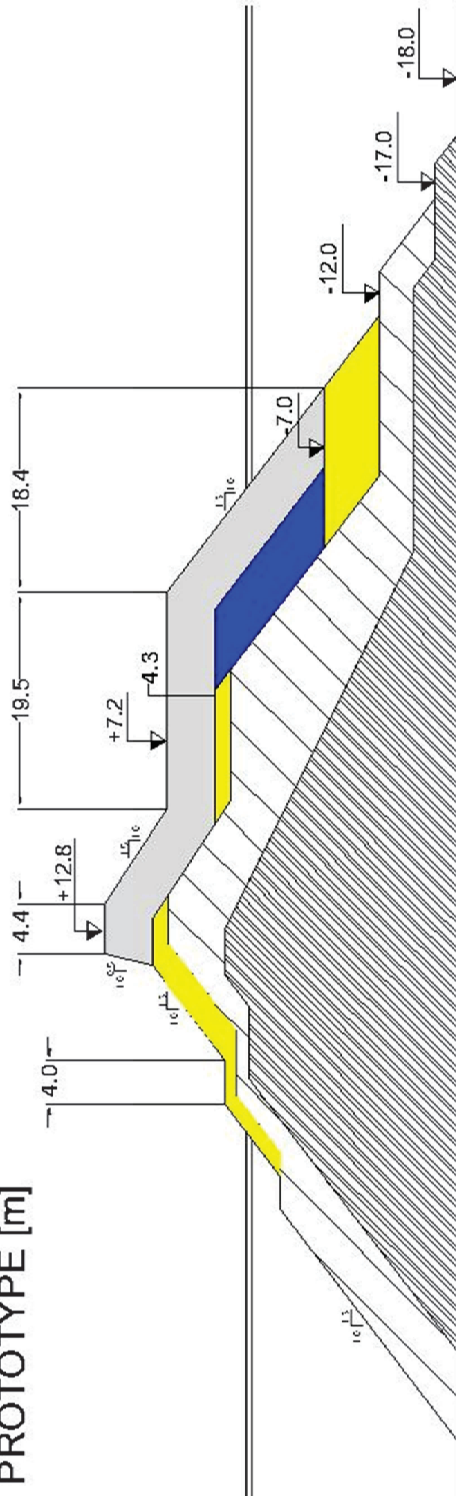
PROTOTYPE [m]
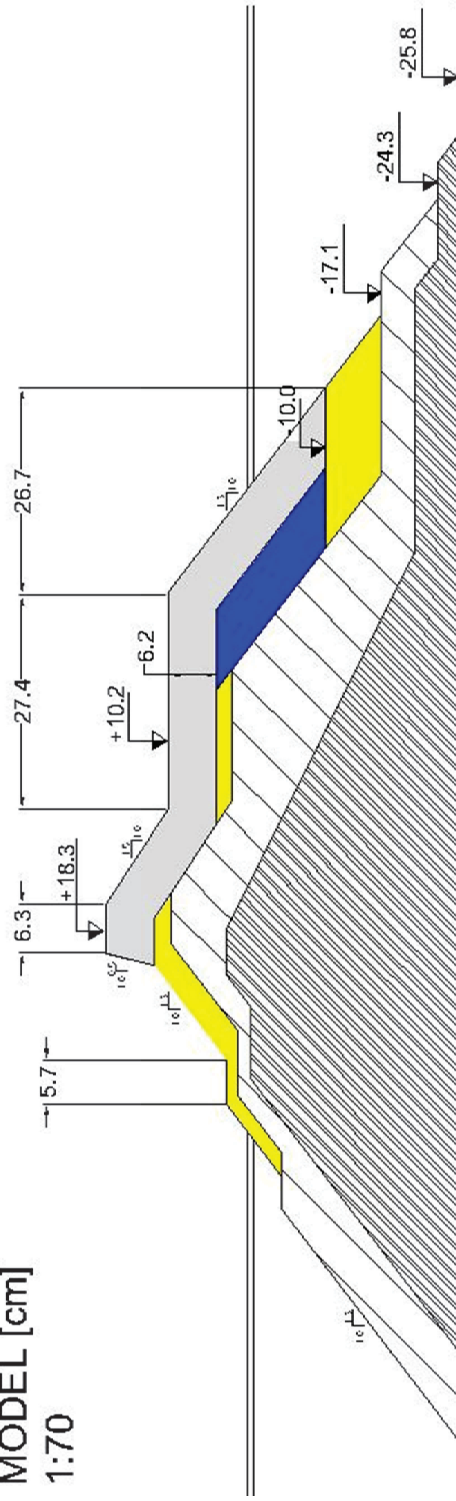
MODEL [cm]
1:70

Figure C.4. Prototype and model cross section of the breakwater in the setups 4 and 5

Master Thesis, spring 2013   Altea Cámara Aguilera   NTNU

APPENDIX D. PROFILES DISTRIBUTION

Six profiles are extracted from the laser data at each run. The location of these profiles is show in the figure below. There is a distance between profile of 10 cm and between the lateral walls and the closest profiles 5 cm.
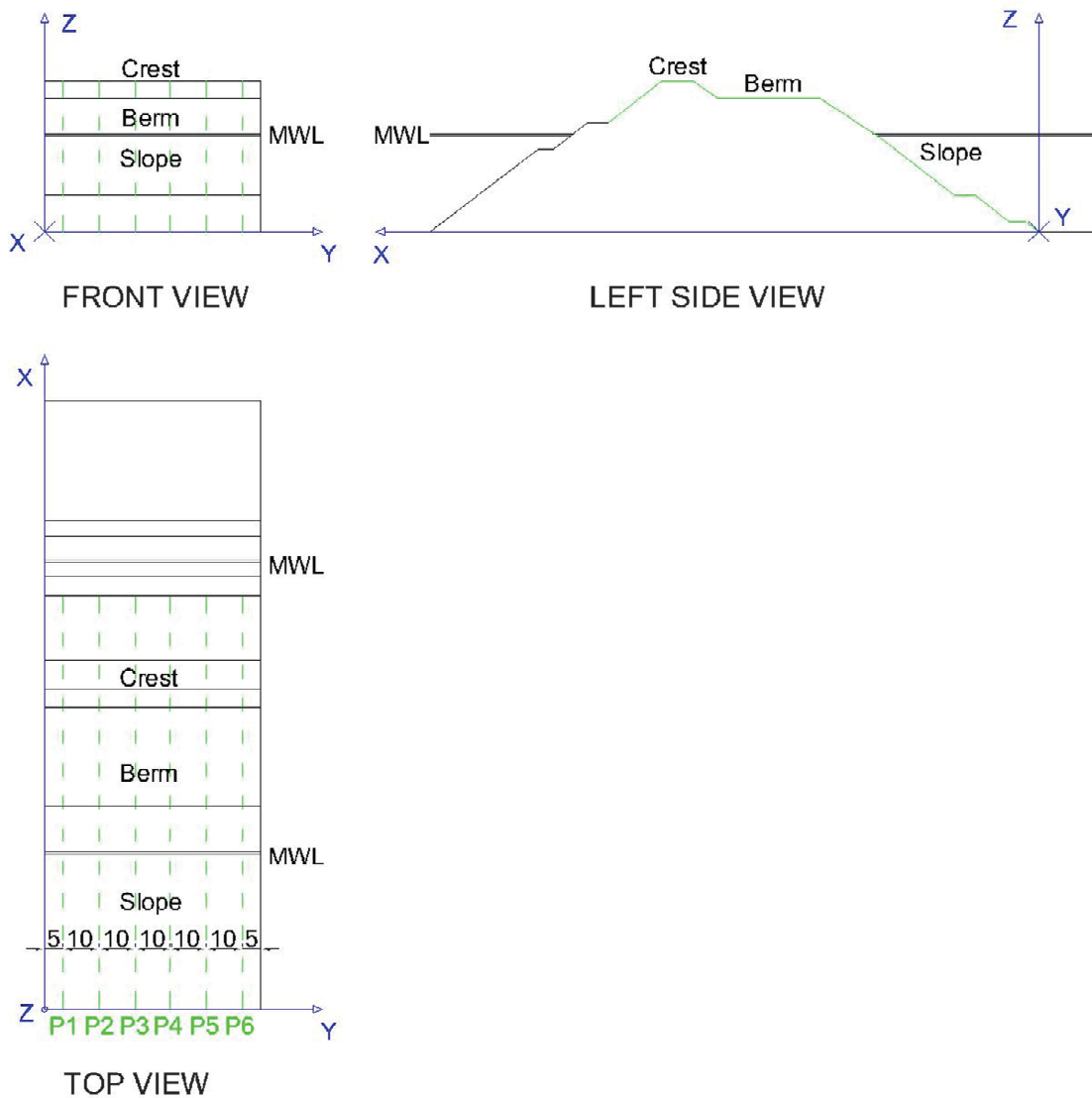
Figure D.1. Views of the profile distribution.

APPENDIX E. WAVE RECORDS AND CALCULATIONS

The water level during the tests was registered by 7 wave gauges. With the data recorded by the 5 five gauges situated at deep water a reflection analysis was made. For this analysis different parameters from the incoming wave spectrum were obtained, as the significant wave height in deep water, the mean wave period, the peak wave period and the number of waves. This data is registered in the tables below. Afterwards, the shoaling effect due to the slope existing between the deep water wave gauges and the structure was calculated. Ks was extracted from the figure 3.22 at Goda (2000).
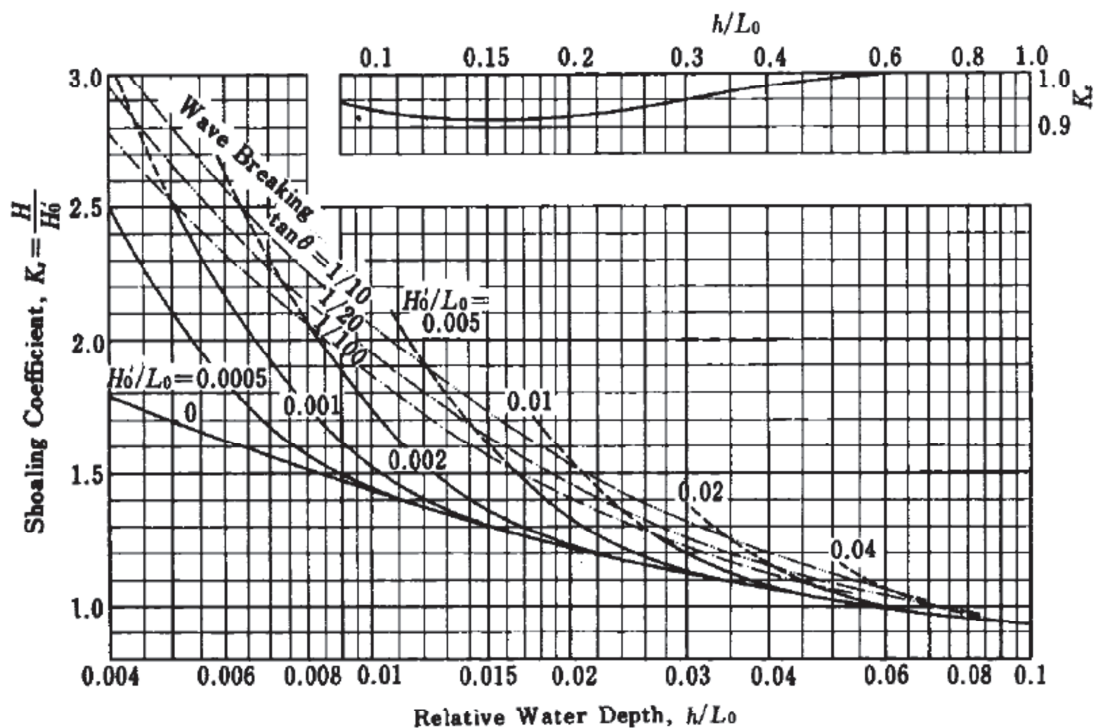
Fig. 3.22. Diagram of nonlinear wave shoaling.

Figure E.1. Diagram of nonlinear wave shoaling from Goda (2000)

With the value of the wave height that was acting at the structure, the values of Ho, To, HoTo, Ho√To and s_{mo} where calculated.

In the tables below are registered all the values calculated.

SETUP 1

Table E.1. Wave records and calculation from setup 1

	Output from reflection analysis (model scale)				Shoaling calculation		Waves at the breakwater (prototype scale)			Wave parameters			
	Tp [s]	Tz [s]	H$_0$ [m]	Number of waves	Ks	Hs [m]	Tp [s]	Tz [s]	Hs [m]	Ho	HoTo	Ho√To	s$_{mo}$
Step 1	1.296	1.032	0.051	1058	0.93	0.047	10.9	8.7	3.3	1.08	19.38	4.58	0.028
	1.296	1.028	0.05	1063	0.93	0.047	10.9	8.6	3.3	1.08	19.3	4.57	0.028
Step 2	1.403	1.135	0.063	962	0.96	0.061	11.8	9.5	4.3	1.41	27.67	6.25	0.03
	1.403	1.126	0.063	970	0.96	0.061	11.8	9.5	4.3	1.41	27.58	6.24	0.031
Step 3	1.495	1.234	0.082	885	0.98	0.08	12.6	10.4	5.6	1.85	39.5	8.55	0.034
	1.495	1.229	0.081	889	0.98	0.08	12.6	10.3	5.6	1.85	39.4	8.53	0.034
Step 4	1.941	1.336	0.102	818	1.09	0.111	16.3	11.2	7.8	2.47	55.95	11.62	0.04
	1.693	1.331	0.101	821	1.01	0.102	14.2	11.2	7.2	2.36	54.66	11.37	0.037
Step 5	1.941	1.446	0.109	755	1.1	0.12	16.3	12.1	8.4	2.79	70.09	13.98	0.037
	1.941	1.445	0.11	756	1.1	0.121	16.3	12.1	8.5	2.79	70.19	14.01	0.037
Step 6	1.693	1.346	0.114	812	1.02	0.115	14.2	11.3	8.1	2.67	62.4	12.91	0.041
	1.693	1.346	0.114	812	1.02	0.115	14.2	11.3	8.1	2.67	62.39	12.9	0.041
Step 7	1.253	1.034	0.049	1057	0.93	0.045	14.2	11.3	3.2	1.05	24.61	5.09	0.016
	1.432	1.124	0.062	972	0.95	0.059	14.2	11.3	4.1	1.36	31.86	6.59	0.021
	1.495	1.23	0.079	888	0.96	0.076	14.2	11.3	5.3	1.75	40.86	8.45	0.027
	1.693	1.331	0.096	821	1	0.096	14.2	11.3	6.7	2.22	51.93	10.74	0.034
	1.941	1.331	0.111	758	1.1	0.122	16.3	11.2	8.5	2.81	65.05	13.53	0.044
	1.693	1.442	0.118	812	1.05	0.124	14.2	12.1	8.7	2.86	71.6	14.31	0.038

SETUP 2

Table E.2. Wave records and calculation from setup 2

	Output from reflection analysis (model scale)				Shoaling calculation		Waves at the breakwater (prototype scale)			Wave parameters			
	Tp [s]	Tz [s]	H_0 [m]	Number of waves	Ks	Hs [m]	Tp [s]	Tz [s]	Hs [m]	Ho	HoTo	HovTo	s_{mo}
Step 1	1.268	1.034	0.046	1058	0.93	0.043	10.7	8.7	3.0	1.00	17.99	4.25	0.026
	1.422	1.028	0.045	1063	0.975	0.044	11.9	8.6	3.1				
Step 2	1.489	1.125	0.060	962	0.98	0.059	12.5	9.5	4.1	1.38	26.86	6.08	0.030
	1.432	1.121	0.061	970	0.975	0.060	12.0	9.4	4.2				
Step 3	1.495	1.227	0.079	885	0.98	0.077	12.6	10.3	5.4	1.80	38.25	8.29	0.033
	1.495	1.226	0.079	889	0.98	0.078	12.6	10.3	5.5				
Step 4	1.693	1.330	0.101	818	1.01	0.102	14.2	11.2	7.1	2.38	55.03	11.44	0.037
	1.820	1.332	0.101	821	1.03	0.104	15.3	11.2	7.3				
Step 5	1.941	1.442	0.112	755	1.08	0.120	16.3	12.1	8.4	2.79	69.84	13.95	0.037
	1.941	1.443	0.112	756	1.08	0.121	16.3	12.1	8.4				
Step 6	1.820	1.451	0.121	753	1.03	0.124	15.3	12.2	8.7	2.88	72.47	14.44	0.038
	1.820	1.449	0.121	754	1.03	0.125	15.3	12.2	8.7				
Step 7	1.253	1.038	0.050	1053	0.925	0.046	10.5	8.7	3.2	1.07	19.25	4.53	0.028
	1.432	1.126	0.063	970	0.975	0.061	12.0	9.5	4.3	1.42	27.80	6.29	0.031
	1.495	1.229	0.080	889	0.98	0.078	12.6	10.3	5.5	1.81	38.72	8.38	0.033
	1.693	1.333	0.098	819	1.01	0.099	14.2	11.2	7.0	2.30	53.21	11.06	0.036
	1.941	1.444	0.112	757	1.08	0.122	16.3	12.1	8.5	2.81	70.48	14.07	0.037
	1.820	1.448	0.123	755	1.03	0.126	15.3	12.2	8.8	2.92	73.50	14.66	0.039

SETUP 3

Table E.3. Wave records and calculation from setup 3

	Output from reflection analysis (model scale)				Shoaling calculation		Waves at the breakwater (prototype scale)			Wave parameters			
	Tp [s]	Tz [s]	H_0 [m]	Number of waves	Ks	Hs [m]	Tp [s]	Tz [s]	Hs [m]	Ho	HoTo	Ho√To	s_{mo}
Step 1	1.154	1.031	0.051	1060	0.92	0.047	9.7	8.7	3.3	1.08	19.29	4.57	0.028
	1.154	1.025	0.051	1066	0.92	0.047	9.7	8.6	3.3				
Step 2	1.403	1.128	0.064	969	0.95	0.061	11.8	9.5	4.3	1.41	27.56	6.23	0.031
	1.403	1.124	0.064	971	0.95	0.061	11.8	9.4	4.3				
Step 3	1.569	1.232	0.082	887	0.98	0.080	13.2	10.3	5.7	1.86	39.84	8.61	0.034
	1.569	1.231	0.082	887	0.98	0.081	13.3	10.3	5.6				
Step 4	1.941	1.340	0.100	815	1.1	0.110	16.3	11.3	7.7	2.56	59.66	12.36	0.039
	1.941	1.341	0.102	815	1.1	0.112	16.3	11.3	7.8				
Step 5	1.941	1.451	0.114	752	1.1	0.126	16.3	12.2	8.8	2.91	73.38	14.61	0.038
	1.941	1.452	0.114	752	1.1	0.126	16.3	12.2	8.8				
Step 6	1.941	1.455	0.125	751	1.1	0.137	16.3	12.2	9.6	3.17	79.98	15.91	0.041
	1.941	1.453	0.124	752	1.1	0.137	16.3	12.2	9.6				
Step 7	1.154	1.028	0.050	1062	0.92	0.046	9.7	8.6	3.2	1.06	18.88	4.47	0.028
	1.403	1.128	0.063	968	0.95	0.060	11.8	9.5	4.2	1.38	27.06	6.11	0.030
	1.569	1.234	0.081	885	0.97	0.079	13.2	10.4	5.5	1.82	38.95	8.41	0.033
	1.781	1.341	0.099	815	1.02	0.101	15.0	11.3	7.1	2.34	54.47	11.28	0.036
	1.932	1.458	0.115	749	1.07	0.123	16.2	12.3	8.6	2.84	71.96	14.30	0.037
	1.932	1.462	0.125	747	1.07	0.135	16.2	12.3	9.4	3.11	79.14	15.70	0.040

Table E.4. Wave records and calculation from setup 4

	Output from reflection analysis (model scale)				Shoaling calculation		Waves at the breakwater (prototype scale)			Wave parameters			
	Tp [s]	Tz [s]	H_0 [m]	Number of waves	Ks	Hs [m]	Tp [s]	Tz [s]	Hs [m]	Ho	HoTo	HoVTo	s_{mo}
Step 1	1.296	1.033	0.050	1058	0.94	0.047	10.9	8.7	3.26	1.41	25.82	6.03	0.028
	1.296	1.030	0.050	1061	0.94	0.047	10.9	8.7	3.27				
Step 2	1.403	1.128	0.062	968	0.95	0.059	11.8	9.5	4.10	1.78	35.65	7.96	0.030
	1.495	1.125	0.062	971	0.96	0.059	12.6	9.5	4.16				
Step 3	1.495	1.233	0.079	886	0.965	0.077	12.6	10.4	5.36	2.31	50.59	10.81	0.032
	1.495	1.231	0.079	887	0.965	0.077	12.6	10.3	5.36				
Step 4	1.693	1.341	0.095	815	1	0.095	14.2	11.3	6.68	2.89	68.80	14.09	0.034
	1.693	1.338	0.096	816	1	0.096	14.2	11.2	6.72				
Step 5	1.941	1.448	0.110	754	1.1	0.121	16.3	12.2	8.47	3.57	91.90	18.12	0.036
	1.820	1.442	0.110	757	1.06	0.116	15.3	12.1	8.13				
Step 6	1.820	1.446	0.118	755	1.07	0.126	15.3	12.1	8.83	3.80	97.64	19.25	0.039
	1.820	1.445	0.118	756	1.07	0.126	15.3	12.1	8.81				
Step 7	1.253	1.032	0.050	1059	0.93	0.046	10.5	8.7	3.22	1.39	25.48	5.95	0.028
	1.432	1.121	0.062	975	0.95	0.059	12.0	9.4	4.15	1.79	35.63	7.98	0.030
	1.432	1.221	0.079	895	0.95	0.075	12.0	10.3	5.26	2.27	49.23	10.56	0.032
	1.700	1.325	0.096	824	1	0.096	14.3	11.1	6.72	2.89	68.21	14.05	0.035
	1.820	1.439	0.110	759	1.035	0.113	15.3	12.1	7.93	3.42	87.46	17.29	0.035
	1.820	1.445	0.120	756	1.055	0.126	15.3	12.1	8.83	3.80	97.75	19.28	0.039

SETUP 5

Table E.5. Wave records and calculation from setup 5

	Output from reflection analysis (model scale)				Shoaling calculation		Waves at the breakwater (prototype scale)			Wave parameters			
	Tp [s]	Tz [s]	H_0 [m]	Number of waves	Ks	Hs [m]	Tp [s]	Tz [s]	Hs [m]	Ho	HoTo	HovTo	Som
Step 1	1.154	1.033	0.050	1058	0.92	0.046	9.7	8.7	3.2	1.40	25.61	5.98	0.028
	1.154	1.027	0.050	1064	0.92	0.046	9.7	8.6	3.3				
Step 2	1.495	1.131	0.062	966	0.96	0.059	12.6	9.5	4.2	1.79	35.97	8.02	0.030
	1.495	1.128	0.062	968	0.96	0.059	12.6	9.5	4.2				
Step 3	1.495	1.232	0.078	886	0.96	0.075	12.6	10.4	5.3	2.26	49.56	10.59	0.032
	1.495	1.228	0.078	889	0.96	0.075	12.6	10.3	5.3				
Step 4	1.693	1.331	0.093	820	1	0.093	14.2	11.2	6.5	2.82	66.72	13.71	0.034
	1.693	1.330	0.094	821	1	0.094	14.2	11.2	6.6				
Step 5	1.820	1.444	0.110	757	1.05	0.115	15.3	12.1	8.1	3.48	89.35	17.63	0.036
	1.820	1.443	0.110	757	1.05	0.116	15.3	12.1	8.1				
Step 6	1.941	1.448	0.119	754	1.1	0.131	16.3	12.2	9.2	3.96	102.00	20.10	0.040
	1.941	1.449	0.119	754	1.1	0.131	16.3	12.2	9.2				
Step 7	1.253	1.035	0.050	1055	0.92	0.046	10.5	8.7	3.2	1.38	25.47	5.94	0.027
	1.432	1.128	0.063	968	0.95	0.060	12.0	9.5	4.2	1.80	36.05	8.05	0.030
	1.495	1.230	0.080	888	0.96	0.077	12.6	10.3	5.4	2.33	50.91	10.88	0.033
	1.693	1.332	0.097	820	1.01	0.098	14.2	11.2	6.8	2.95	69.85	14.35	0.035
	1.941	1.448	0.112	754	1.1	0.123	16.3	12.2	8.6	3.70	95.28	18.77	0.037
	1.941	1.456	0.122	750	1.1	0.135	16.3	12.2	9.4	4.06	105.05	20.64	0.041

APPENDIX F. RECESSION

RECESSION VALUES

Table F.1. Maximum recession values measured at the six profiles at each wave step, the heigth at which they were measured and the non-dimensional recession equivalent. Setup 1

	Profile	Rec [mm]	Rec/D_{n50}	Z [mm]	Average Rec/D_{n50}
Step 1	10	0	0		0
	P2	0	0		
	P3	0	0		
	P4	0	0		
	P5	0	0		
	P6	0	0		
Step2	P1	6.959	0.214	192	0.233
	P2	6.959	0.214	212	
	P3	8.616	0.265	247	
	P4	20.43	0.629	250	
	P5	2.386	0.073	247	
	P6	0	0.000		
Step 3	P1	8.45	0.260	190	0.763
	P2	11.04	0.340	229	
	P3	0	0.000		
	P4	70	2.154	257	
	P5	51.65	1.589	250	
	P6	7.585	0.233	178	
Step 4	P1	18.79	0.578	208	1.589
	P2	39.84	1.226	216	
	P3	39.1	1.203	240	
	P4	69.26	2.131	257	
	P5	89.69	2.760	274	
	P6	53.27	1.639	263	
Step 5	P1	30.13	0.927	254	1.730
	P2	50.07	1.541	378	
	P3	33.8	1.040	237	
	P4	65.78	2.024	257	
	P5	89.61	2.757	267	
	P6	68	2.092	267	
Step 6	P1	65.8	2.025	317	2.435
	P2	60.48	1.861	200	
	P3	95.5	2.938	300	
	P4	89.59	2.757	265	
	P5	90.7	2.791	264	
	P6	72.85	2.242	262	
Step 7	P1	74.32	2.287	317	2.575
	P2	81.19	2.498	266	
	P3	92.15	2.835	252	
	P4	88.72	2.730	262	
	P5	91.12	2.804	262	
	P6	74.57	2.294	262	

Table F.2. Maximum recession values measured at the six profiles at each wave step, the heigth at which they were measured and the non-dimensional recession equivalent. Setup 2

	Profile	Rec [mm]	Rec/D_{n50}	Z [mm]	Average Rec/D_{n50}
Step 1	P1	41.44	1.275	200	0.746
	P2	0	0.000		
	P3	51.59	1.587	192	
	P4	0.4783	0.015	193	
	P5	52.03	1.601	194	
	P6	0	0.000		
Step2	P1	29.11	0.896	195	1.261
	P2	52.95	1.629	210	
	P3	67.69	2.083	190	
	P4	1.6222	0.050	193	
	P5	62	1.908	190	
	P6	32.5	1.000	198	
Step 3	P1	70.3	2.163	195	1.519
	P2	65.27	2.008	210	
	P3	67.69	2.083	192	
	P4	2.94	0.090	198	
	P5	62	1.908	182	
	P6	28	0.862	133	
Step 4	P1	71.05	2.186	194	1.637
	P2	89.57	2.756	212	
	P3	65.33	2.010	190	
	P4	3.3	0.102	198	
	P5	62	1.908	187	
	P6	28	0.862	198	
Step 5	P1	78.52	2.416	196	1.640
	P2	89.95	2.768	212	
	P3	65.33	2.010	255	
	P4	1.12	0.034	193	
	P5	57.77	1.778	188	
	P6	27.03	0.832	198	
Step 6	P1	97.5	3.000	193	3.146
	P2	106.4	3.274	212	
	P3	132.7	4.083	194	
	P4	92.4	2.843	205	
	P5	72.45	2.229	198	
	P6	112	3.446	197	
Step 7	P1	97.5	3.000	203	3.190
	P2	106.4	3.274	250	
	P3	138.5	4.262	193	
	P4	92.4	2.843	200	
	P5	75.3	2.317	196	
	P6	112	3.446	200	

Table F.3. Maximum recession values measured at the six profiles at each wave step, the height at which they were measured and the non-dimensional recession equivalent. Setup 3

	Profile	Rec [mm]	Rec/D_{n50}	Z [mm]	Average Rec/D_{n50}
Step 1	P1	0	0.000		
	P2	0	0.000		
	P3	2.68	0.082	200	
	P4	1.772	0.055	180	0.037
	P5	0.82	0.025	174	
	P6	1.91	0.059	250	
Step2	P1	0	0.000		
	P2	23.62	0.727	184	
	P3	0	0.000		
	P4	0	0.000		0.137
	P5	0.92	0.028	276	
	P6	2.27	0.070	256	
Step 3	P1	0	0.000		
	P2	44.26	1.362	180	
	P3	10.43	0.321	255	
	P4	0	0.000		0.451
	P5	29.4	0.905	176	
	P6	3.92	0.121	280	
Step 4	P1	44.98	1.384	183	
	P2	44	1.354	180	
	P3	0	0.000		
	P4	0.85	0.026	180	0.567
	P5	20.72	0.638	180	
	P6	0	0.000		
Step 5	P1	23.7	0.729	183	
	P2	28.7	0.883	179	
	P3	37	1.138	242	
	P4	69.93	2.152	236	1.447
	P5	60.13	1.850	310	
	P6	62.61	1.926	287	
Step 6	P1	65.56	2.017	205	
	P2	29.77	0.916	180	
	P3	48.6	1.495	316	
	P4	73.71	2.268	225	1.747
	P5	62.6	1.926	305	
	P6	60.41	1.859	287	
Step 7	P1	52.21	1.606	184	
	P2	34.02	1.047	180	
	P3	53.51	1.646	236	
	P4	77.11	2.373	266	1.751
	P5	62.6	1.926	270	
	P6	61.93	1.906	195	

Table F.4. Maximum recession values measured at the six profiles at each wave step, the height at which they were measured and the non-dimensional recession equivalent. Setup 4

	Profile	Rec [mm]	Rec/D_{n50}	Z [mm]	Average Rec/D_{n50}
Step 1	P1	0	0.000		0.567
	P2	37	1.138	182	
	P3	0	0.000		
	P4	0	0.000		
	P5	26.51	0.816	178	
	P6	46.97	1.445	201	
Step2	P1	0	0.000		0.945
	P2	37	1.138	192	
	P3	9	0.277	235	
	P4	39.43	1.213	196	
	P5	50.4	1.551	200	
	P6	48.34	1.487	201	
Step 3	P1	37.76	1.162	234	1.565
	P2	37.59	1.157	190	
	P3	57.43	1.767	220	
	P4	42.52	1.308	324	
	P5	77	2.369	204	
	P6	52.83	1.626	290	
Step 4	P1	27.2	0.837	240	2.208
	P2	115.8	3.563	187	
	P3	111.3	3.425	168	
	P4	44.7	1.375	198	
	P5	81.18	2.498	203	
	P6	50.41	1.551	290	
Step 5	P1	44.65	1.374	260	2.911
	P2	96.94	2.983	204	
	P3	111.1	3.418	320	
	P4	111.5	3.431	301	
	P5	91.35	2.811	294	
	P6	112	3.446	274	
Step 6	P1	116	3.569	295	5.070
	P2	171	5.262	284	
	P3	198.2	6.098	310	
	P4	163	5.015	306	
	P5	150	4.615	293	
	P6	190.4	5.858	300	
Step 7	P1	175	5.385	304	6.741
	P2	225	6.923	303	
	P3	245.2	7.545	310	
	P4	266.1	8.188	322	
	P5	183.8	5.655	310	
	P6	219.3	6.748	305	

Table F.5. Maximum recession values measured at the six profiles at each wave step, the height at which they were measured and the non-dimensional recession equivalent. Setup 5

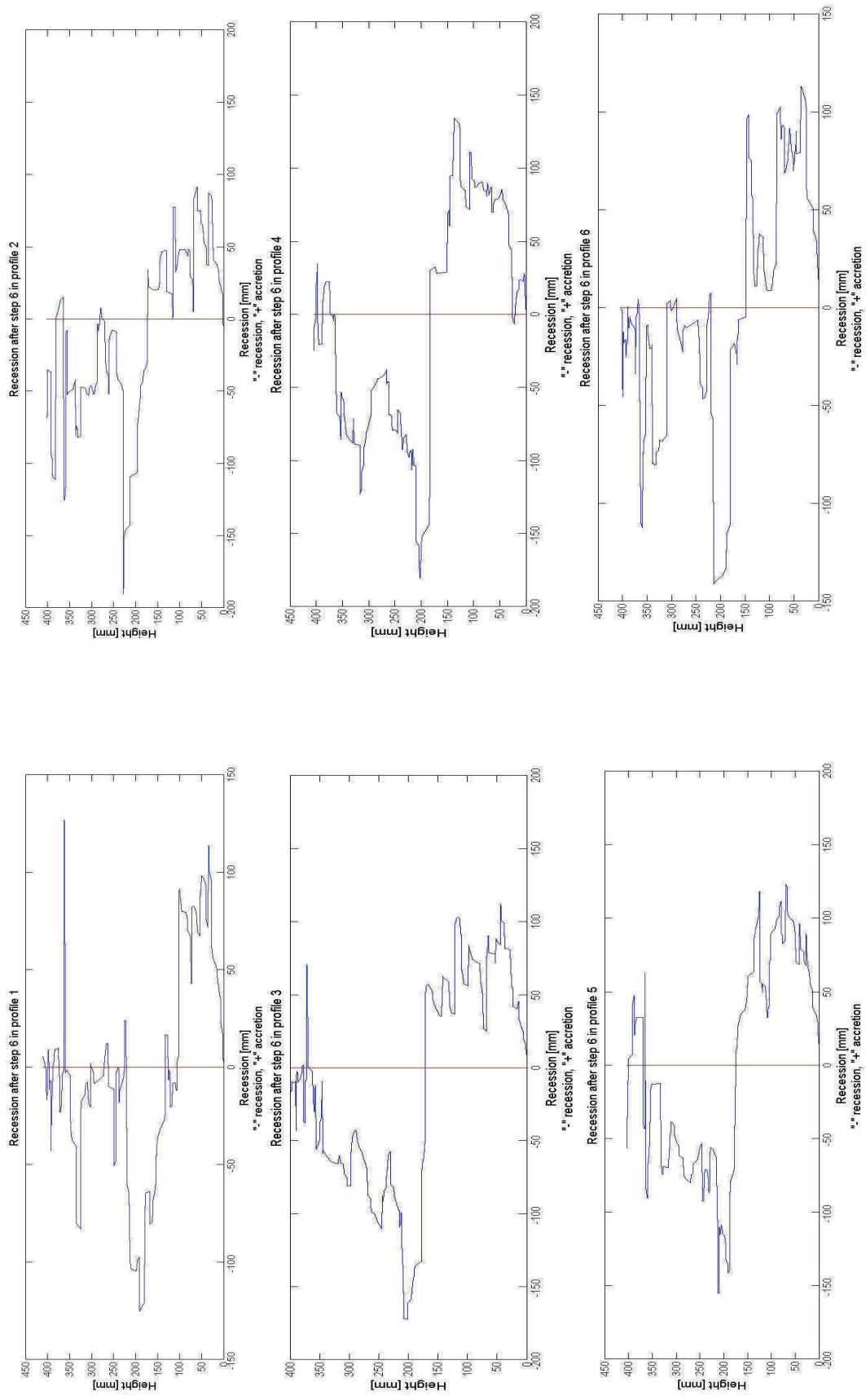|	Profile	Rec [mm]	Rec/D_{n50}	Z [mm]	Average Rec/D_{n50}
Step 1	P1	23.64	0.763	204	0.602
	P2	15.78	0.509	185	
	P3	22	0.710	190	
	P4	29.81	0.962	189	
	P5	20.74	0.669	198	
	P6	0	0.000		
Step2	P1	34.9	1.126	175	1.508
	P2	47.35	1.527	196	
	P3	20.61	0.665	193	
	P4	85.05	2.744	193	
	P5	77.49	2.500	202	
	P6	15	0.484	200	
Step 3	P1	83.85	2.705	285	2.035
	P2	37.8	1.219	236	
	P3	65.7	2.119	310	
	P4	64.16	2.070	256	
	P5	51	1.645	300	
	P6	76	2.452	238	
Step 4	P1	84.43	2.724	286	2.363
	P2	84.71	2.733	208	
	P3	66.5	2.145	314	
	P4	72.45	2.337	256	
	P5	81.9	2.642	204	
	P6	49.5	1.597	243	
Step 5	P1	62.71	2.023	206	2.653
	P2	87.19	2.813	208	
	P3	72.58	2.341	207	
	P4	101.5	3.274	339	
	P5	96.46	3.112	316	
	P6	72.96	2.354	207	
Step 6	P1	63.11	2.036	286	2.692
	P2	88.76	2.863	208	
	P3	75.8	2.445	205	
	P4	103.6	3.342	336	
	P5	96.53	3.114	321	
	P6	73	2.355	206	
Step 7	P1	63.69	2.055	287	2.766
	P2	85.76	2.766	209	
	P3	77.7	2.506	203	
	P4	118.5	3.823	323	
	P5	96.52	3.114	311	
	P6	72.33	2.333	206	
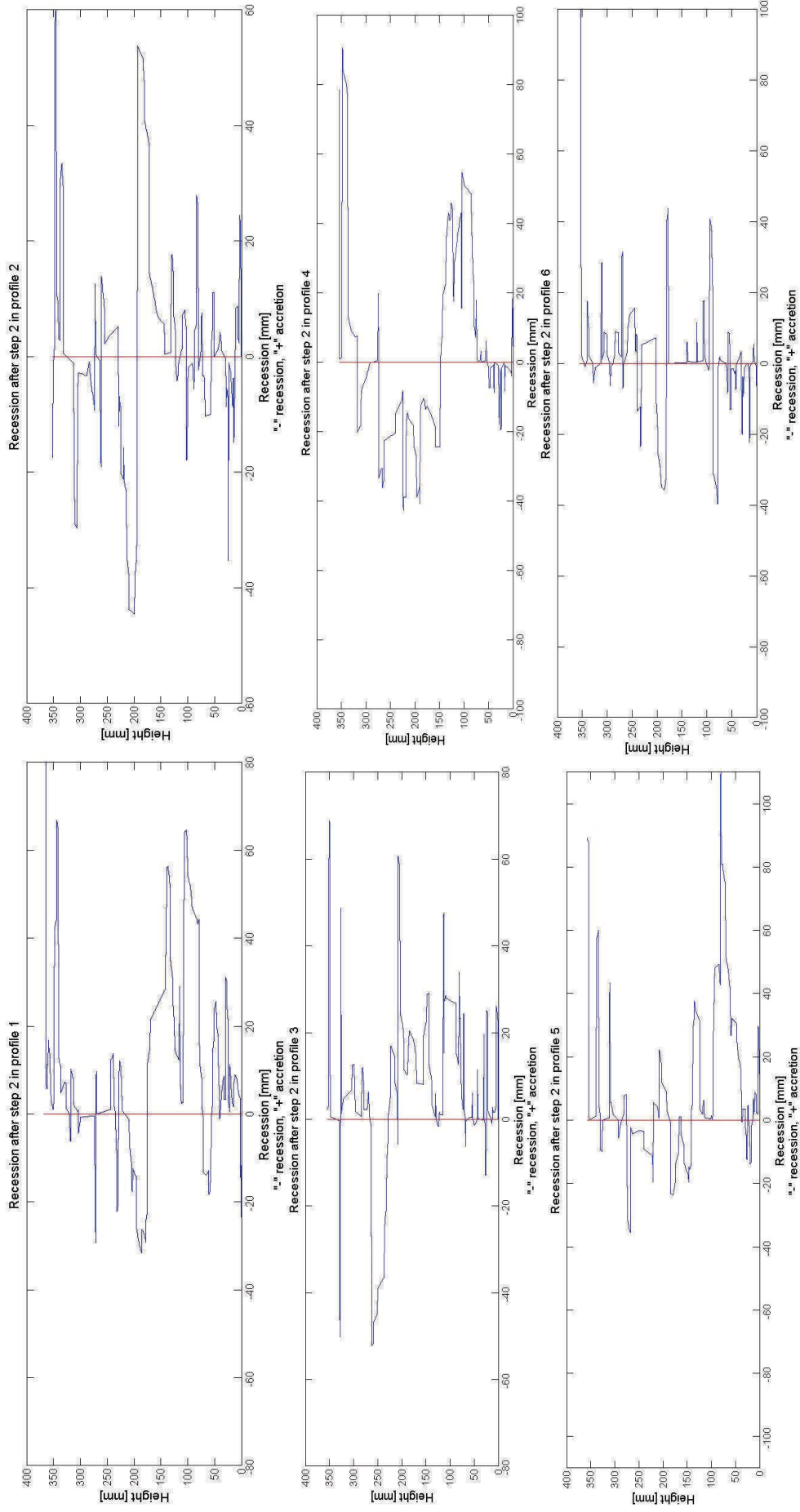
Figure F.1. Recession at each height at all the profiles after wave step 2. Setup 1

STEP 3
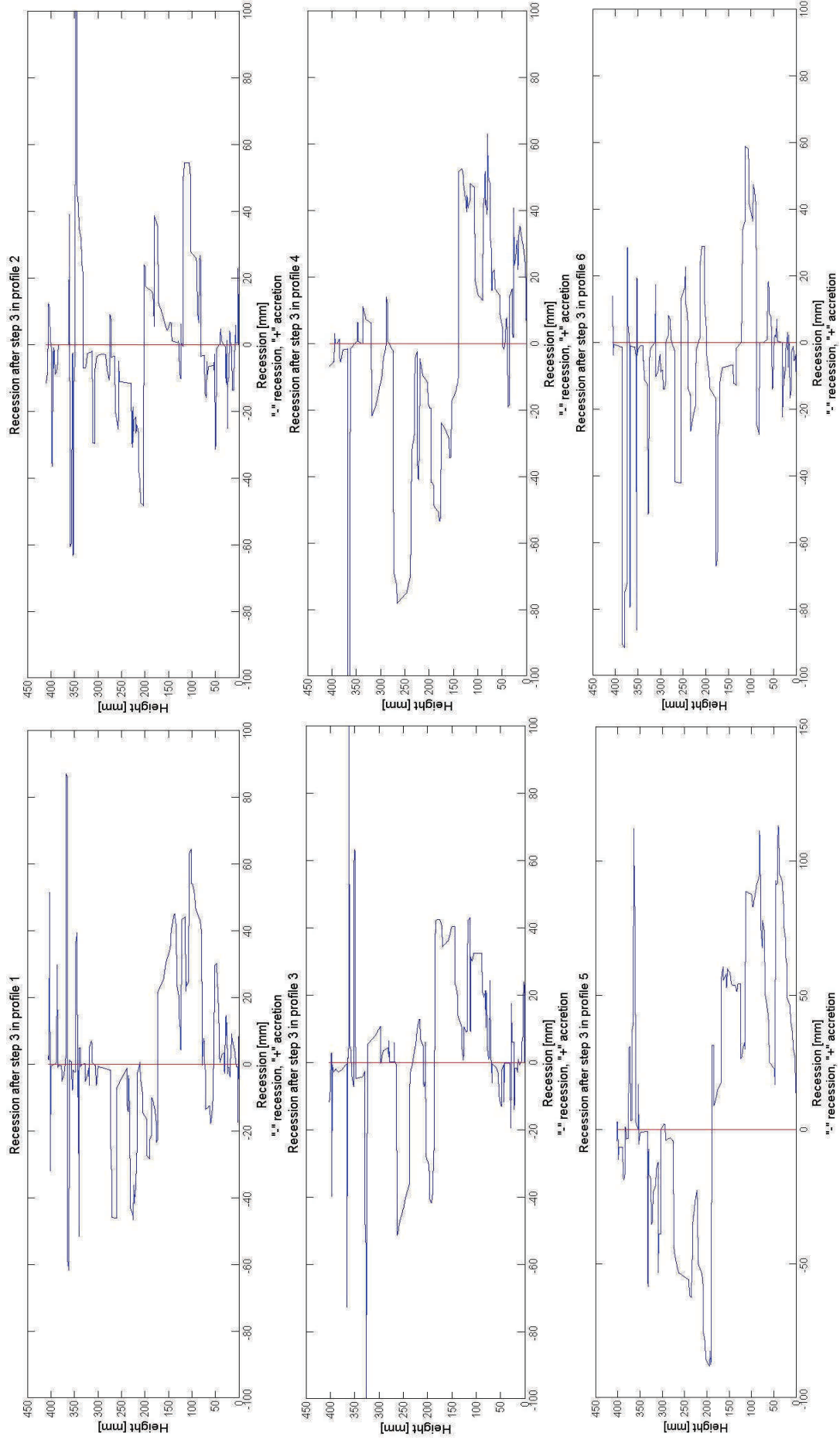
Figure F. 2. Recession at each height at all the profiles after wave step 3. Setup 1
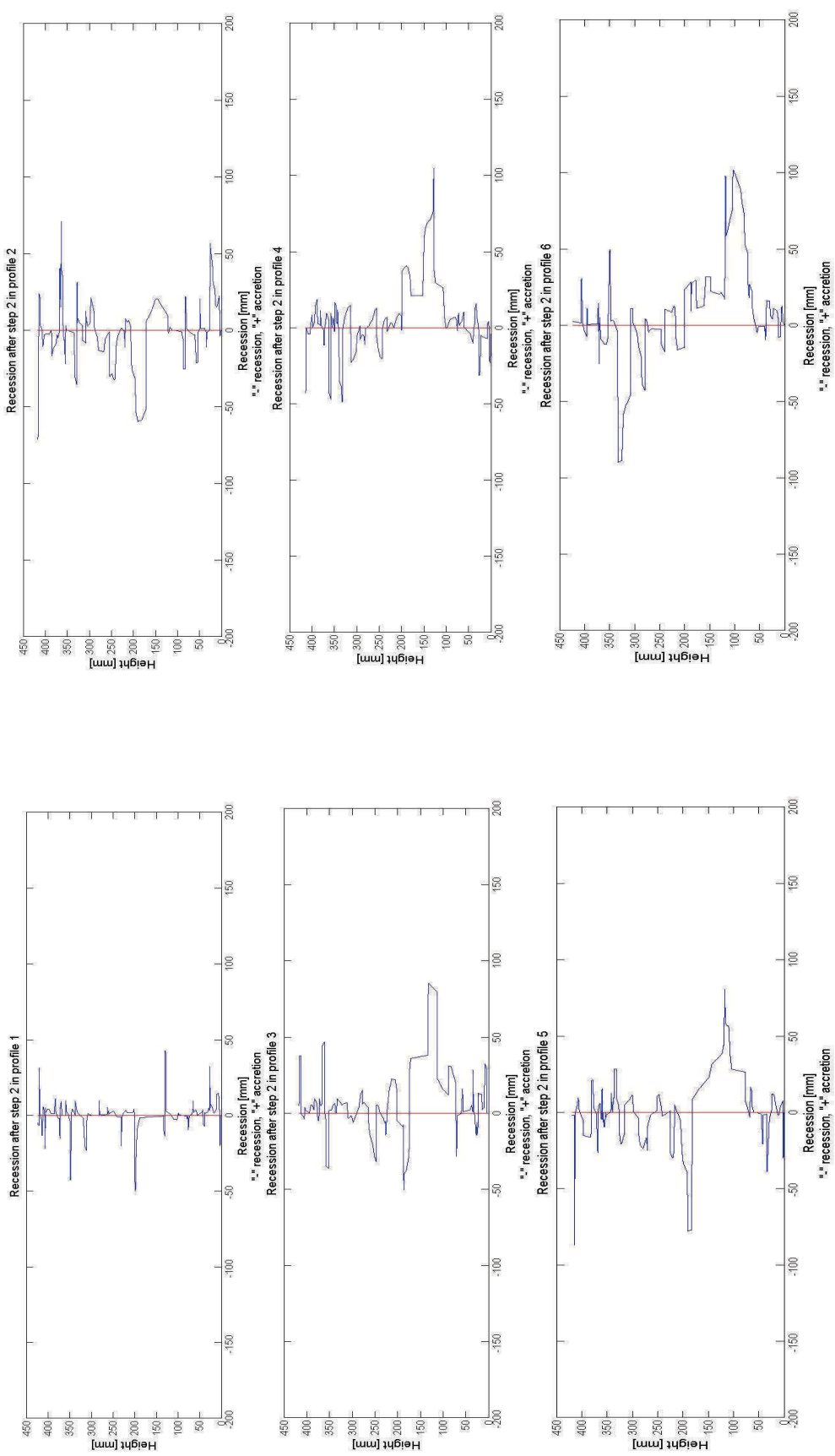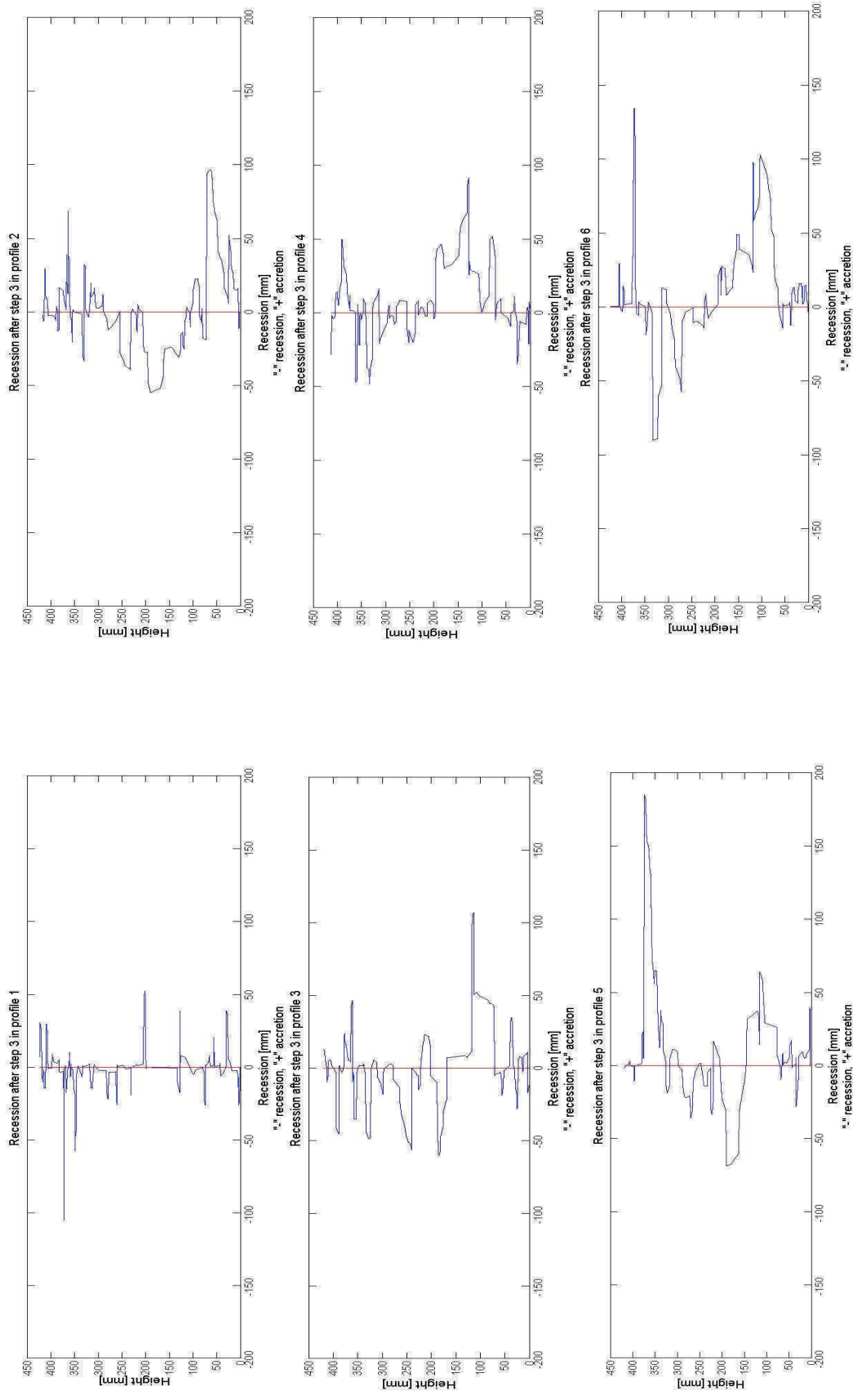
STEP 4

Recession after step 4 in profile 2

Recession after step 4 in profile 4

Recession after step 4 in profile 6

Recession after step 4 in profile 1

Recession after step 4 in profile 3

Recession after step 4 in profile 5
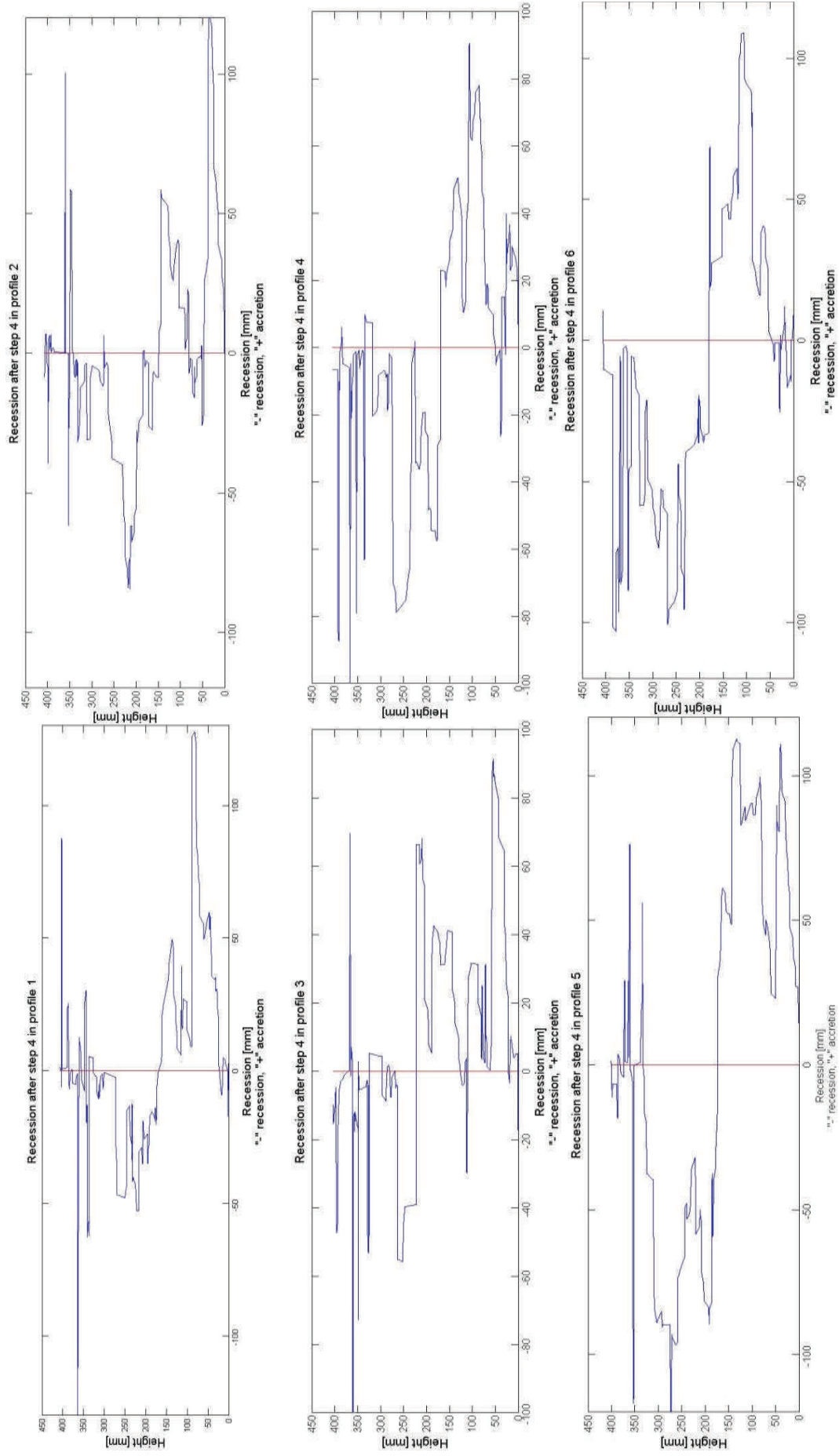
Figure F. 3. Recession at each height at all the profiles after wave step 4. Setup 1

Master Thesis, spring 2013   Altea Cámara Aguilera   NTNU
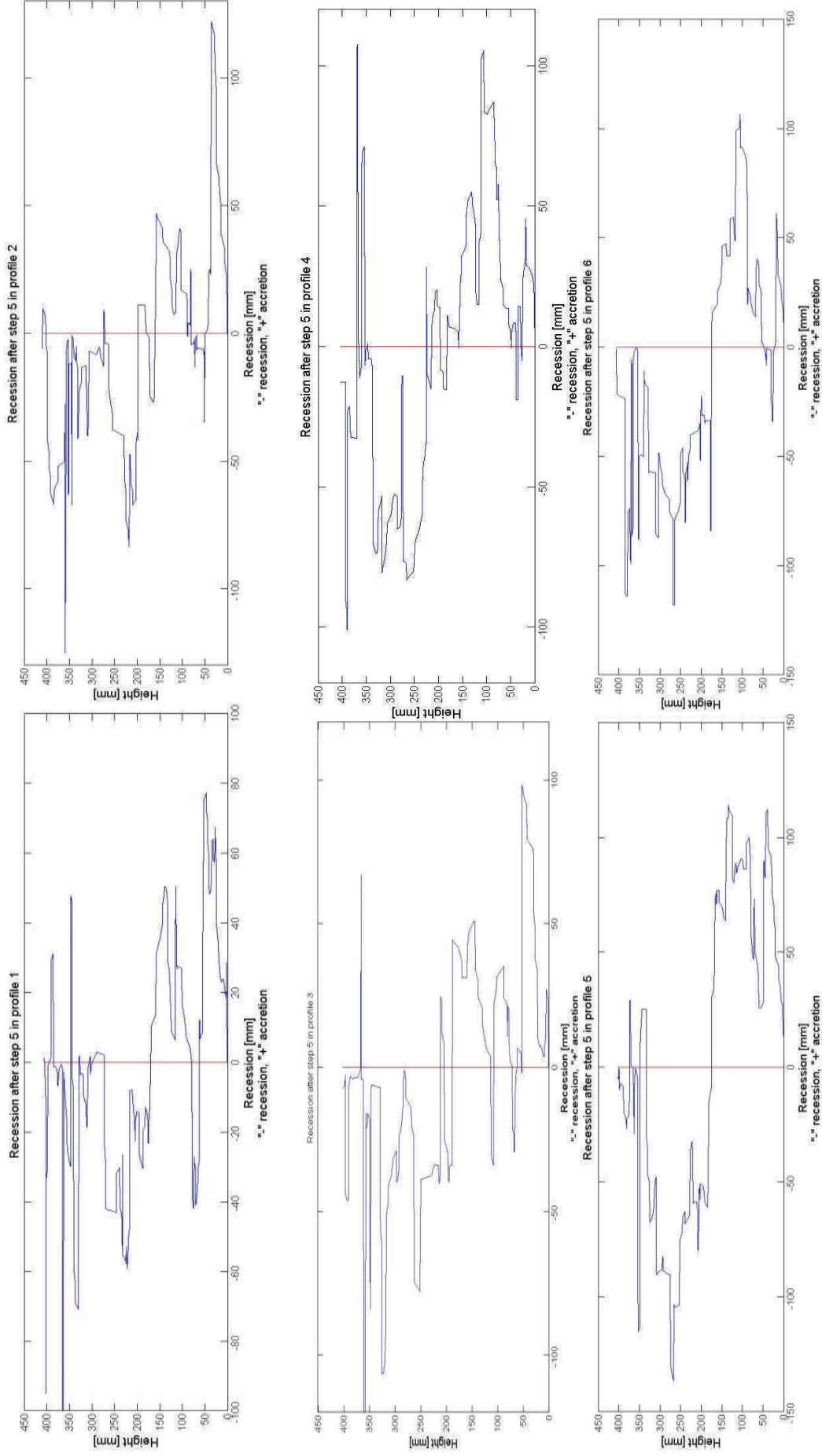
STEP 5

Figure F. 4. Recession at each height at all the profiles after wave step 5. Setup 1

Master Thesis, spring 2013   Altea Cámara Aguilera   NTNU
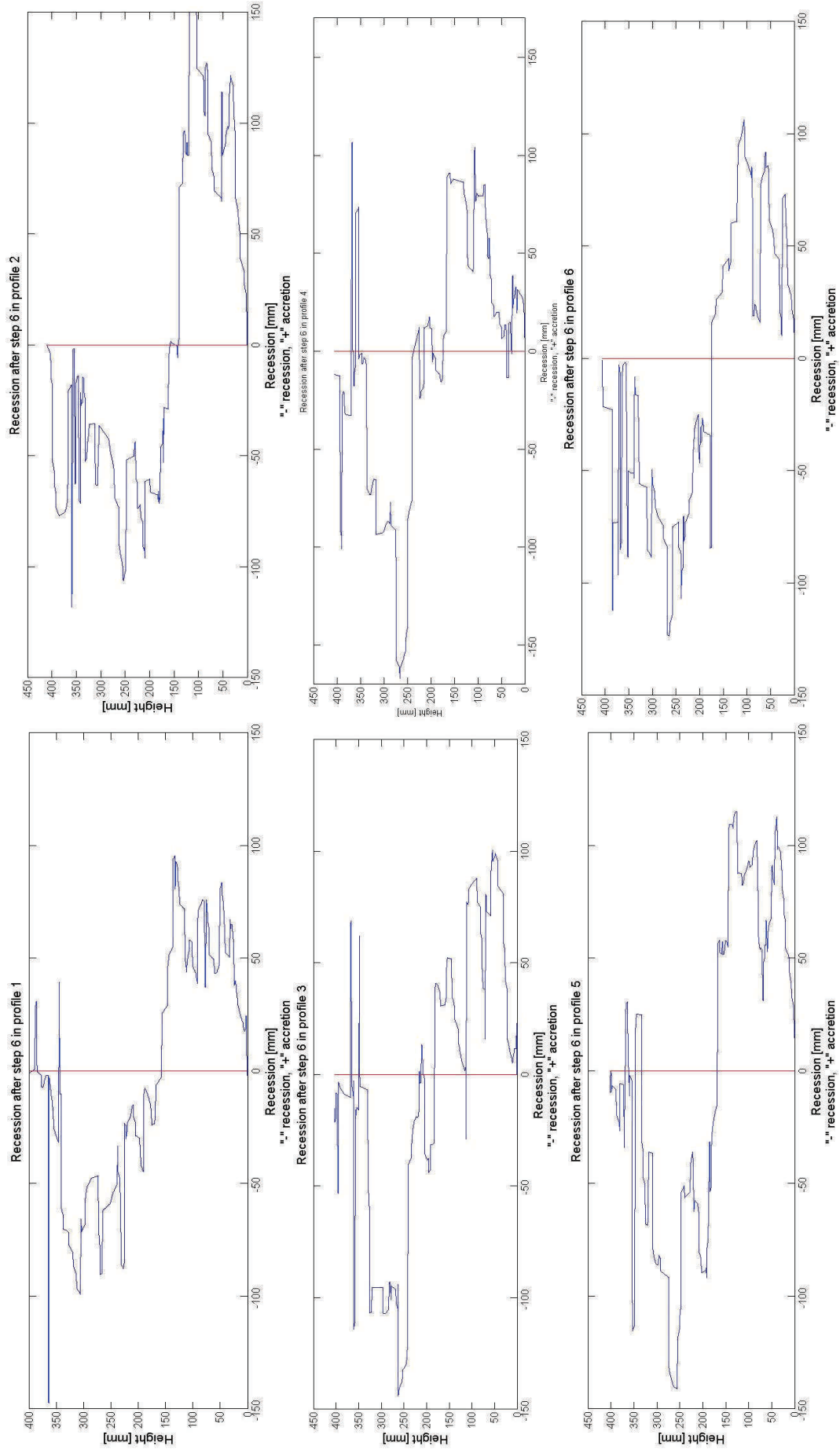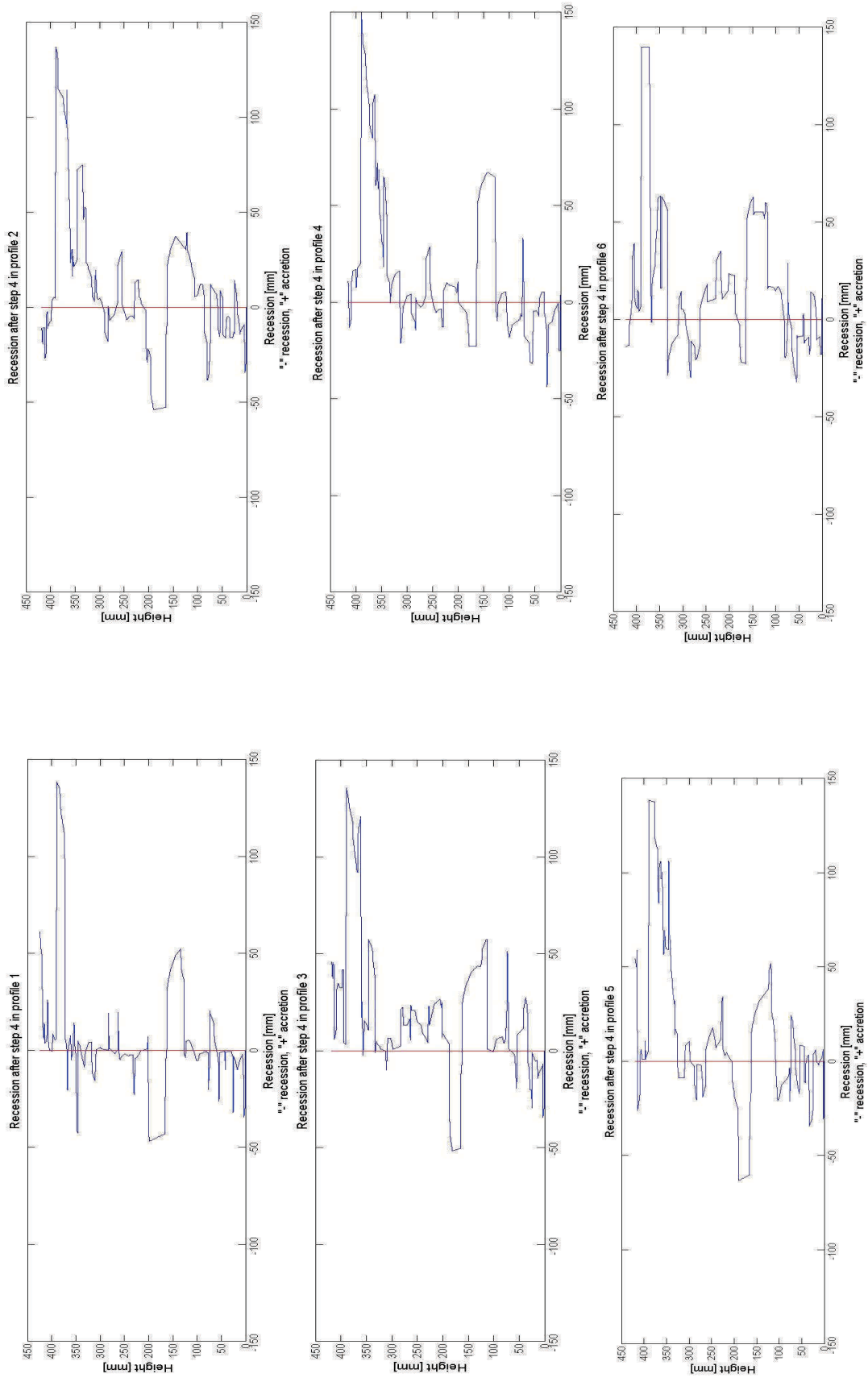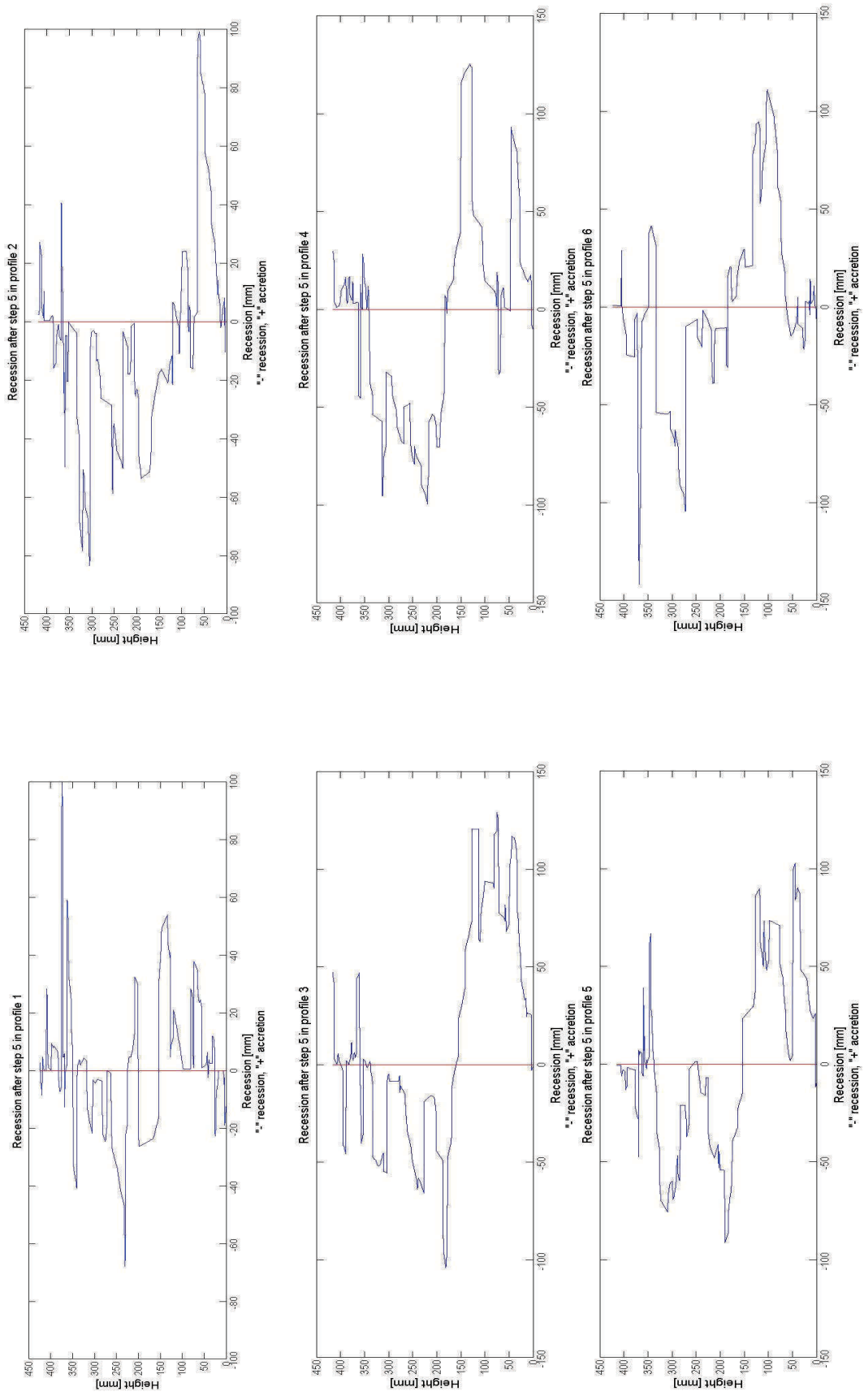
STEP 6

Figure F. 5. Recession at each height at all the profiles after wave step 6. Setup 1

STEP 7
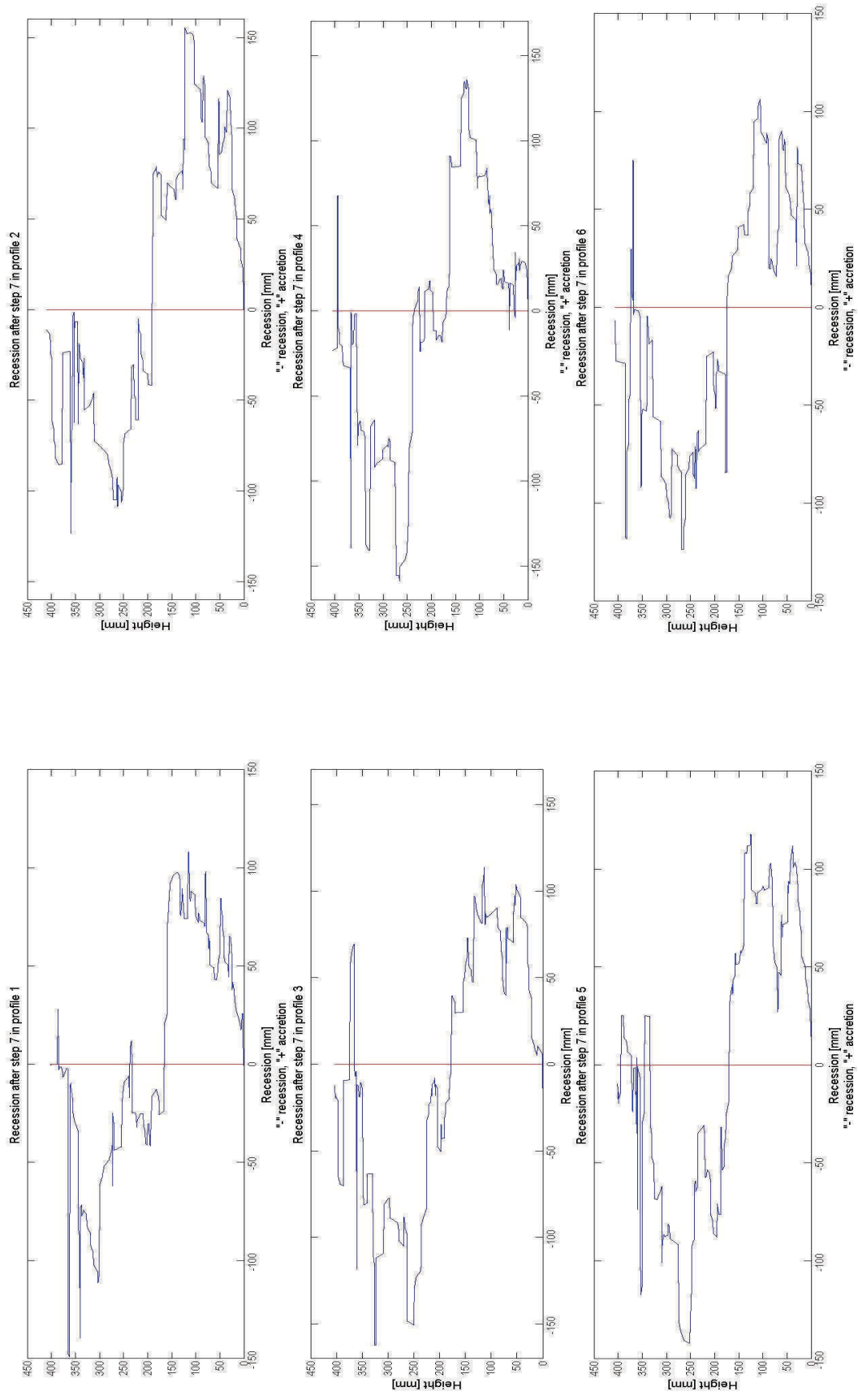
Figure F. 6. Recession at each height at all the profiles after wave step 7. Setup 1

Master Thesis, spring 2013   Altea Cámara Aguilera   NTNU
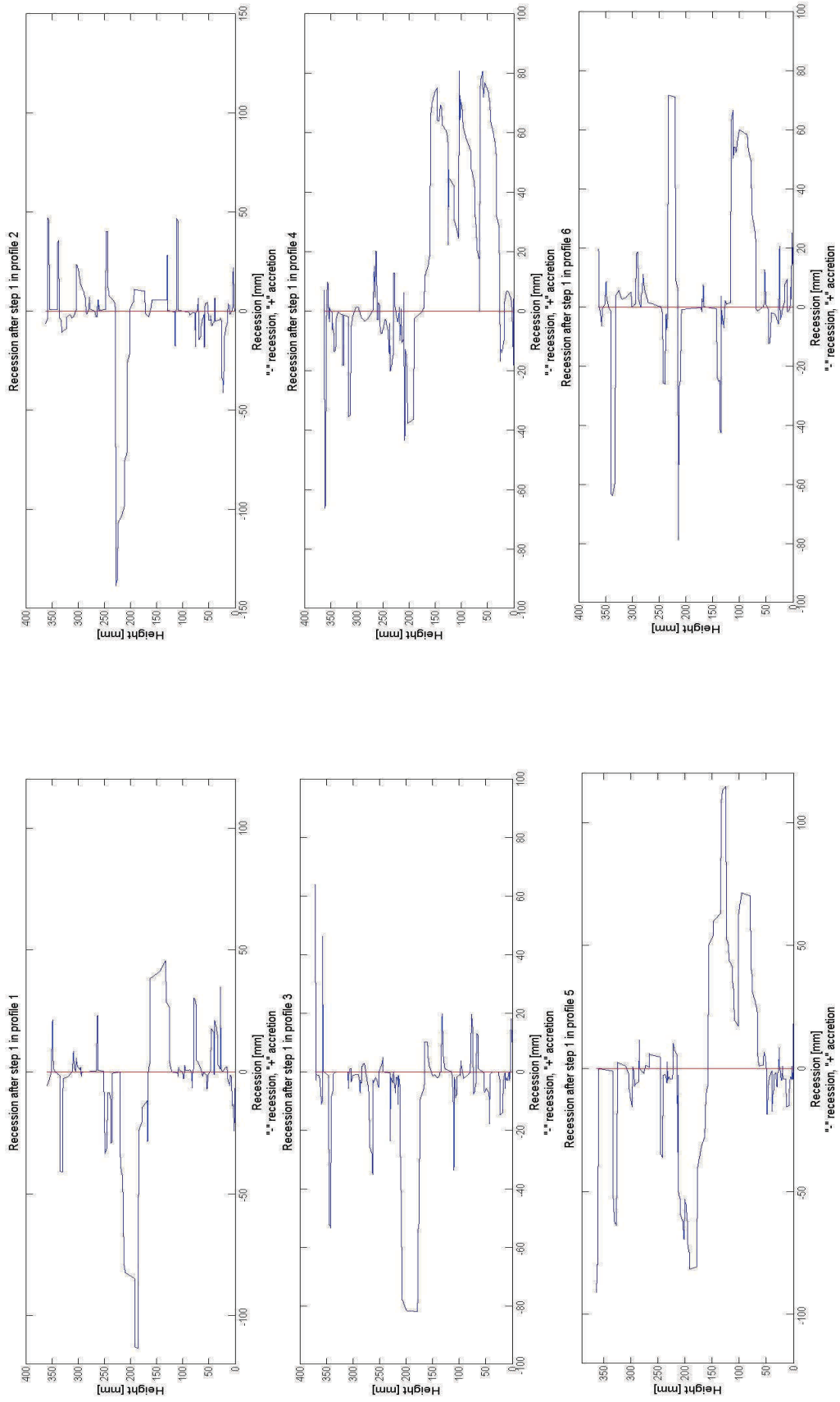
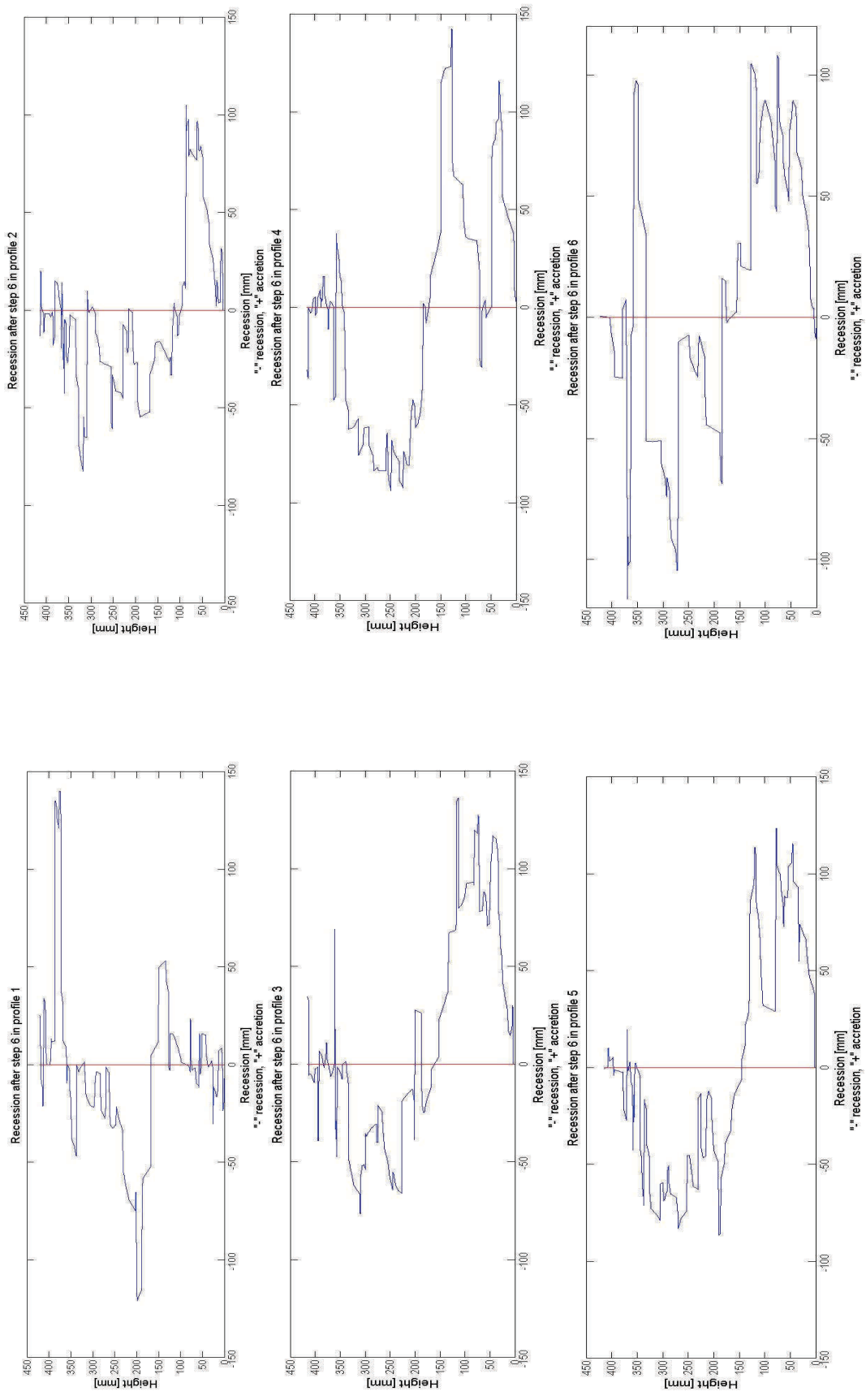Figure F. 7. Recession at each height at all the profiles after wave step 1. Setup 2
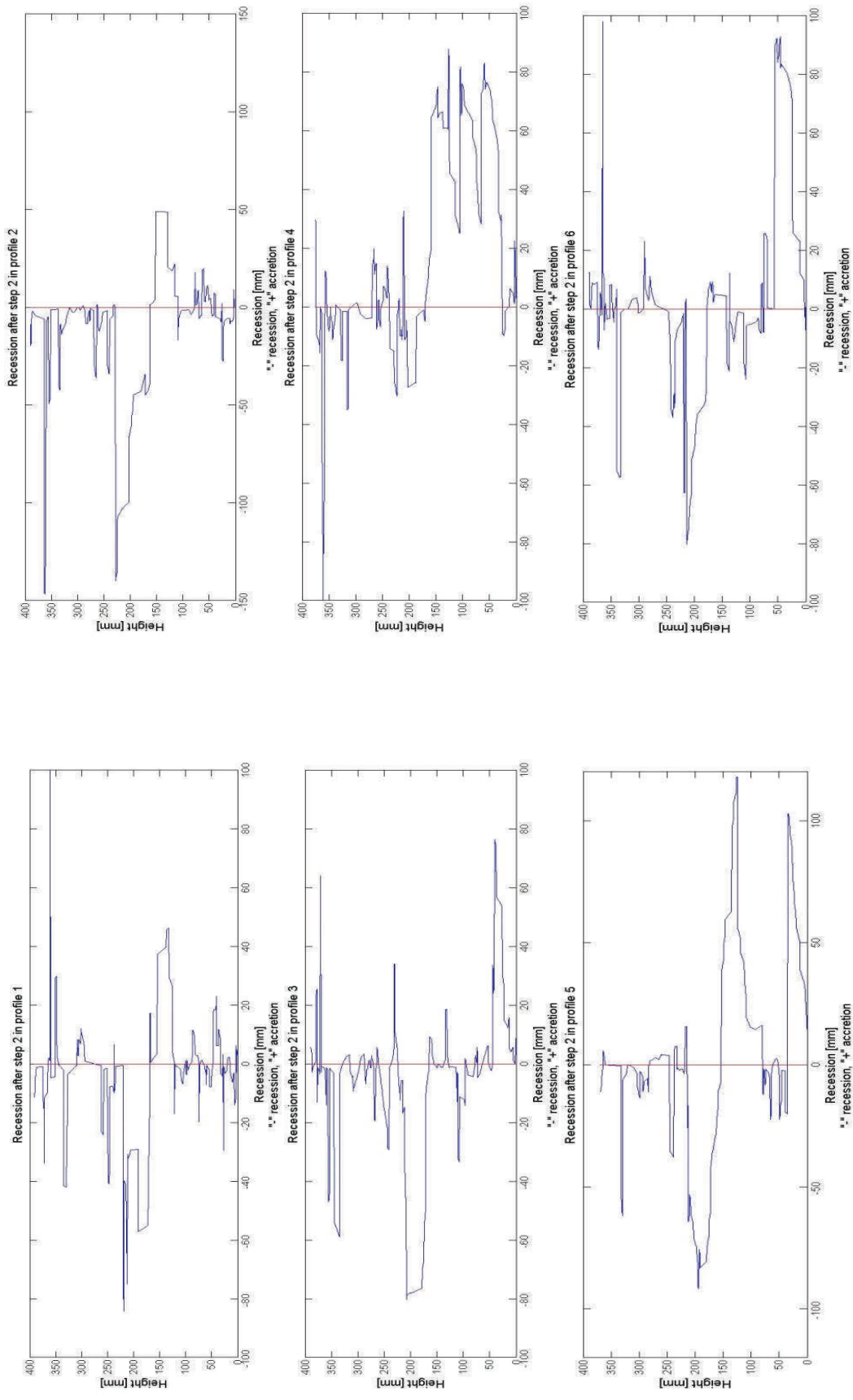
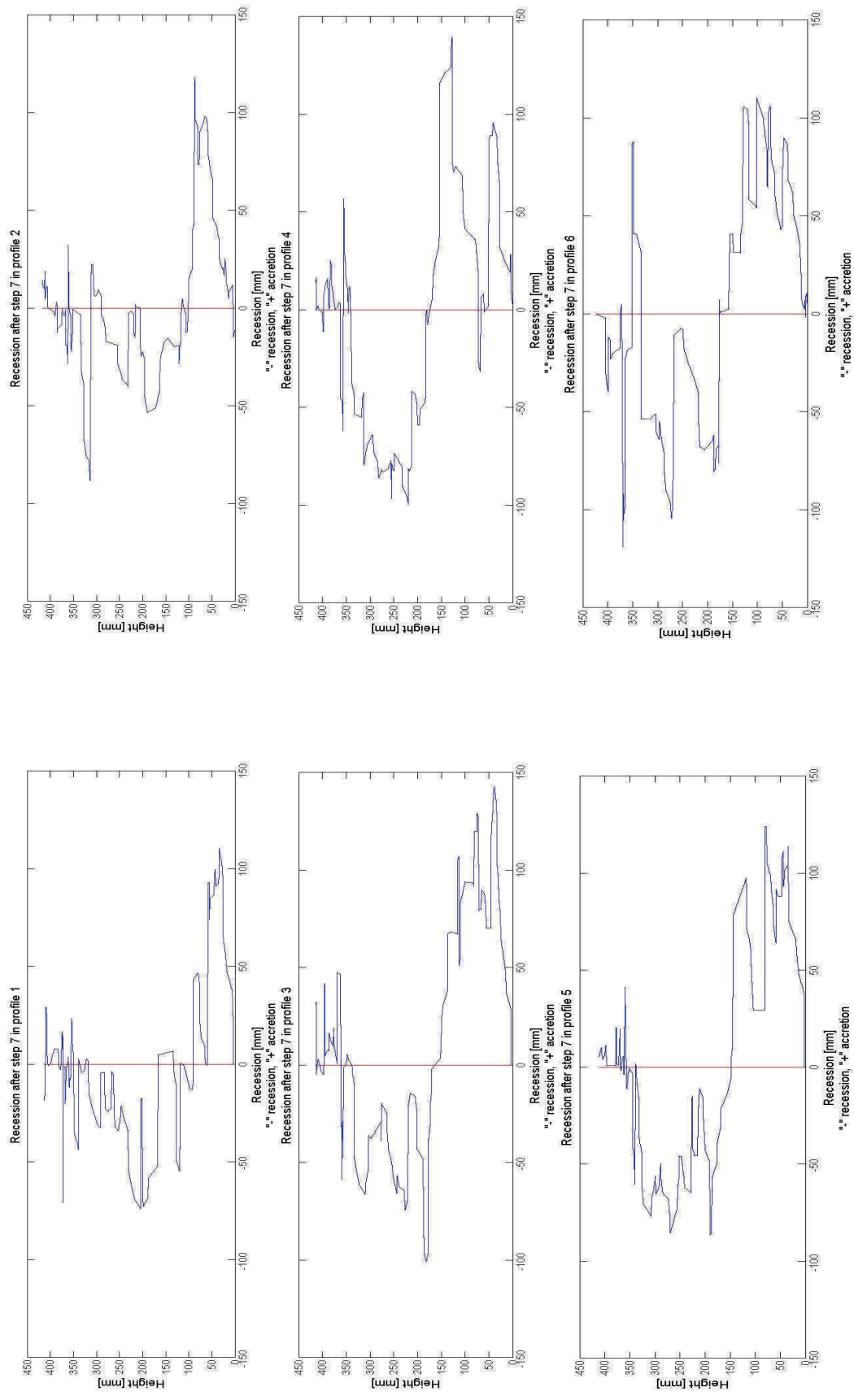Figure F. 8. Recession at each height at all the profiles after wave step 2. Setup 2

STEP 3
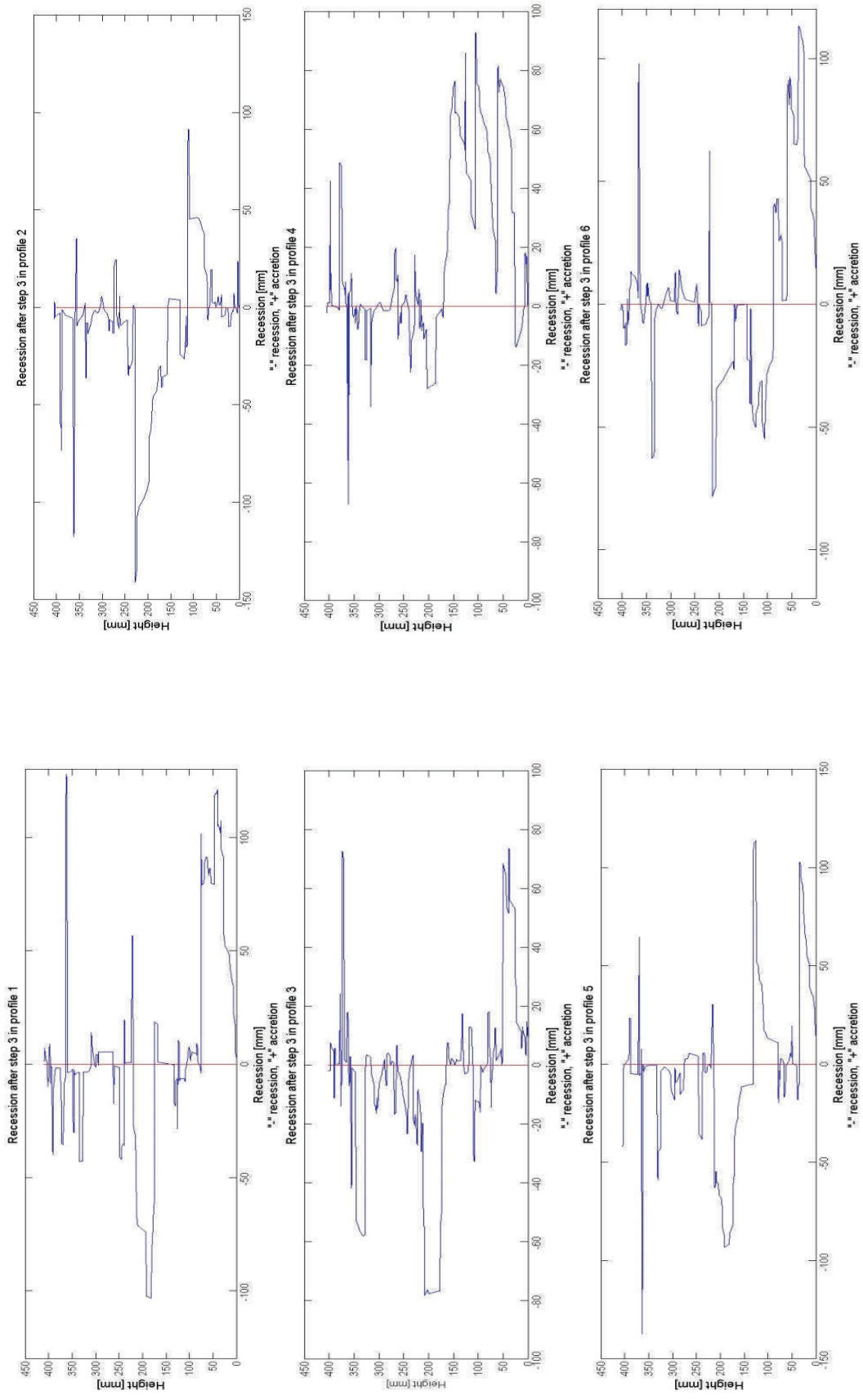
Figure F. 9. Recession at each height at all the profiles after wave step 3. Setup 2

STEP 4
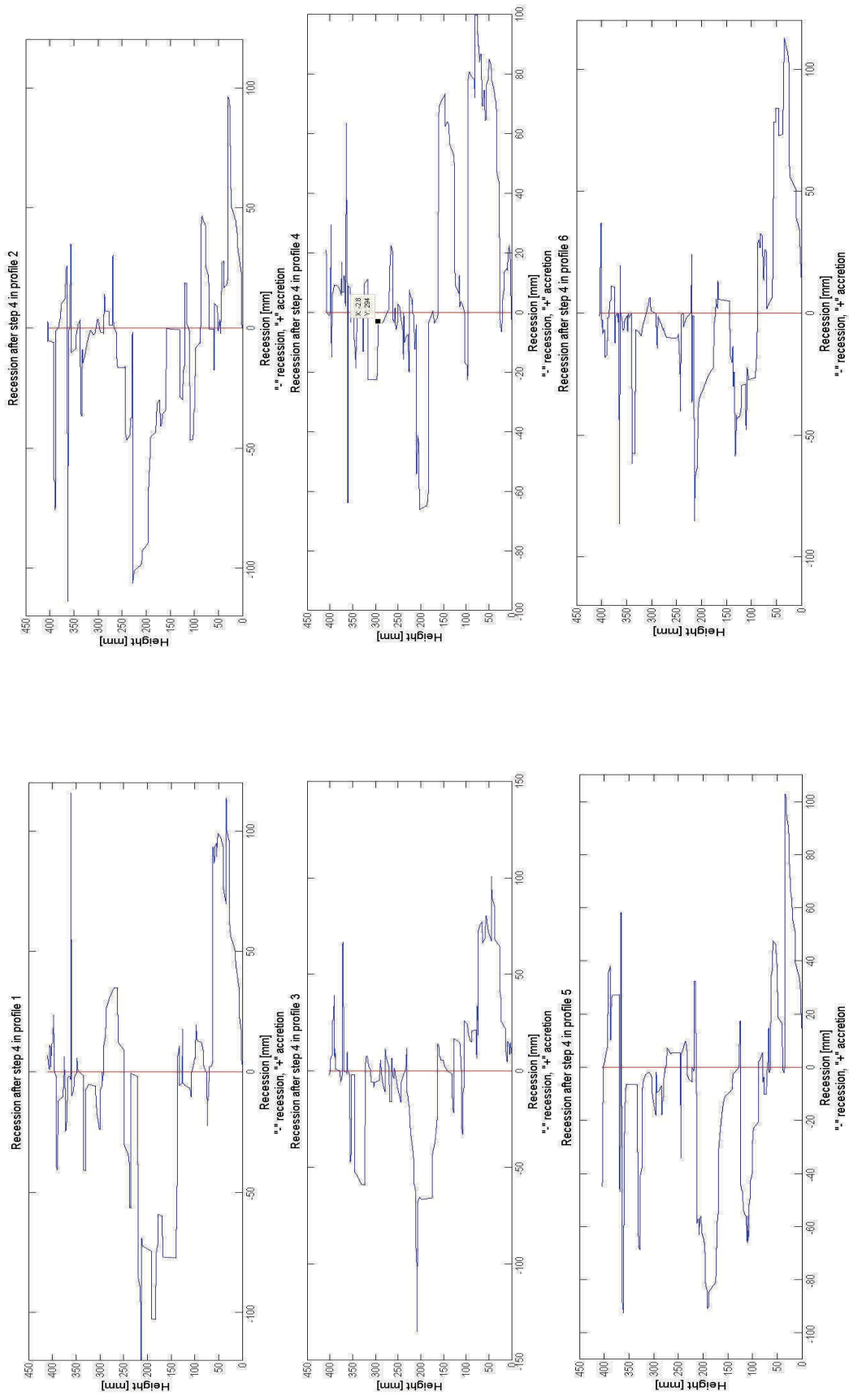
Figure F. 10. Recession at each height at all the profiles after wave step 4. Setup 2

Master Thesis, spring 2013   Altea Cámara Aguilera   NTNU
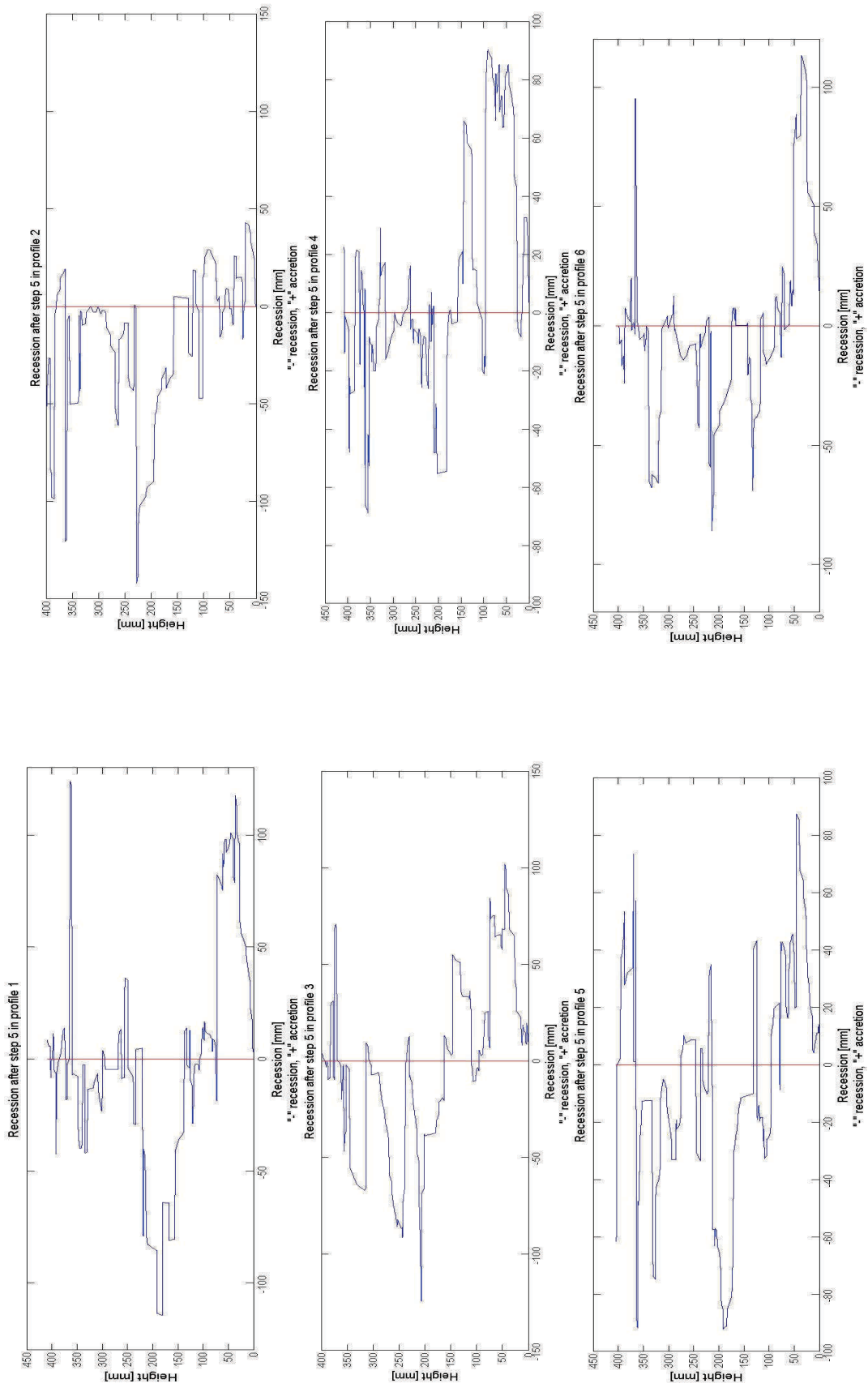
Figure F. 11. Recession at each height at all the profiles after wave step 5. Setup 2

Master Thesis, spring 2013   Altea Cámara Aguilera   NTNU

STEP 6

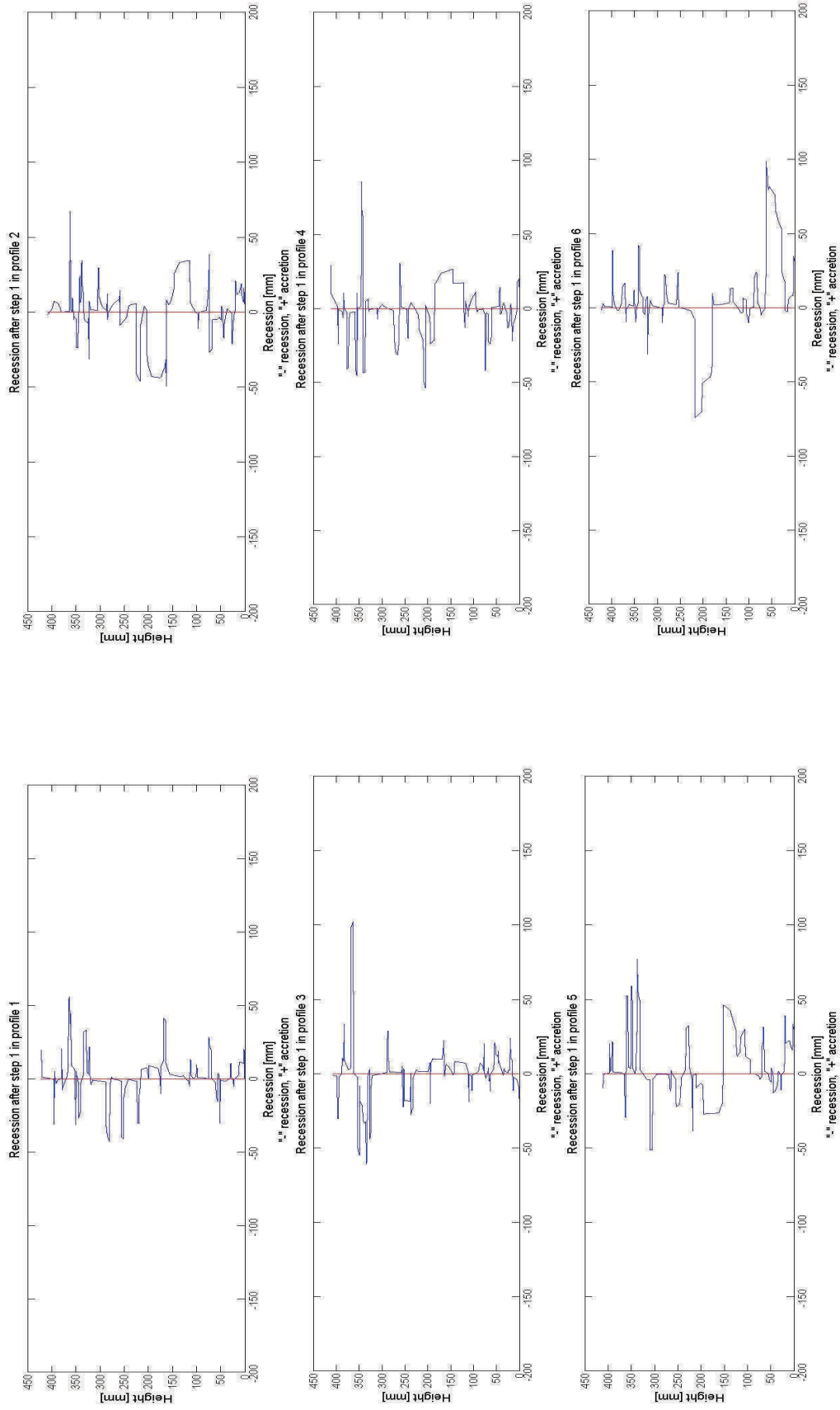**Figure F. 12. Recession at each height at all the profiles after wave step 6. Setup 2**
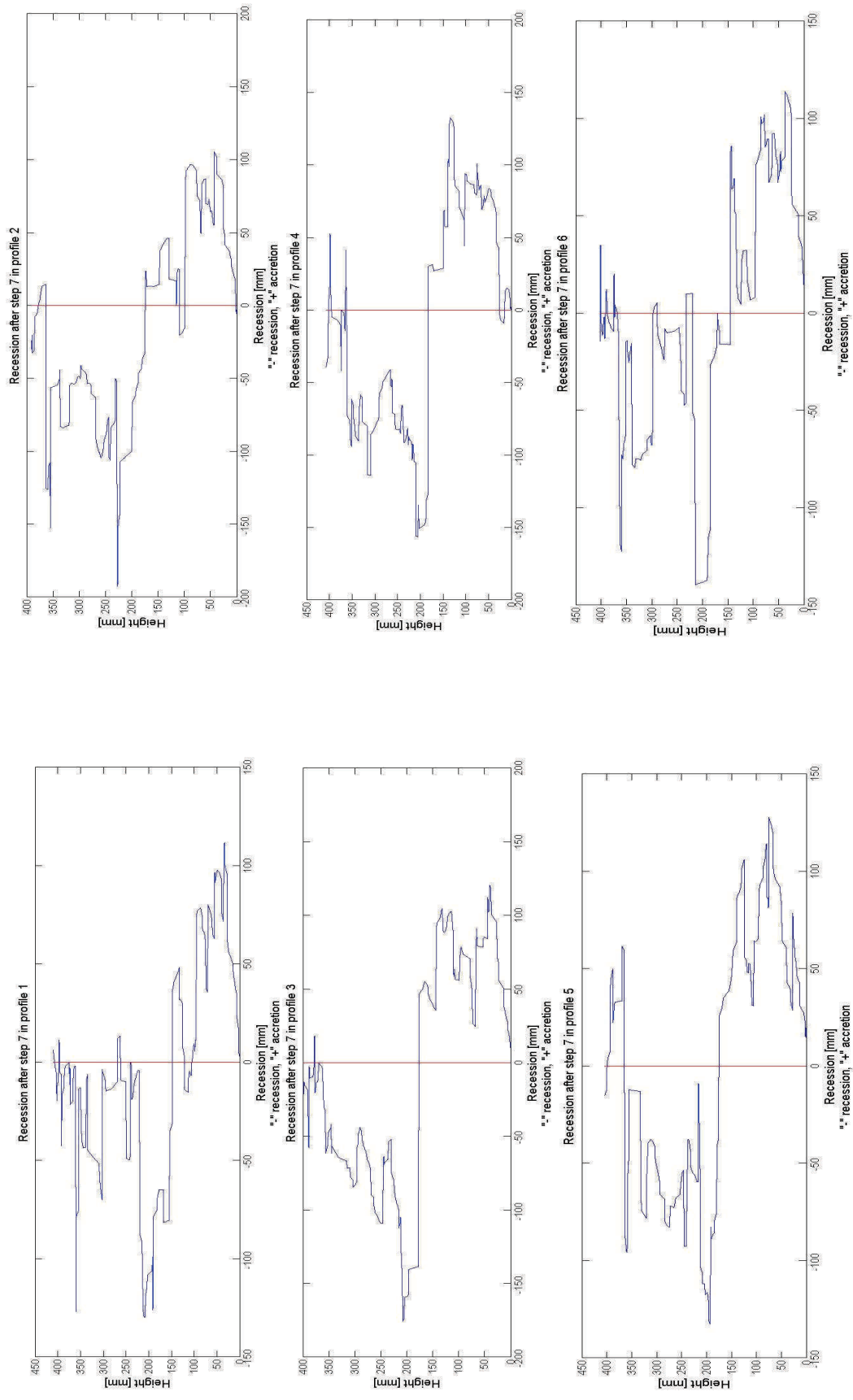
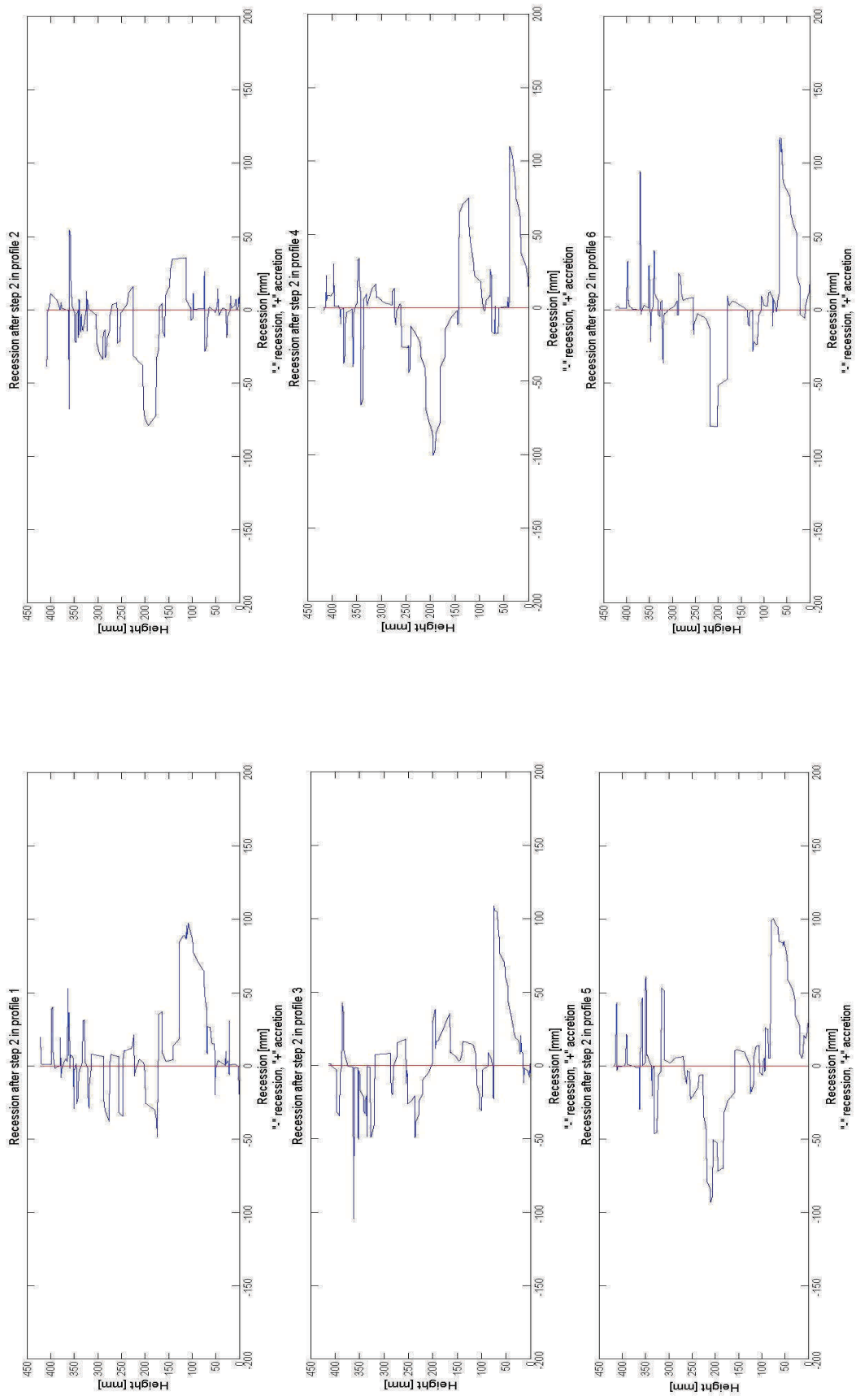**Figure F. 13. Recession at each height at all the profiles after wave step 7. Setup 2**
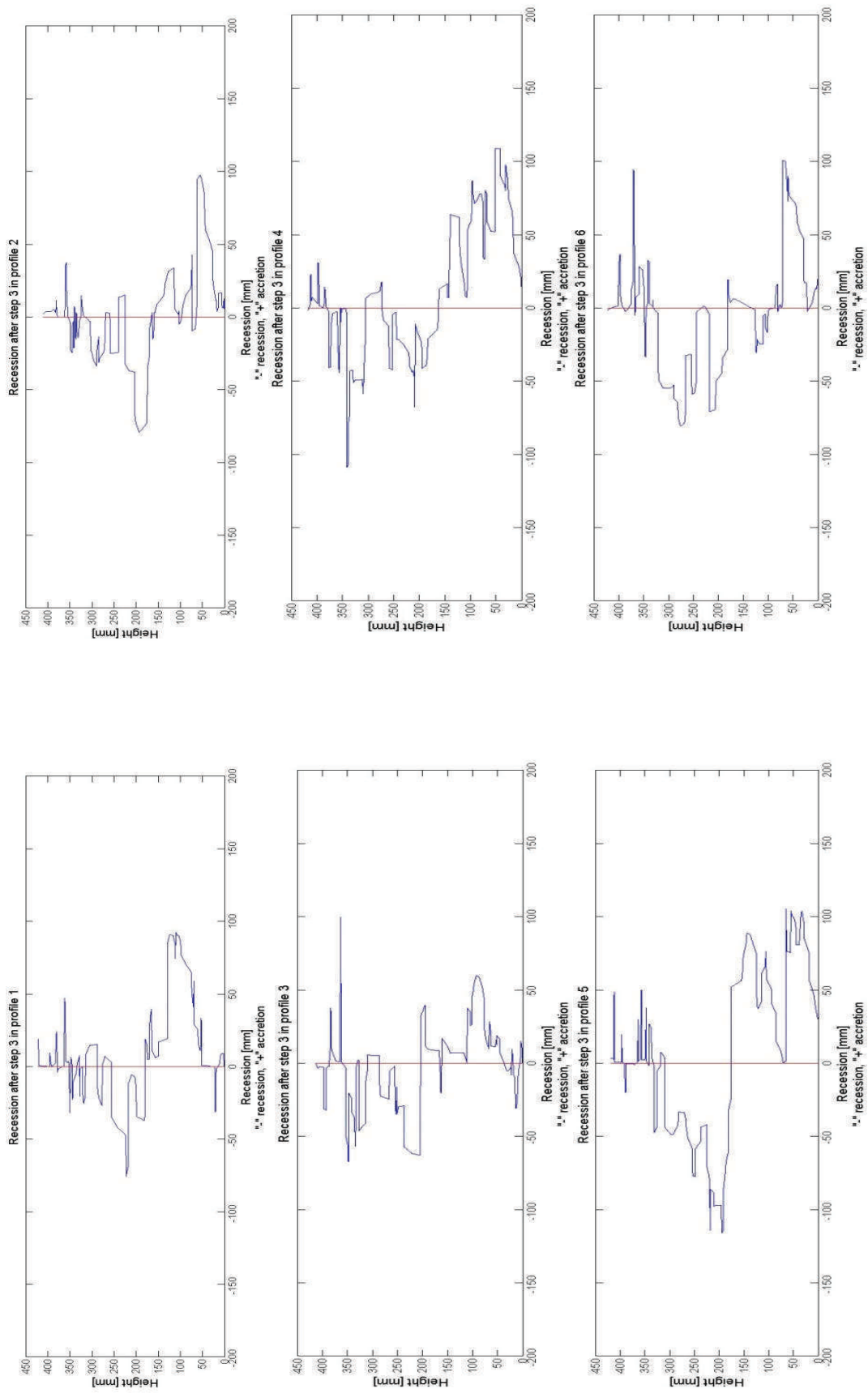
Figure F. 14. Recession at each height at all the profiles after wave step 2. Setup 3

STEP 3

Figure F. 15. Recession at each height at all the profiles after wave step 3. Setup 3

Figure F. 16. Recession at each height at all the profiles after wave step 4. Setup 3

Master Thesis, spring 2013   Altea Cámara Aguilera   NTNU

Figure F. 17. Recession at each height at all the profiles after wave step 5. Setup 3

Figure F. 18. Recession at each height at all the profiles after wave step 6. Setup 3

Figure F. 19. Recession at each height at all the profiles after wave step 7. Setup 3

Figure F. 20. Recession at each height at all the profiles after wave step 1. Setup 4
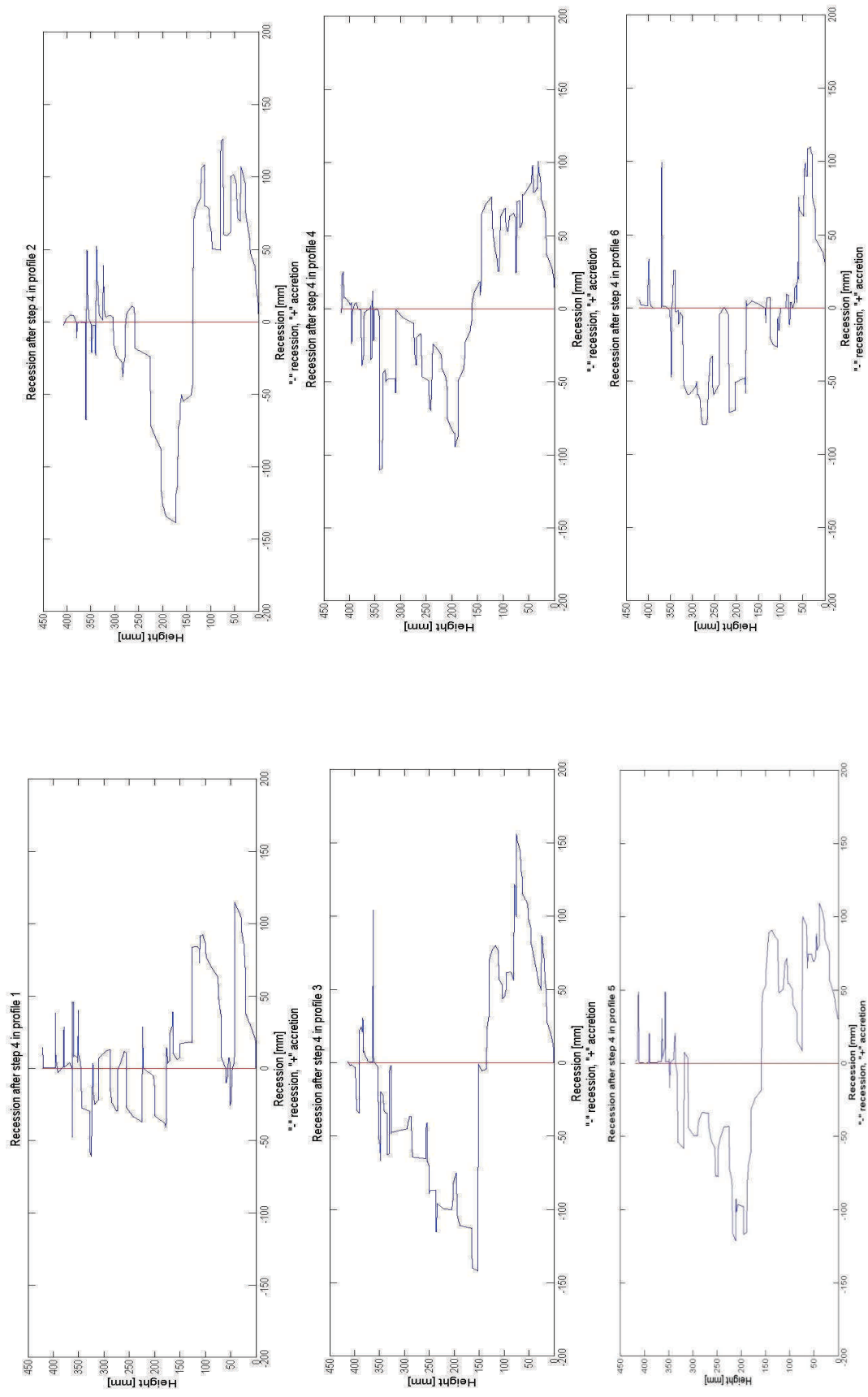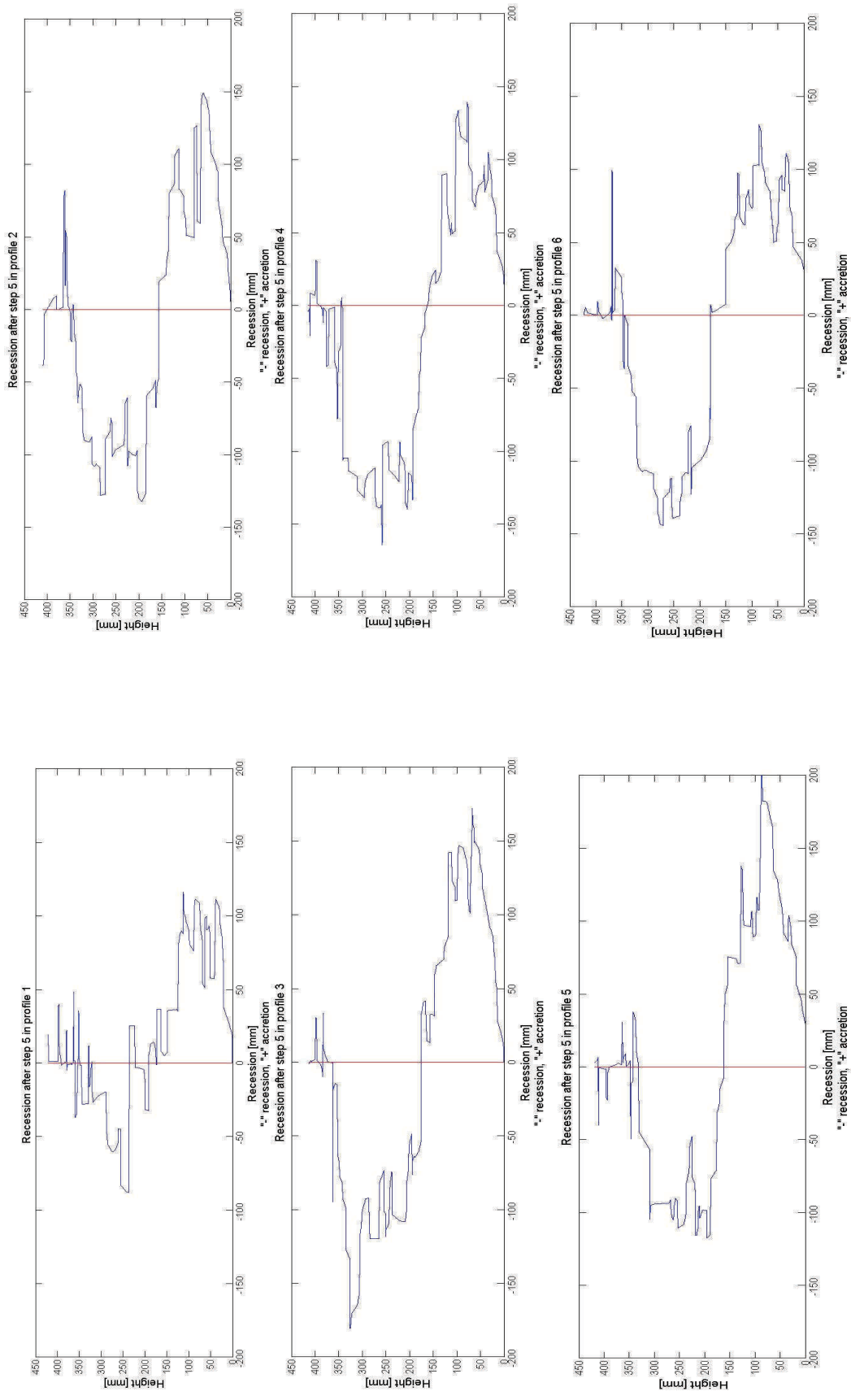
Figure F. 21. Recession at each height at all the profiles after wave step 2. Setup 4

STEP 3

Figure F. 22. Recession at each height at all the profiles after wave step 3. Setup 4

Figure F. 23. Recession at each height at all the profiles after wave step 4. Setup 4

Figure F. 24. Recession at each height at all the profiles after wave step 5. Setup 4

STEP 6

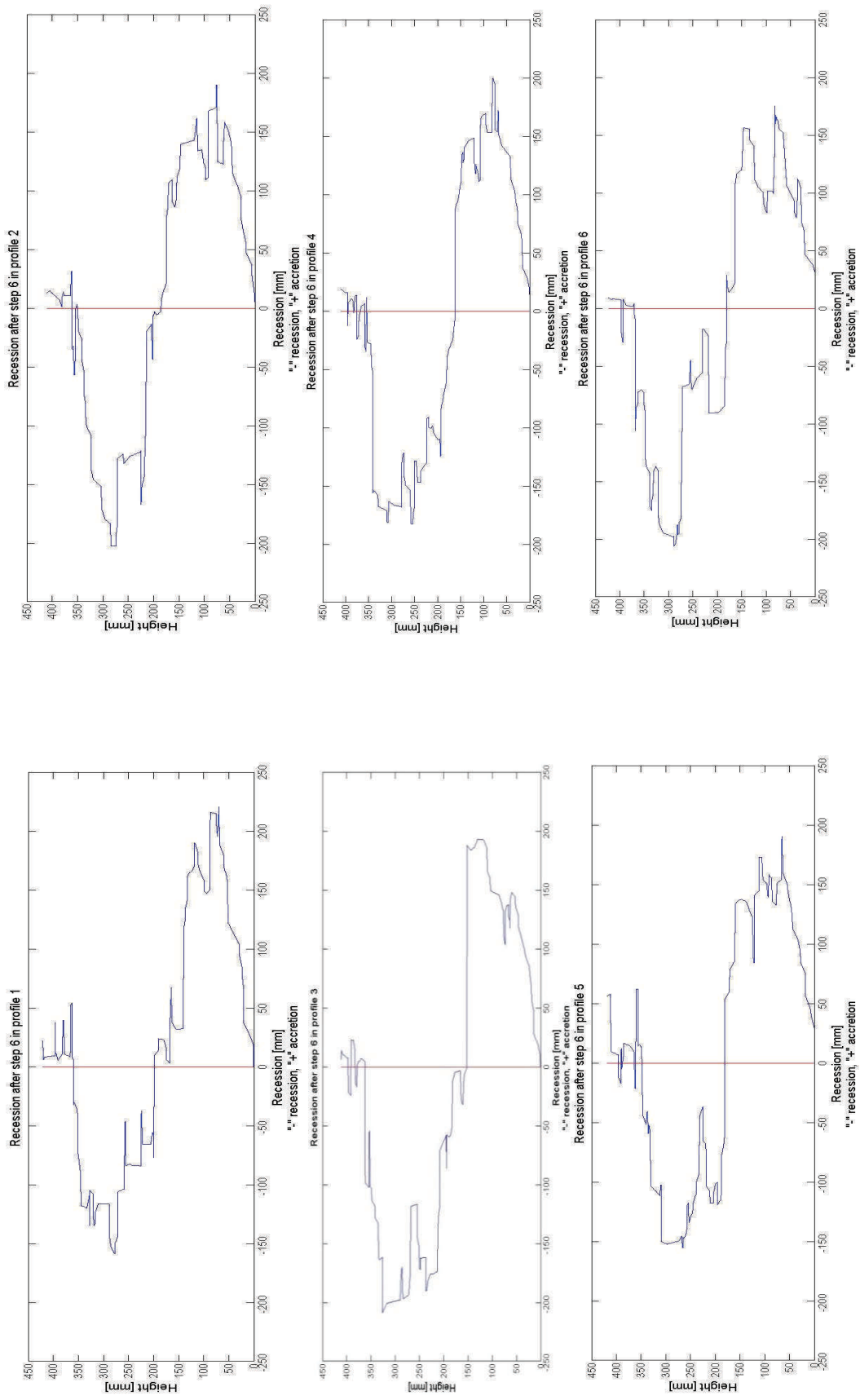

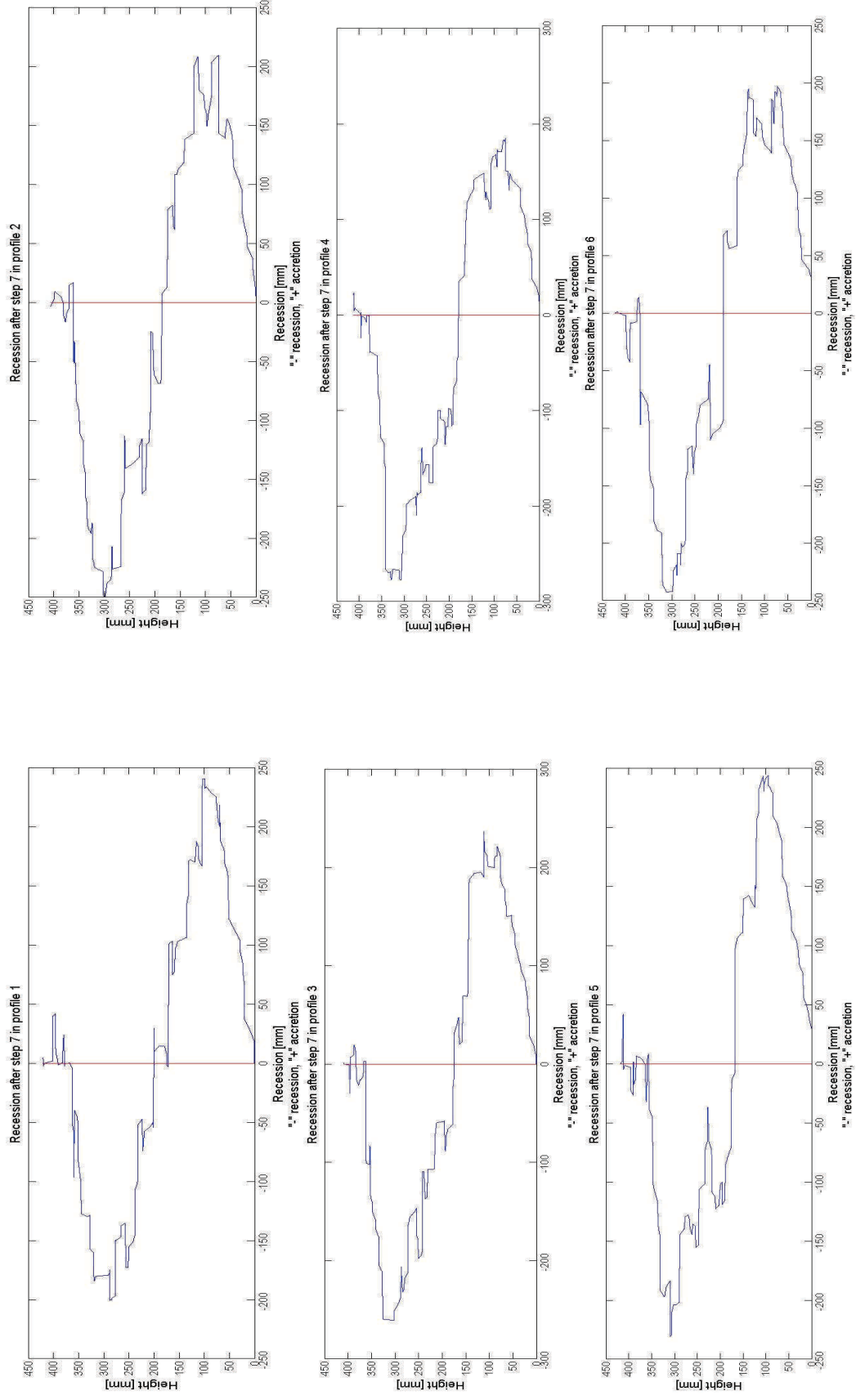Figure F. 25. Recession at each height at all the profiles after wave step 6. Setup 4

STEP 7

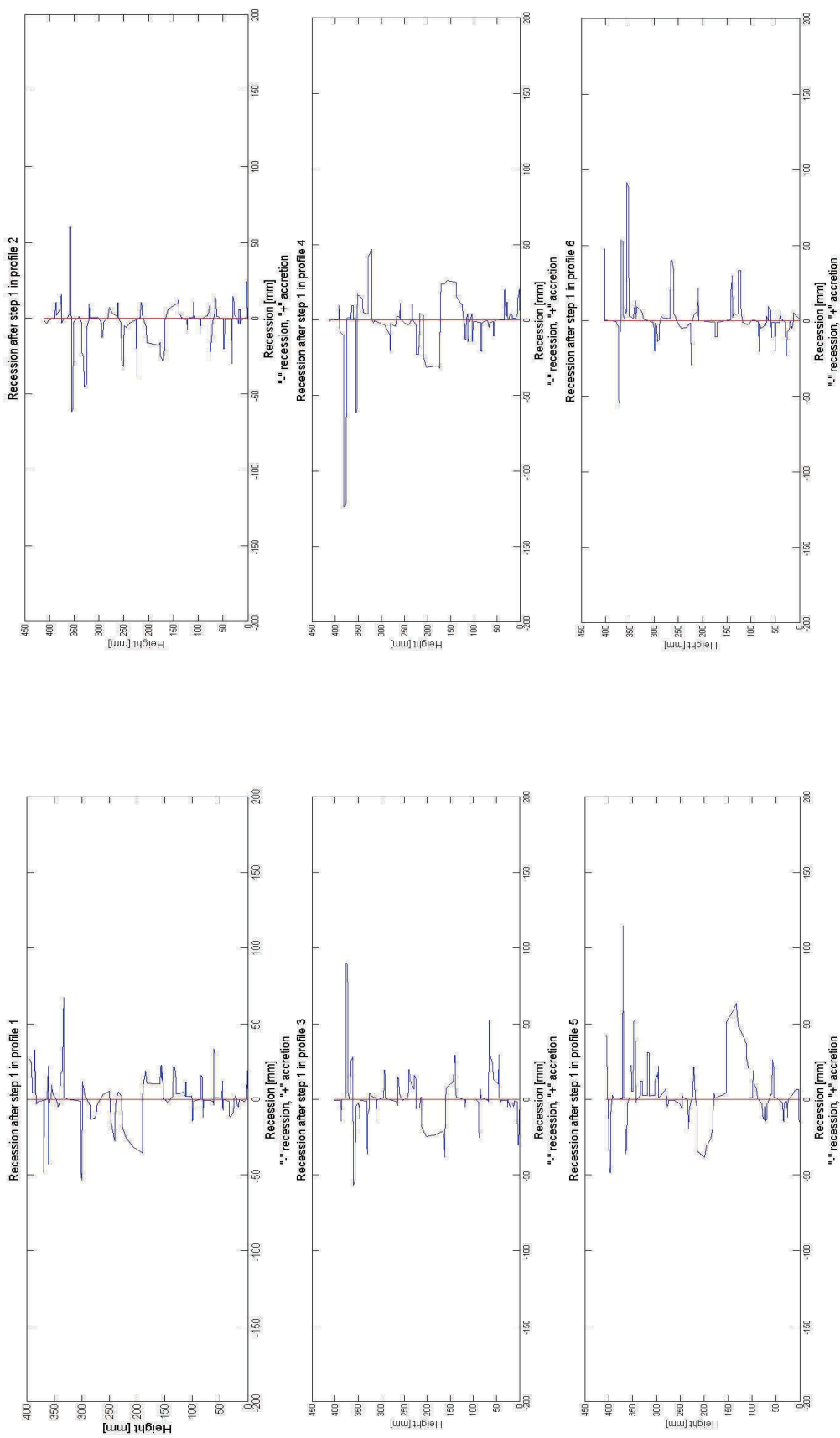**Figure F. 26. Recession at each height at all the profiles after wave step 7. Setup 4**

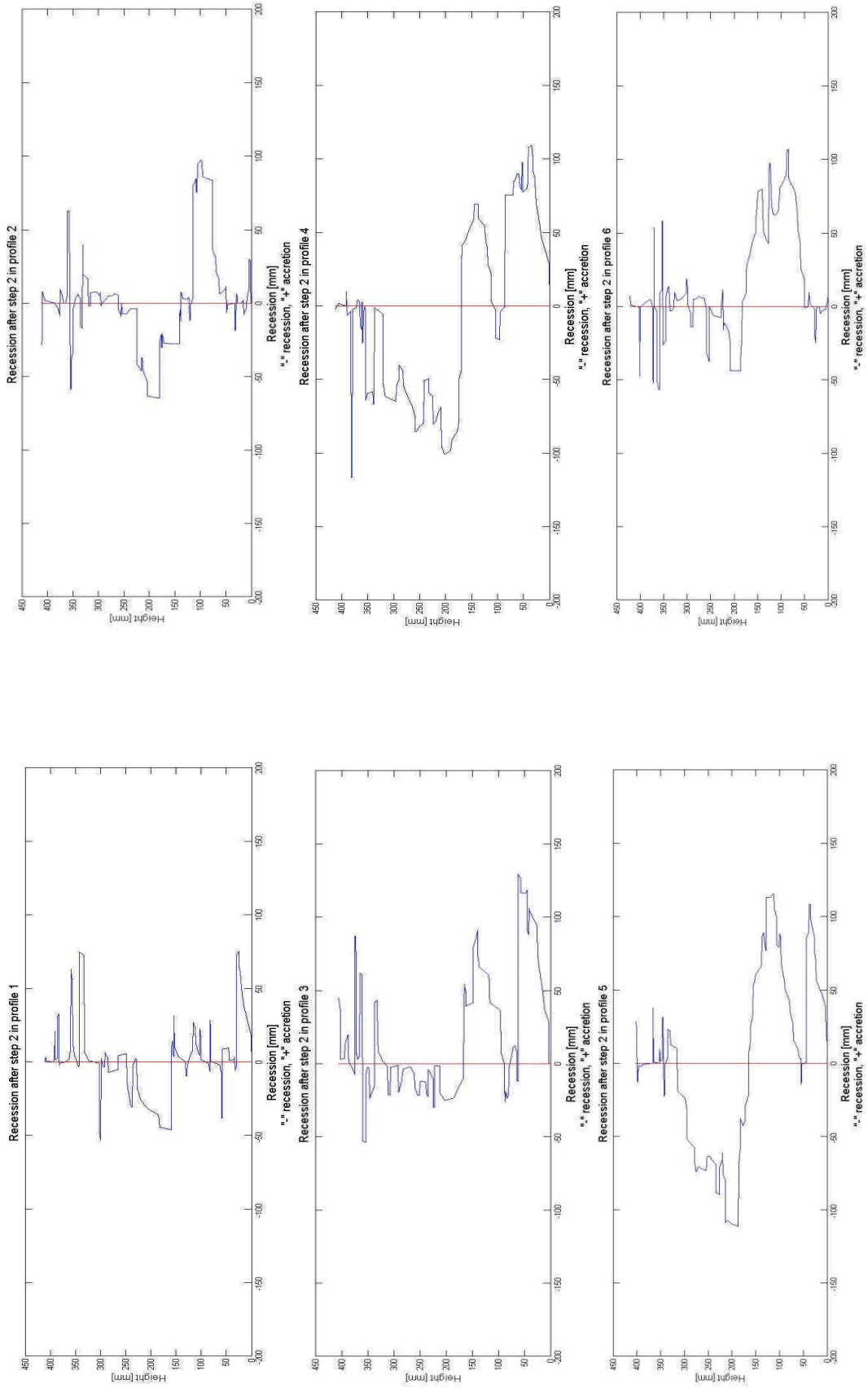**Figure F. 27. Recession at each height at all the profiles after wave step 1. Setup 5**

Figure F. 28. Recession at each height at all the profiles after wave step 2. Setup 5

Figure F. 29. Recession at each height at all the profiles after wave step 3. Setup 5

STEP 4

Recession after step 4 in profile 1

Recession after step 4 in profile 2

Recession after step 4 in profile 3

Recession after step 4 in profile 4

Recession after step 4 in profile 5

Recession after step 4 in profile 6

Figure F. 30. Recession at each height at all the profiles after wave step 4. Setup 5

STEP 5

Figure F. 31. Recession at each height at all the profiles after wave step 5. Setup 5
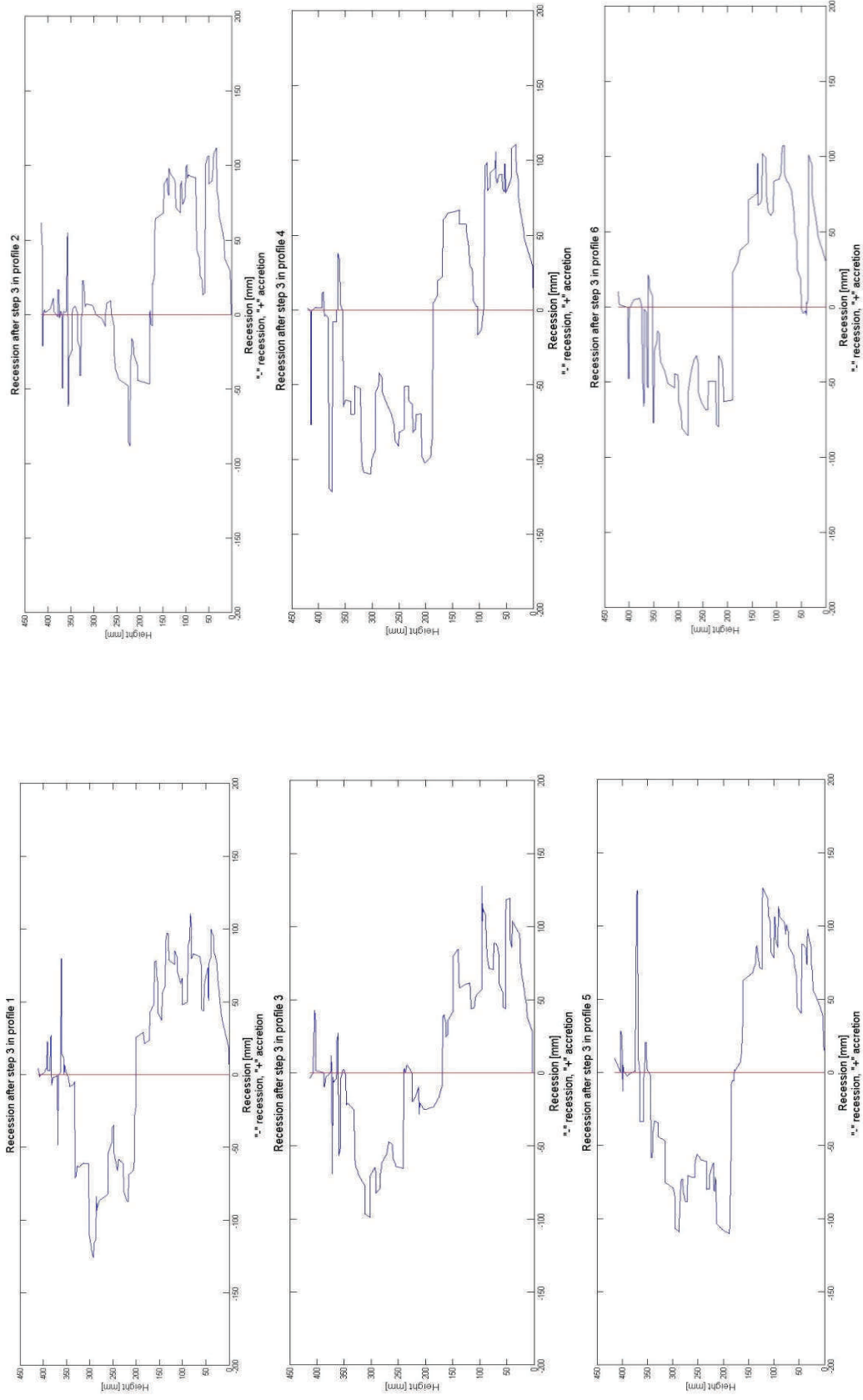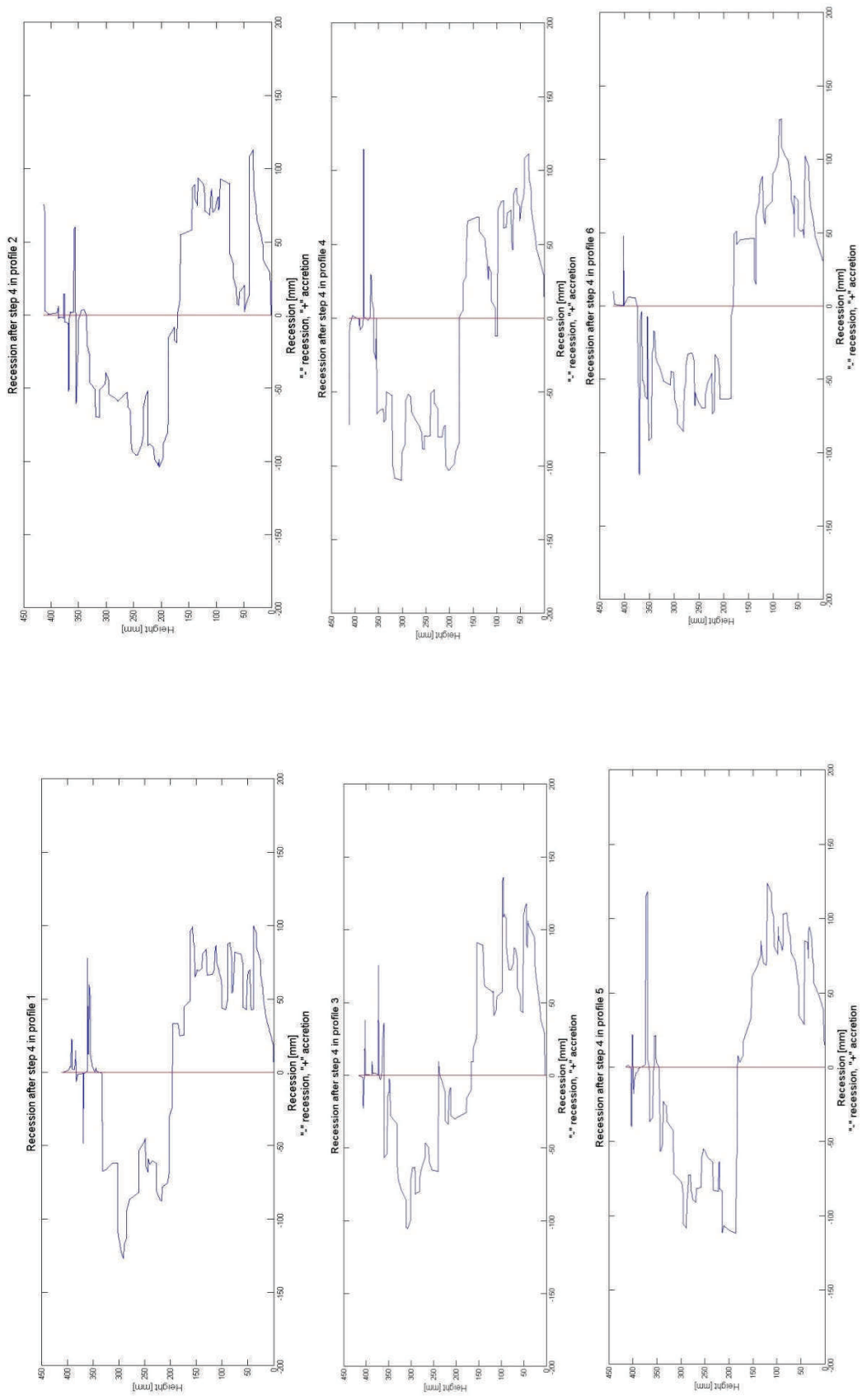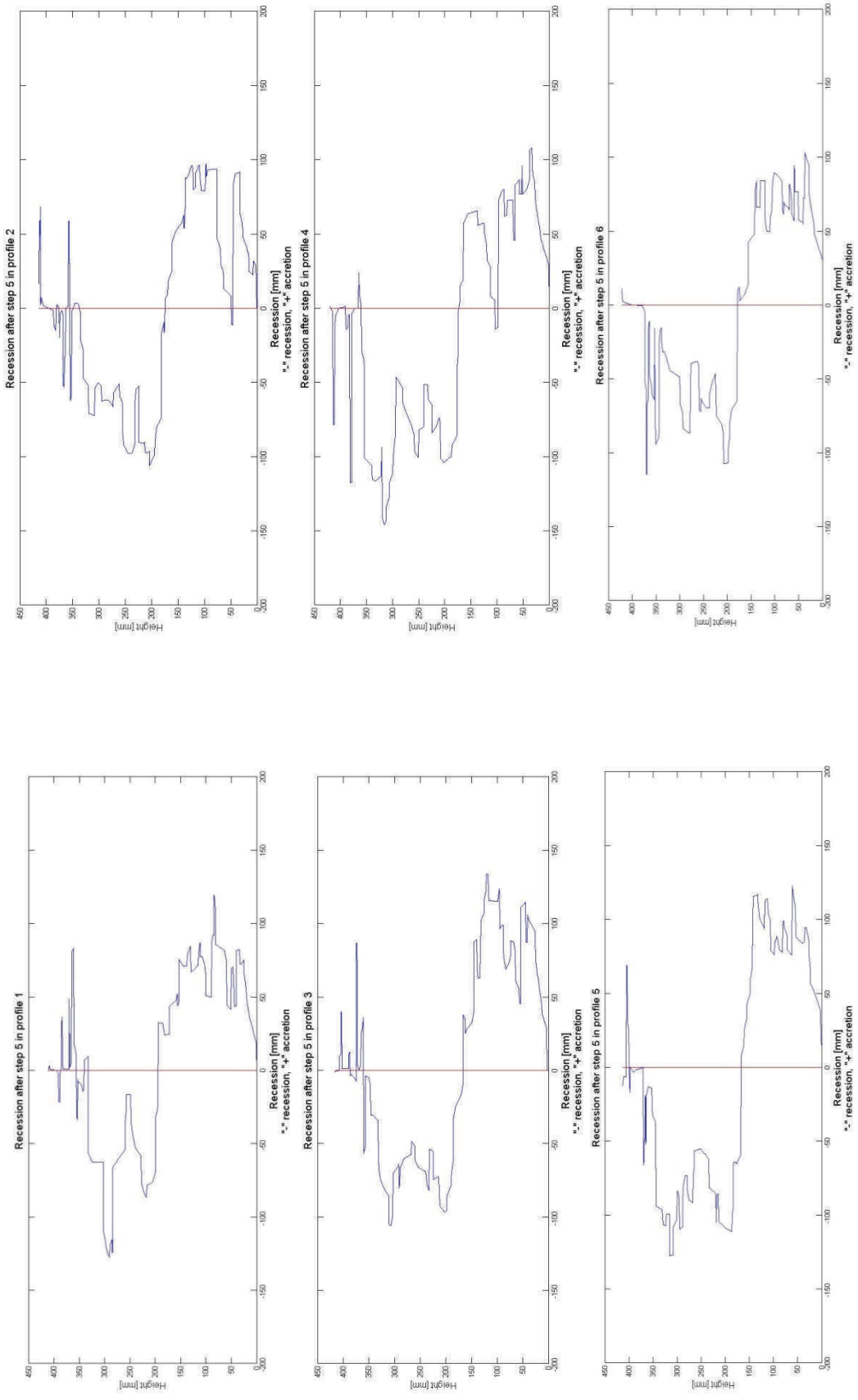
Figure F. 32. Recession at each height at all the profiles after wave step 6. Setup 5

STEP 7
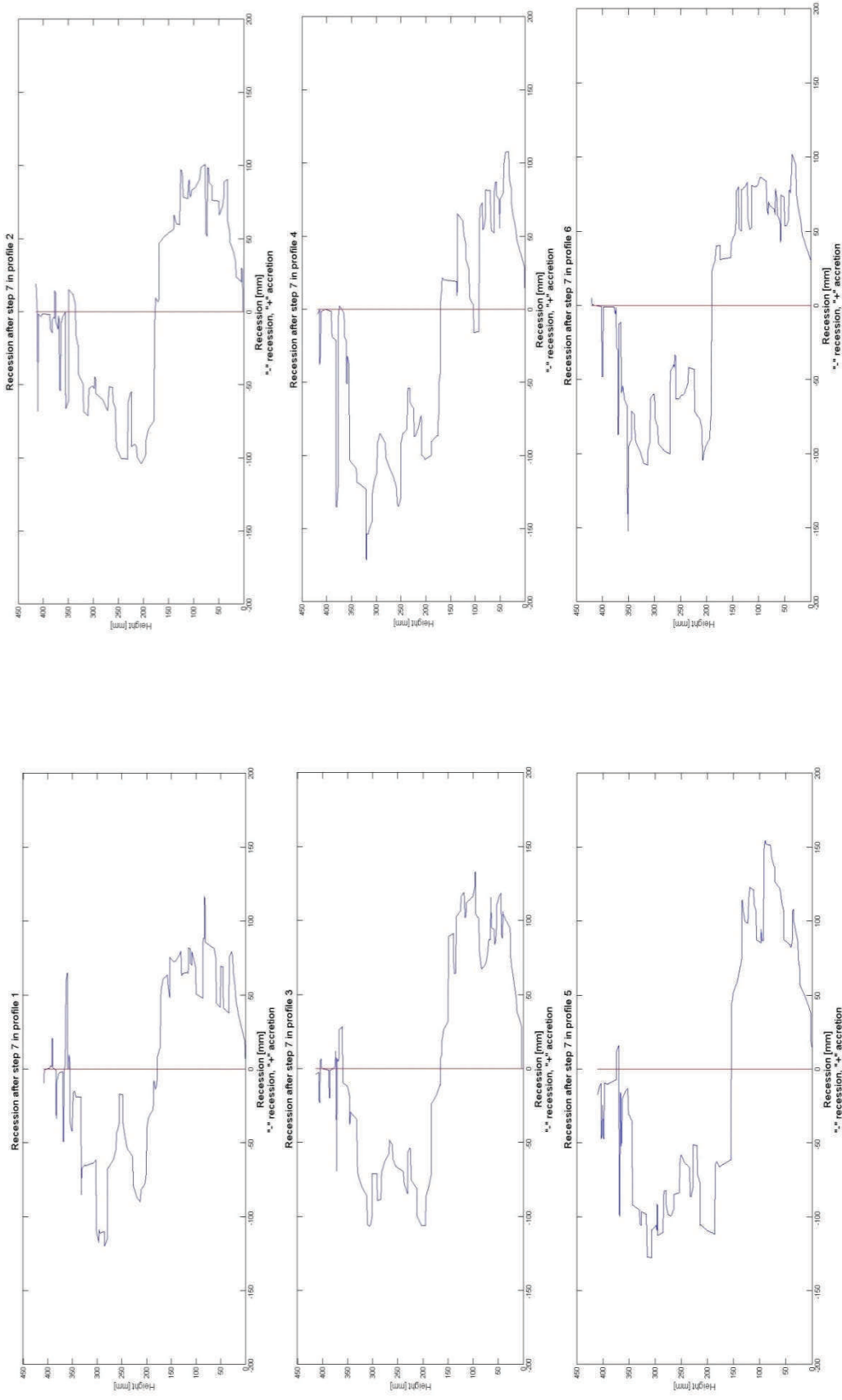
Figure F. 33. Recession at each height at all the profiles after wave step7. Setup 5

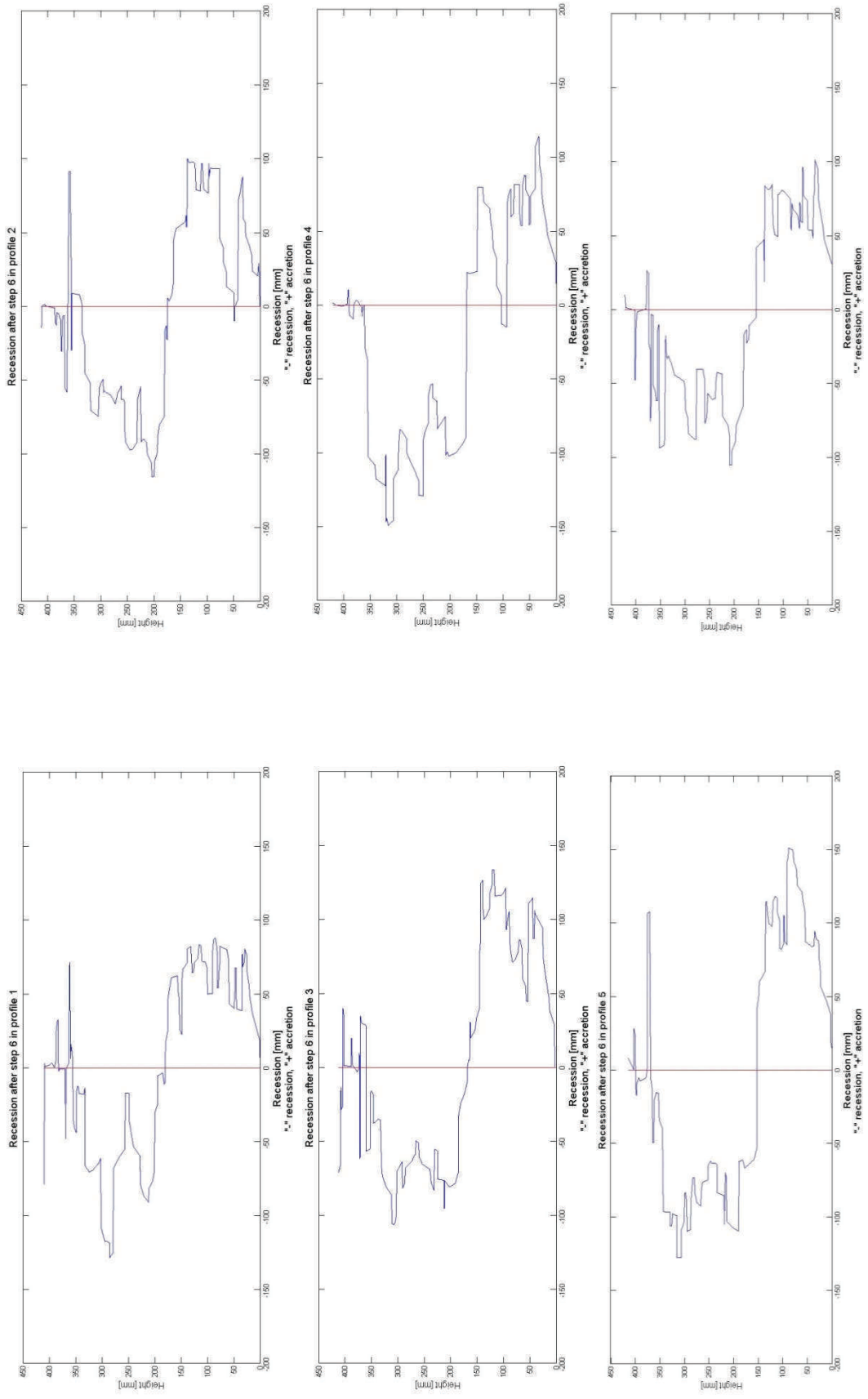# APPENDIX G. PICTURES

SETUP 1

Figure 1. Core material

Figure 2. Rock IV

Figure 3. Rock III

Figure 4. Rock II

Figure 5. First layer concrete cubes   **Figure 6. Second layer concrete cubes**

Figure 7. Outside profile

Figure 8. Breakwater after running wave step one

Figure 9. Breakwater front after step 3

Figure 10. Breakwater front after step 4

Figure 11. Breakwater front after step 5

Figure 12. Breakwater front after step

Figure 13. Breakwater profile after step 6

SETUP 2

Figure 14. Detail of the first rows

Figure 15. Breakwater before any wave test   **Figure 16. Breakwater after wave step one**

Figure 17. Breakwater after wave step two   **Figure 18. Breakwater after wave step three**

Figure 19. Breakwater after wave step four

Figure 20. Breakwater after wave step five

Figure 21. Breakwater after wave step six

Figure 22. Breakwater after wave step seven

SETUP 3

The yellow cubes are the ones of the second layer of the berm.

Figure 23. First layer of concrete cubes

Figure 24. Detail of the first row of cubes
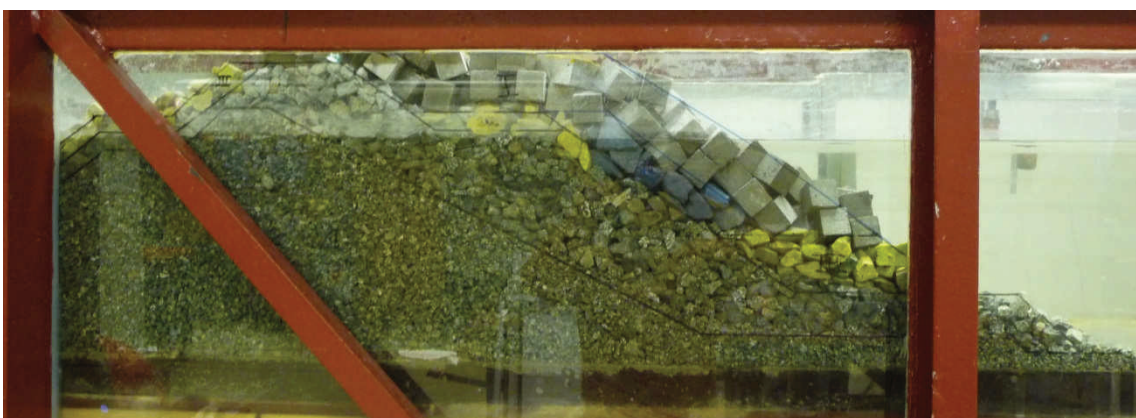
Figure 25. Profile before any wave step

Figure 26. Breakwater before any wave step

Figure 27. Breakwater after wave step one

Figure 28. Breakwater after wave step two

Figure 29. Breakwater after wave step three

Figure 30. Breakwater after wave step four

Figure 31. Breakwater after wave step five

Figure 32. Breakwater after wave step six

Figure 33. Breakwater after wave step seven

SETUP 4

Green cubipods: second layer of the slope

Orange cubipods: Second layer of the berm

Figure 34. First layer of cubipods

Figure 35. Profile of the model before any wave step

Figure 36. Detail of the first rows of cubipods

Figure 37. Breakwater before any wave step

Figure 38. Breakwater after wave step one

Figure 39. Breakwater after wave step two

Figure 40. Breakwater after wave step three

Figure 41. Breakwater after wave step four

Figure 42. Breakwater after wave step five

Figure 43. Breakwater after wave step six

Figure 44. Breakwater after wave step seven

SETUP 5

Figure 45. First layer of cubipods

Figure 46. Profile of the model before any wave step

Figure 47. Detail of the first rows of cubipods

Figure 48. Breakwater before any wave step

Figure 49. Breakwater after wave step one

Figure 50. Breakwater after wave step two

Figure 51. Breakwater after wave step three

Figure 52. Breakwater after wave step four

Figure 53. Breakwater after wave step five

Figure 54. Breakwater after wave step six

Figure 55. Breakwater after wave step seven

APPENDIX H. MYHRA (2005) TESTS

Myhra (2005) tested two berm breakwaters, the Sirevåg berm breakwater, Figure H.1, and the Alternative berm breakwater with a narrower and higher shoulder and also a higher crest, Figure H.2. Both were tested with different construction method of the armour layer, pell-mell vs. orderly placement, but at the comparisons done at this thesis, the data from pell-mell placement model is used. The main difference between these two models is the start of the armour layer. The prototype in Sirevåg was constructed with a placement of the armour stones from elevation -1.0 m, while n the alternative breakwater design, the class-I armour stones is placed down to level -7.0 m in prototype scale.
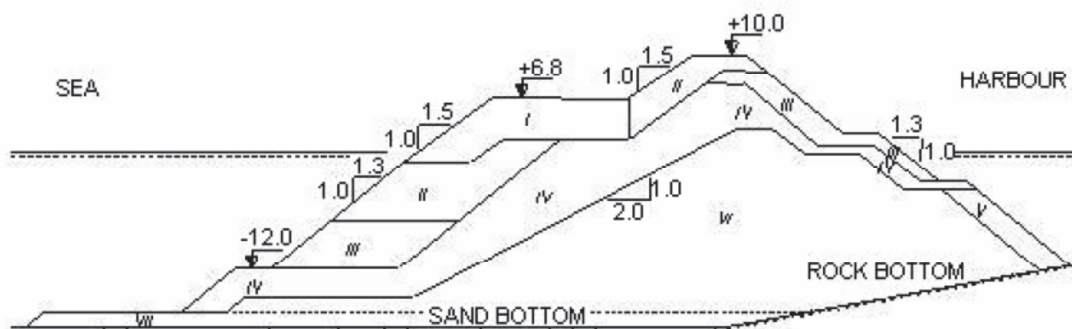
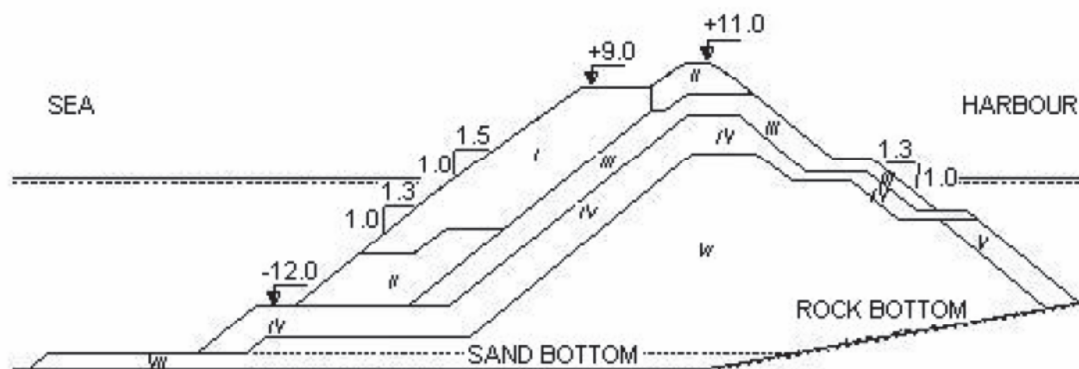

Figure H.1. Sirevåg berm breakwater

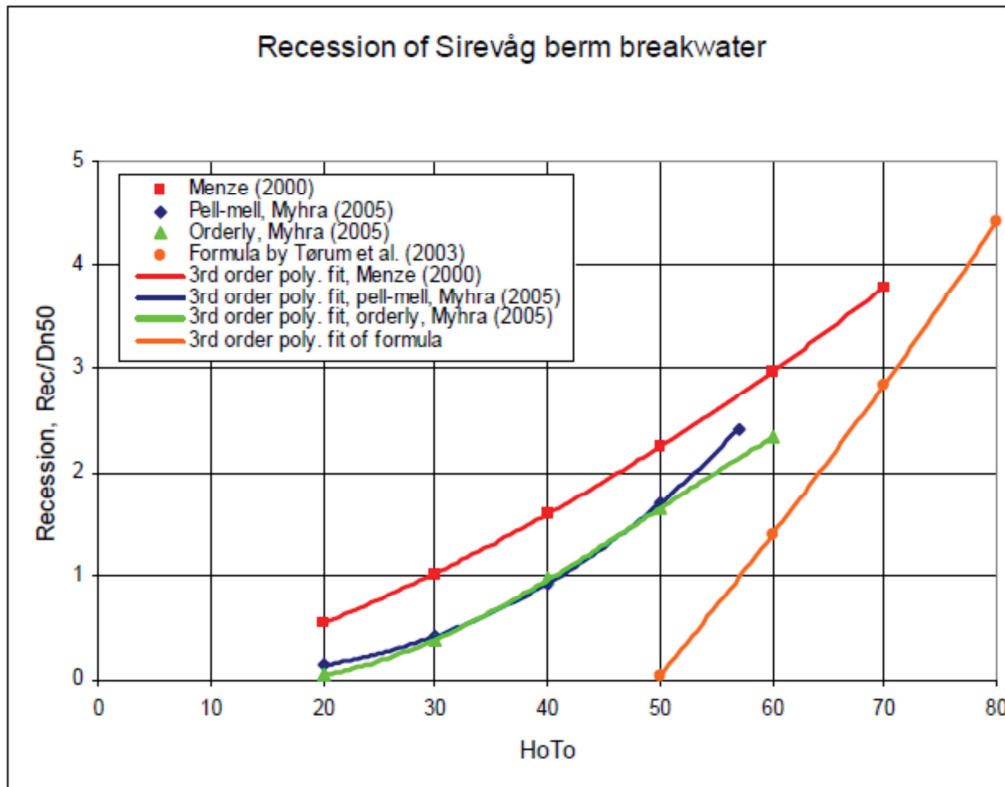**Figure H.2. Alternative breakwater tested by Myhra (2005).**

Figure H.3. Recession, Sirevåg berm breakwater. All tests are performed at a multilayer berm breakwater, while the formula by Tørum et al. (2003) is for a homogenous berm breakwater (Myhra 2005)

APPENDIX I. PRE-THESIS. TASK DESCRIPTION

October 2012

Master Thesis Spring 2012 Previous Text
Berm breakwaters with concrete cubes as armour units
Altea Cámara Aguilera

It has been tested that berm breakwaters are more stable under certain conditions than conventional breakwaters, Rao et al. (2012). They have also the advantages of its great tolerance in placement accuracy and the lower mass of the individual armour stones that makes possible the construction with less specialized equipment and labor (Tørum et al. 2011).

The acquisition of large armour stones can be difficult in some locations. A solution could be to use concrete blocks in the armour layer, where the largest rocks are needed.

Only a few experimental studies about berm breakwaters with concrete blocks have been performed, as the one by Subba Rao et al. (2012). They studied the influence in the stability of the berm breakwater produced by the change in different wave parameters and storm duration. This study was very similar to ours but it had a different modelling. They used a physical model with a scale of 1:30 and three layers berm breakwater. Their test was carried in a 2D wave flume with regular waves. Our test will be also carried in a 2D wave flume but we will use irregular waves. Our model scale will be 1:70-1:80 and our model will be a multilayer berm breakwater.

Our tests will be carried out on a scale model of the Sirevåg berm breakwater in order to compare the results with the several investigations completed about it. Some of these studies are the thesis carried out by Menze (2000), Myhra (2005) and Westeng (2011) at NTNU. Menze studied the behaviour of multilayer berm breakwaters, testing two stone densities in two different set-ups, with three dimensional tests. Myhra investigated the recession of two berm breakwaters with different construction design, in two models, one of the Sirevåg breakwater and an alternative model with narrower and higher berm. Westeng studied the recession of two different berm breakwaters, a model of the Sirevåg breakwater and a similar one with class II armour at the upper front of the berm.

All the test runs consisted in replicas of the two major storms recorded close to the Sirevåg harbour, in addition with different wave series. AS we will work at the

same wave flume that Myhra (2005), our test will be similar his, which slightly changed the test of Menze so as to the largest wave could be generated with the available wave generator. It consisted of wave steps of two 25 minutes series that corresponded to approximately 2700 waves for the lowest wave height and 2000 waves for the highest wave height. The main storms were simulated based on the data from the Norwegian Mapping Authority and the analysis from the data documented made by Tørum et al. (2003) and Tørum et al. (2005).

A laser will be used to profile the breakwater before and after each run. At the Myhra test, performed in the same wave flume that ours, the laser sampled profiles at a distance of 100 mm between each other. This profile distance is a frequently used parameter for berm breakwater with D_{n50} between two and three centimetres (Tørum et al. 2011). Menze (2000), Myhra (2005) and Westeng (2011) followed the same procedure to calculate the recession. The data of the laser was first smoothened and then, the recession over the height of the breakwater was calculated. The maximum value of the recession was defined to be within a peak of a width of at least D_{n50}. Westeng also calculated the recession as its more general definition, that is, at the top of the berm. He concluded that the two methods to a large extent gave equal results. Visual observations and pictures were also made in the three tests after each run. This helps to have a better idea of the alterations in the breakwater. In addition, all moved stones where counted and their actual positions were noted. The visual observations were helped by painting each layer of stones in a different colour.

After the storm in 2005, the Sirevåg berm breakwater showed clear signs of reshaping at a location with a shoal in front, Myhra (2005). Because of this, at the Myhra test, a shoal was built into the wave flume and it confirmed that the reshaping was mainly owing to the shoal. This test also indicates that the duration of the storm is of less importance for the reshaping. I think that this fact could be taking into consideration in our model.

Our task is to test a modification of the Sirevåg breakwater replacing the class I stone with concrete cubes of 43 tons. The design waves will be $H_{s,100}=7.0$ m, $T_z=10.6$ s. HoTo=48. We will obtain the recession for the same wave conditions used by Myhra. We will compare the results with the previous test in order to conclude if this modification in a berm breakwater is favourable or at least has the same behaviour than the traditional berm breakwater. We will also compare the result with the different recession formulae to know the usefulness of the formulae with concrete blocks.

This will be the beginning of a whole study. Other tests that study different performances and aspects of the breakwater should follow it, such a different layer configuration and different morphology that suits better to a berm breakwater with

concrete cubes, the different concrete armours, and the permeability and overtopping in each of them, etc.

References

Menze, A. (2000): Stability of multilayer berm breakwaters. Master thesis. Norwegian University of Science and Technology, Department of Civil and Transport Engineering, and Lieichtweiss Institut für Wasserbau, Technical University of Braunschweig.

Myhra, H. (2005): Berm breakwaters. Influence of construction method and storm duration on stability. Ice ride-up. Master thesis, Norwegian University of Science and Technology, Department of Civil and Transport Engineering.

Rao, S., Shirlal, K.G., Rao, B. and Prashanth, J. (2012): Berm breakwater study with concrete cubes – an experimental approach. Proceedings of the 8th International Conference on Coastal and Port Engineering in Developing Countries. COPEDEC , Madras, Chennai, India, 20 – 24 February, 2012.

Tørum, A., Arntsen, Ø., Mathiesen, M. and Bjørdal S. (2003): Sirevåg berm breakwater. Comparison between hydraulic model and prototype behaviour. NTNU Report IBAT/MB R1. Prepared for the Norwegian Coastal Administration.

Tørum, A., Løset, S. and Myhra (2005): Sirevåg berm breakwater – comparison between model and prototype reshaping. International Coastal Symposium, Höfn, Iceland, 5-8 June 2005.

Tørum, A., Moghim, N.M, Westeng, K., Hidayati, N. and Arntsen, Ø. (2011): on berm breakwaters: recession, crown wall wave forces, reliability. Accepted for publication in Coastal Engineering Elsevier.

Westeng, K.O. (2011): Berm breakwaters – a modified version. Master Thesis, Norwegian University of Science and Technology, Department of Civil and Transport Engineering.